SOUTH AFRICAN MARINE COMPOUNDS AS ANTICANCER AGENTS

Thesis presented by

Catherine Evelyn Whibley

In fulfillment of the requirements for the degree of

Doctor of Philosophy

in

Medical Biochemistry

Faculty of Health Sciences
University of Cape Town

October 2006

Supervised by
Dr Denver T. Hendricks
Department of Medical Biochemistry
University of Cape Town

Co-supervised by
Professor Michael T. Davies-Coleman
Department of Chemistry
Rhodes University

ACKNOWLEDGEMENTS

Many thanks to the following people for their assistance with this project :

Dr. Shirley Parker-Nance and Dr. Toufiek Samaai for the identification of the source marine organisms.

Past and present students and staff in the Department of Chemistry, Rhodes University, especially Andy Soper, Brent Scheepers and Albert van Wyk.

Dr. Rob Keyzers, for the superhuman chemistry.

Staff of the oesophageal cancer lab – especially Robert Samuels (for always going the extra mile), and Hajira Karjiker and Lamize Viljoen (for keeping the lab running smoothly).

Past and present students in the oesophageal cancer lab – especially Widaad Zemanay for all the moral support, and Kate Hadley and Michelle Skelton for their friendship.

Dr. Virna Leaner and her students – Pauline Forrester and Michelle Maritz – for all the suggestions, contributions and assistance with the Caski/TAM 67 work and the microarrays, and for input on this thesis.

Dr. Sharon Prince and Amaal Abrahams for the use of the luminometer, and useful discussions.

Students and staff in the Department of Haematology, UCT, especially Rianna, Glenda, Caryn and Jai for the access to the flow cytometer, and always being willing to help.

The funding agencies who have supported me during my PhD – National Research Foundation, Harry Crossley Foundation, University of Cape Town and the Deutscher Akademischer Austauschdienst (DAAD).

Professor M. Iqbal Parker, for all his assistance.

Finally my supervisors :

Dr. Denver Hendricks, for pushing me to do my best at all times, and providing such a supportive environment for my PhD work.

Prof Mike Davies-Coleman, for all the encouragement, and for making this project possible with the supply of all marine extracts and compounds.

TABLE OF CONTENTS

DEDICATION

For my wonderful husband

Thank you for your endless patience, love and support

You can have me back now!

ABSTRACT

Oesophageal cancer is the most common cause of cancer related deaths among black males in South Africa. Currently there are very limited treatment options, and patients have a very poor prognosis, due in part to the late stage at which this cancer is usually detected.

In this thesis we describe the establishment of a screening assay using an oesophageal cancer cell line as a model. It was our hope that this screen would allow us to identify compounds which have activity against oesophageal cancer, that could be used as lead agents for further development of chemotherapeutic agents.

Once our screen was established, we tested a wide range of extracts from southern African marine organisms, supplied by our collaborators from Rhodes University, South Africa. The marine environment represents a rich, untapped repository of novel and interesting compounds, and through our collaboration we had access to a wide range of marine-derived extracts and compounds.

During the course of this project we provided screening data to assist in activity-directed fractionation from five active marine extracts, giving rise to 15 compounds of varying activity. These included several groups of novel active compounds such as the makaluvic acids from the sponge *Strongylodesma aliwaliensis* and the malonganenones from the octocoral *Leptogorgia gilchristii.* The identification of a number of novel, active compounds through our screening program highlights the potential of marine organisms from the southern African coast as a source of novel drug leads.

We also examined the mechanism of action of a group of triprenyl quinones and hydroquinones previously identified from the Arminacean nudibranch *Leminda millecra* by our collaborators. We showed that these compounds cause a cell cycle block in oesophageal cancer cells, followed by cell death by apoptosis, and not necrosis. The action of these compounds was shown to be a result of their ability to produce reactive oxygen species (ROS). Treatment with ROS scavengers decreased apoptosis levels in KLM treated cells, and the levels of ROS produced by these compounds was directly proportional to their activity (as measured by IC_{50} analysis). Further, the activation of several cellular antioxidant pathways by treatment with

KLM155 was demonstrated, and the involvement of AP1 signalling in the cellular responses to KLM treatment was examined.

The production of ROS is an attractive chemotherapeutic approach since recent evidence indicates that tumours are under increased oxidative stress, and thus the production of ROS may be sufficient to induce apoptosis in cancer cells, while normal cells survive. Our results thus indicate that this group of compounds may be good drug leads for the development of effective chemotherapeutic agents for oesophageal cancer.

CHAPTER 1

LITERATURE REVIEW

1.1. Oesophageal cancer

Oesophageal cancer occurs with high frequency in many parts of the world, and most often patients have a poor prognosis due to late diagnosis. As this discussion highlights, there is a clear need to understand this disease better and improve on the treatment options currently available to increase the survival rate of oesophageal cancer patients.

1.1.1. Description

Tumours of the oesophagus have been classified as epithelial and non-epithelial tumours. Of these, tumours of the epithelium are the most common, and the two predominant forms of epithelial tumours of the oesophagus are squamous cell carcinoma (SCC) and adenocarcinoma (1;2).

WHO classification defines SCC of the oesophagus as "a malignant epithelial tumour with squamous cell differentiation, microscopically characterized by keratinocyte-like cells with intercellular bridges and/or keratinization". SCC is found predominantly in the upper two-thirds of the oesophagus in 85-90% of cases (2). Squamous cell carcinoma accounts for 50-60% of all oesophageal cancer worldwide (3).

Adenocarcinoma is "a malignant epithelial tumour of the oesophagus with glandular differentiation arising predominantly from Barrett mucosa in the lower third of the oesophagus" (2). Adenocarcinoma accounts for 40 to 50% of all oesophageal malignancies worldwide (3).

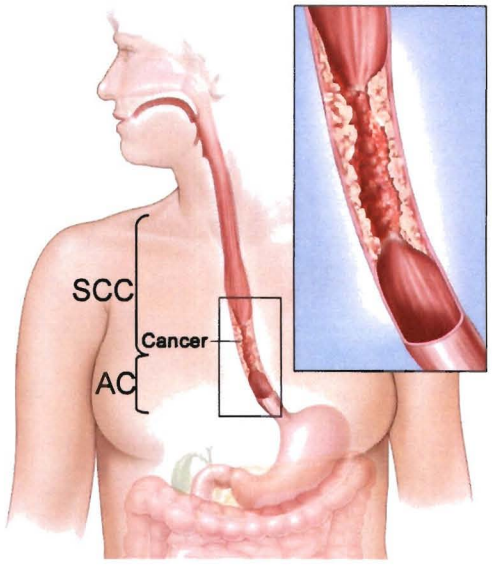

Figure 1.1. Location of the oesophagus, and the most common sites of adenocarcinoma and squamous cell carcinoma.
The most common sites for squamous cell carcinoma (SCC) and adenocarcinoma (AC) are indicated. The tumour in the inset has constricted the diameter of the oesophagus and may interfere with swallowing. (Image from www.cancer.gov.)

1.1.2. Incidence

Oesophageal cancer is the eighth most common form of cancer worldwide with an age-standardised incidence ratio (ASIR) of 11.5 per 100 000 for males and 4.7 per 100 000 for females. Oesophageal cancer is the 6th most frequent cancer among males, and the 9th most common cancer among females (http://www-dep.iarc.fr/).

The incidence of oesophageal cancer varies widely with geographical location, especially when divided into the 2 major forms – squamous cell carcinoma and adenocarcinoma. Adenocarcinoma is more prevalent in developed countries, and SCC is more prevalent in developing countries, with hotspots in China, South America, east and southern Africa, and the Middle East (2) with rates as high as 28.1 per 100 000 in some areas (http://www-dep.iarc.fr/).

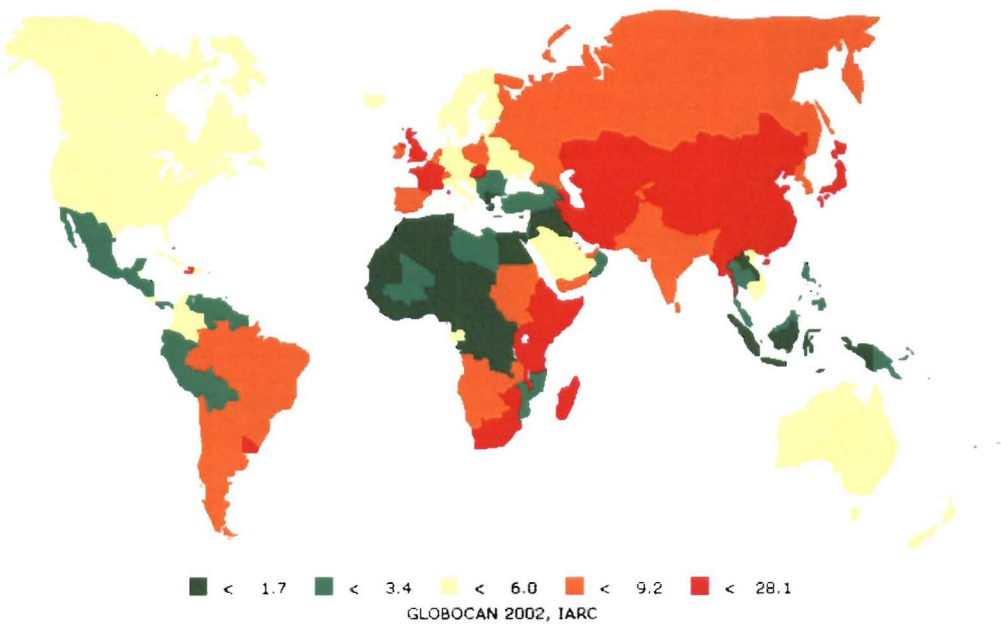

Figure 1.2. Geographical distribution of oesophageal cancer among males.
Map showing the ASIR of oesophageal cancer among males. Areas of high incidence include parts of Asia, the south-east coast of Africa, Italy and France, and a small area in South America. (Image from http://www-dep.iarc.fr/)

In South Africa, the predominant form of oesophageal cancer is SCC (1;4) with an overall ASIR for males of 12.6 per 100 000, and 5.6 per 100 000 for females. Considering the high incidence of SCC in South Africa, the work in this project focused on SCC of the oesophagus. Currently oesophageal cancer is the third most

common cancer among males (at 6% of all cancers), and the fourth most common cancer among women (at 3% of all cancers) in South Africa. While these figures are only slightly higher than the worldwide incidence, when incidence is considered among different population groups in South Africa, much higher rates are observed.

Black males are the group most at risk of developing oesophageal cancer in South Africa, with oesophageal cancer the second leading cancer affecting black males (at 14% of all cancers), second only to prostate cancer. The ASIR for this group is 16.2 per 100 000 (4).

Black females are also at high risk of developing oesophageal cancer with this cancer the third leading cancer causing 6% of all cancers after cervical (35% of all cancers) and breast (15% of all cancers). The ASIR for this group is 7 per 100 000.

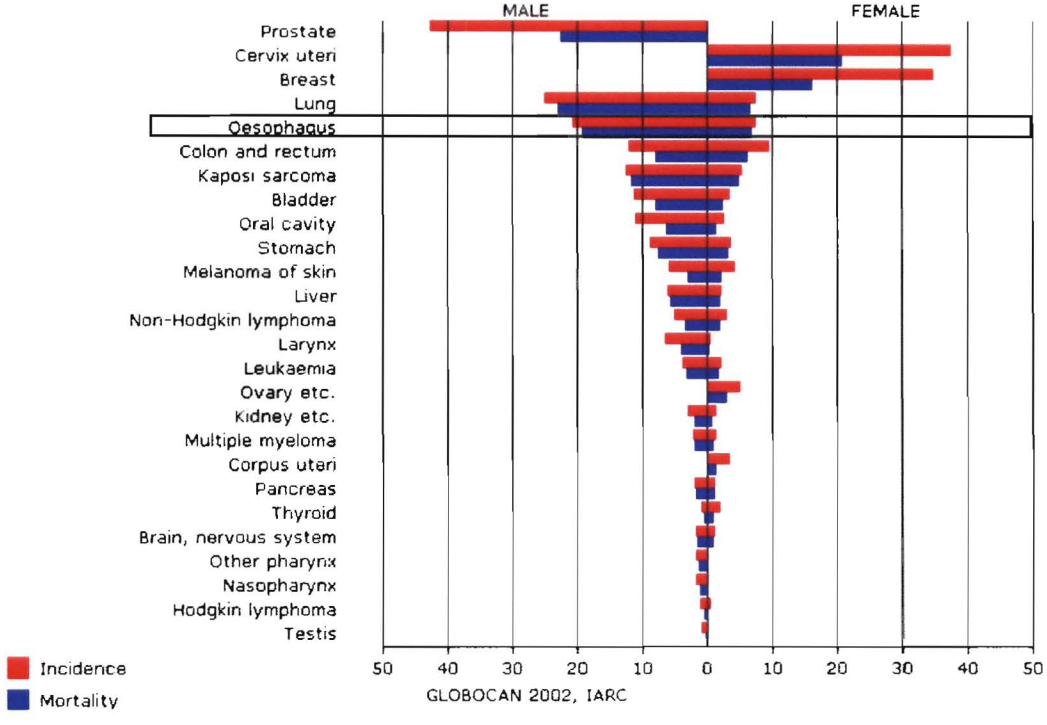

Figure 1.3. Cancer incidence and mortality figures for South Africa.
Oesophageal cancer is among the most common cancers for both males and females in South Africa, and the third most common incidence cancer in males, and the fourth most common incidence cancer among females. (Image from http://www-dep.iarc.fr/)

The current 5 year survival rate for patients diagnosed with oesophageal cancer is only 14%, which is extremely poor, but is an improvement on the survival rate from the 1970's, when only 4% of oesophageal cancer patients survived at 5 years after

diagnosis (5). This is due, in part, to improved surgical techniques and earlier detection.

Since this cancer has such high prevalence in South Africa, it presents a high burden of disease. Combined with the poor prognosis and late diagnosis, it causes a great number of mortalities. As such there is a need for novel chemotherapeutic agents to help treat this disease.

1.1.3. Aetiology

Whereas adenocarcinoma has been strongly linked to gastric reflux and Barretts oesophagus (6), the aetiology of squamous cell carcinoma of the oesophagus is less clearly defined. In developed countries there is a strong correlation between smoking and drinking, and the risk of developing SCC (about 90% in the USA, France and Italy). However, in less developed countries the percentage of SCC attributable to smoking and drinking drops to 50% in South Africa, 20% in Iran, and as low as 1% in Henan province in China (2). Other environmental and behavioural risk factors include drinking of extremely hot beverages, low levels of fresh fruit and vegetables in the diet, maize as a staple diet and consumption of *Fusarium* contaminated food (often maize) (1;2). There is some evidence that infection with Human Papilloma Virus (HPV) may be associated with oesophageal cancer, with HPV detected in 15% to 75% of oesophageal tumours (7;8). In addition, normal polymorphisms in xenobiotic metabolizing enzymes may affect the risk of developing squamous cell carcinoma of the oesophagus in individuals exposed to the same environmental background (9;10).

1.1.4. Staging

Oesophageal cancer is staged according to the degree of tumour invasion, involvement of regional lymph nodes, and presence of distant metastasis. These combine to give 4 stages as detailed in Figure 1.4. At Stage 0, also called carcinoma in situ, the cancer is superficial and only involves the innermost layer of cells of the oesophagus. Stage I tumours have spread through the epithelial layer and the basement membrane to invade the submucosa. Stage II tumours are divided into two categories, dependant on the involvement of lymph nodes. At Stage III the tumour has invaded all layers of the oesophagus, and may have involved local lymph nodes. Stage IV tumours have spread to local or distant lymph nodes (Stage IVA) and may have spread to distant tissues (Stage IVB) (11).

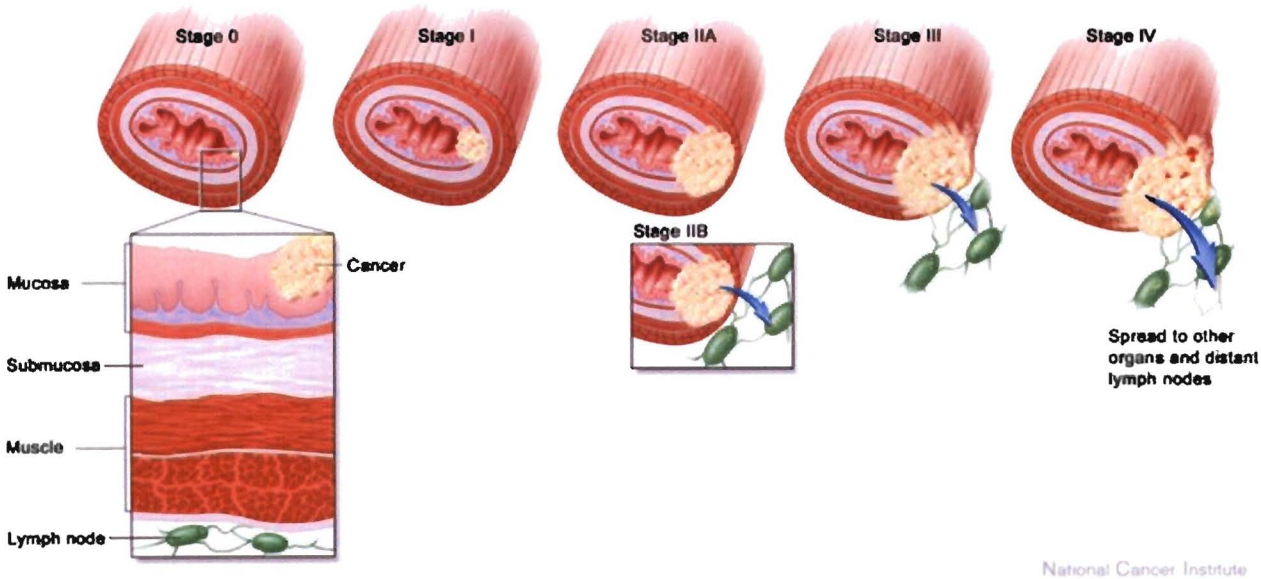

Figure 1.4. Staging of oesophageal cancer.

Oesophageal cancer is staged according to the degree of invasion of the tumour, lymph node involvement, and presence of distant metastases. (Image from www.cancer.gov)

1.1.5. Treatment options

If oesophageal cancer is detected early (Stage I and II), the prognosis is favourable, and treatment generally comprises of surgery, which is often coupled with neoadjuvant chemotherapy (12). However, in most cases, especially in the developing world, detection is only at a late stage (Stage III or IV), at which point the tumour mass has already invaded surrounding tissue and expanded to fill the lumen to obstruct swallowing, and the prognosis is poor (13;14). Due to the poor nutritional status of many of these patients, and the involvement of metastases, surgery is not the ideal option in most of these cases, and chemotherapy or radiotherapy are the options of choice. These may serve to downstage the tumour, allowing surgical intervention (12). In some cases, palliative care is the only option, and may comprise of chemotherapy, radiotherapy, and intubation (15).

At Groote Schuur Hospital in Cape Town, South Africa, in the period 1977 to 2003 a total of 1895 patients presented with oesophageal cancer. Of these, 42% were not suitable for any form of treatment, and received supportive care (16%) and intubation (26%). Nineteen percent of the patients received palliative radiotherapy in an attempt to decrease tumour size, while only 29% (550/1895) of patients received any type of curative treatment. This reflects the late stage at which oesophageal cancer is usually diagnosed in South Africa, and the poor prognosis for these patients. Of the 550 patients receiving treatment of a curative nature, approximately a quarter were suitable for oesophagectomy, with neoadjuvant chemo- and radiotherapy. The remaining patients received radiotherapy or chemotherapy alone, or combined radiotherapy and chemotherapy (equivalent numbers of patients in each group) (Personal correspondence, Dr. C. Dandara, University of Cape Town, South Africa.).

Tew *et al.* identified the following reasons for the poor survival rate of patients with oesophageal cancer (16):

i. Poor screening tools and guidelines
ii. Cancer detection at a late stage
iii. High risk of recurrence after surgery or chemotherapy
iv. Unreliable measurements for response to chemoradiotherapy
v. Limited survival of patients treated with chemotherapy alone with metastatic or non-resectable disease.

These can be grouped into 2 main deficiencies in the current approaches – inadequate identification of patients at an early enough stage to allow treatment (i and ii), and a lack of adequate treatment regimes for all forms of the disease (iii, iv and v).

The poor survival of oesophageal cancer patients has been confirmed in numerous trials in which various combinations of chemotherapy, radiotherapy and surgery have been tested (15;17-20). The most commonly used and effective treatment for oesophageal cancer is a combined cisplatin/5-fluorouracil based chemotherapy, coupled with surgery (21). However, some recent trials show some promising results with newer agents such as paclitaxel, docetaxel and ironetecan having better activity against oesophageal cancer and fewer side effects (12).

1.2. Chemotherapy for oesophageal cancer

The most common chemotherapeutic agents used in the treatment of oesophageal cancer are a combined cisplatin/5-fluorouracil regime (21). This is a synergistic combination with results indicating much higher cell killing in combination, with concentrations of each compound that alone cause only minimal cell death (22;23). This allows administration of each drug at lower concentrations than required if used in isolation, lowering the risks of side-effects.

1.2.1. Cisplatin

Cisplatin (in combination with 5-fluorouracil) is the most commonly used chemotherapeutic agent for oesophageal cancer, and is used widely for the treatment of various solid tumours (24).

Cisplatin is a water-soluble planar complex, comprising of a central platinum atom, bonded by two chlorine atoms and two ammonia molecules organized in a cis-conformation. Interestingly, the trans- conformation is far less active (Figure 1.5).

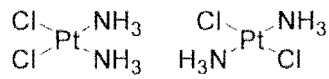

cisplatin transplatin

Figure 1.5. The structures of cisplatin and transplatin.

Cisplatin acts by entering the cell, where the chlorine atoms dissociate leaving a reactive complex that can then interact with DNA, causing intrastrand crosslinking. There is also evidence that cisplatin damages mitochondria, arrests the cell cycle in G2 (probably due to DNA damage), inhibits ATPase activity, and eventually leads to apoptosis, inflammation and cell death (25).

The major, dose limiting side-effect in cisplatin treatment is nephrotoxicity. Other toxicities include ototoxicity, neurotoxicity, and bone marrow suppression. These are suggested to be mediated in part by upregulation of tumour necrosis factor-α (TNF-α) (24).

1.2.2. 5-fluorouracil

5-fluorouracil (5-FU) is a member of a class of nucleoside analogues. The fluorinated pyrimidines were one of the first groups of successful rationally designed anti-neoplastic agents, and were synthesized in 1957 (26). 5-FU, the most well known member of this class, is a uracil analogue, with a fluorine atom substituted at the 5' carbon of the pyrimidine ring (Figure 1.6.).

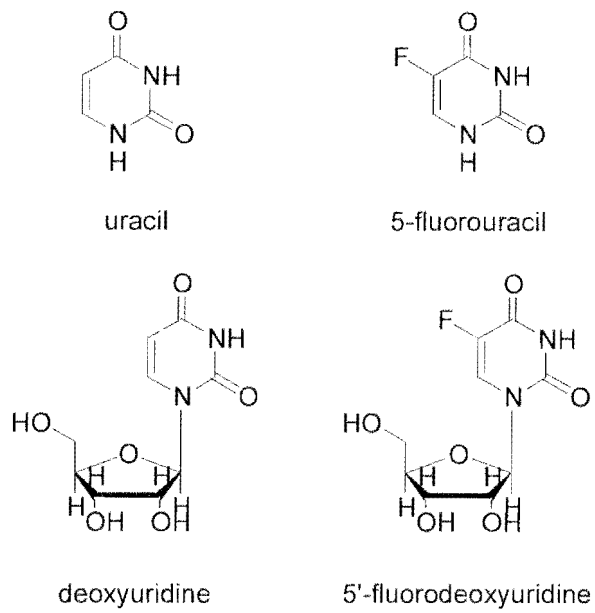

Figure 1.6. The structures of 5-fluorouracil and related compounds.
While uracil is normally metabolised into deoxyuridine, and then incorporated into RNA, 5-fluorouracil is converted into 5-fluorodeoxyuridine, which is then converted to fluorodeoxyuridine monophosphate, which binds tightly to thymidilate synthase.

5-FU alone is known to be toxic to cells via two pathways. The first is by its incorporation into RNA as a false nucleotide, which disrupts many cellular processes. The second, more immediate mechanism is inhibition of thymidilate synthase. 5-FU is metabolized in the cell into FdUMP, which then binds tightly to thymidilate synthase. This prevents the normal functioning of this enzyme, which normally forms thymidilate, an essential precursor for dTTP. This leads to the depletion of dTMP and dTTP, and the inhibition of DNA synthesis and repair. RNA incorporation is a longer-duration event, and kinetic studies of cultured cells treated with 5-FU indicate that there is an initial S-phase block (that could be prevented by dThd), indicative of a block of DNA replication, followed by a later period of cell death that could not be blocked by dThd, and not associated with an S-phase block. This is presumed to be

due to the 5-FU incorporation into RNA, and its effect on RNA processing and functioning (27).

5-fluorouracil is a commonly used therapeutic agent for oesophageal cancer, as well as a range of other solid tumours. It is poorly tumour selective, and thus has a wide toxicity against normal tissue including bone marrow, gastrointestinal epithelial cells, skin, and the central nervous system. Due to its poor selectivity it is often administered in combination with other, more selective agents. Side effects include gastrointestinal epithelial ulceration, myelosuppression, dermatologic toxicity, ocular toxicity, neurotoxicity, cardiac toxicity and biliary sclerosis (28).

1.2.3. Other chemotherapeutic agents

Trials using paclitaxel, irinotecan and docetaxel to treat oesophageal cancer have shown some promise, with slightly better responses and decreased toxicity in comparison to the traditional cisplatin/5-fluorouracil regime (12). However many other agents have been tested against oesophageal cancer with no better response than the standard 5-FU/cisplatin treatment, and in some cases, higher toxicity.

A new era in drug development has seen the development of tailored drugs, designed to inhibit specific pathways, such as the kinase inhibitor Gleevec (29). In the future these tailored therapies would allow an ideal approach for treatment of oesophageal cancer patients, with a biopsy of the tumour allowing identification of particular pathways that can be targeted in each patient, rather than a standard treatment (30). However, unlike the critical alterations/mutations identified in leukemia (bcr-abl), the molecular defects associated with the development of oesophageal cancer are poorly understood.

Clearly for the majority of patients the current treatment options are inadequate, and there is a need to identify more effective therapeutic agents. Screening programs using toxicity against oesophageal cancer cell lines are currently the foremost option to identify new candidate drugs for this disease.

1.3. Drug Discovery

1.3.1. Introduction

The drug discovery process uses many different approaches to obtain new chemotherapeutic agents for the treatment of cancer including rational drug design and screening. The most traditional, and most successful approach to date (in terms of number of compounds identified, and taken to the market) is screening. As our understanding of disease processes improves, rational drug design is becoming more prevalent (30).

Compounds identified in conventional screening programs may very well point the direction towards new therapeutic target molecules. Many groups are now in the process of synthesizing analogues of existing drugs in an attempt to make more specific therapies. This combination of the two approaches is more likely to yield results than either approach in isolation, as in the case of the development of 17-AAG (31).

1.3.2. Rational Drug Design

Rational drug design exploits the knowledge of a particular enzyme target (generally based on the analysis of a protein crystal structure with a substrate molecule bound to the active site) in order to design compounds that will interact specifically with the target, inhibiting it specifically. Until very recently our knowledge of disease at a molecular level was insufficient to allow this. However, with new protein modeling techniques, and the elucidation of disease pathways, a number of rationally designed drugs have entered the market.

Unfortunately our understanding of many diseases, cancer in particular, is still too limited to allow this approach in more than a few rare examples. A few molecular changes have been identified in oesophageal tumours that present potential targets for the development of treatments (16). Since many of these changes are shared with other tumours, drugs developed as therapies for other cancers may prove effective against oesophageal cancer, and *vice versa*. These potential targets include EGFR, Her2/Neu, VEGF and COX2 (16). However, preliminary trials using agents targeted for these molecules (developed for other cancers) has not been promising, highlighting the difficulty in translating *in vitro* results into *in vivo* success (16).

However this will still involve characterization of the target, and design and synthesis of potential inhibitors.

1.3.3. Screening

Examples of drugs identified by screening are cyclophosphamide (nitrogen mustard pro-drug), cisplatin, the vinca alkaloids (from the Madagascan rosy periwinkle formerly *Vinca roseus*, now *Catharanthus roseus*), doxorubicin (antitumor product of *Streptomyces peucetius* (var *caesius*)), and Taxol (from the Paciic yew) (32).

There are several approaches to screening for anticancer agents, based on the screening protocol, and the source of the compounds to be screened. The screening platform varies from toxicity testing against an entire animal to testing for inhibition or activation of a single protein, while compounds can be sourced from synthetic libraries, or natural product programs.

1.3.3.1. Single molecule screening

This type of screening platform tests compounds against a specific target – for example the screens for kinase inhibitors that were used to identify Gleevec (29). Compounds identified in this manner need to be carefully validated, first in a cell system to show biological activity consistent with that seen in the molecular screen, and then in animal systems to elucidate pharmacokinetics and dose effects. It is important to bear in mind that the screening target may not be the only, or even the most effectively inhibited target by the compound, leading to unexpected side effects. Another consideration is that, as in the case of rational drug design, the target needs to have been identified, and thus this approach is of limited use in the case of oesophageal cancer.

1.3.3.2. Whole organism screening

Screening of compounds against an entire organism is seldom performed. In the past the brine shrimp assay was frequently used as a measure of toxicity, and is still used in some cases, while sea-urchin egg assays are used to identify antimitotic agents. There is undoubtably a wealth of information that can be obtained from testing compounds in a whole animal system, such as pharmacokinetics, pharmacodynamics and general cytotoxicity. However, the benefits of a whole animal

screen are outweighed by the expense, time and ethical considerations involved, and thus this is better retained as a second or third level validation.

Traditional *in vivo* tumourigenesis assays involve injecting tumour cell lines into immunocompromised mice, waiting until a tumour develops, and then treating the mice with the compound of interest.

The NCI has recently instituted a hollow fibre *in vivo* test for further characterizing positive hits in the 60 cell line screen, which is an improvement over the traditional *in vivo* tumourigenesis assay. In this protocol, various cell lines are plated into thin tubes (similar to dialysis tubing), and then implanted into the peritoneal cavity of mice. The compound of interest is then administered at various doses, and at the end of the assay the tubes are removed, and the cell number remaining in the tubes is assayed using a conventional MTT (3-(4,5-dimethylthiazol-2-yl)-2,5-diphenyltetrazolium bromide) reagent. This allows testing of factors that aren't compensated for in cell culture including delivery (blood stream, solubility), toxicity to organ systems, pharmacological action (activation/inactivation by metabolic enzymes, detoxification kinetics) and side effects (33).

1.3.3.3. Cell line screening

The most frequently used screening platform for anti-cancer agents is a cell line screen. This is typified by the NCI 60 cell line screen which has been used for high throughput screening of natural and synthetic compounds and has been employed by a large number of research groups to identify potential lead compounds for cancer chemotherapy (34). In the initial years (1960-1982), the NCI screen involved assaying for activity against the mouse leukemia cell lines L1210 and P388. This system had several limitations – first, both cell lines were leukemia in source, which meant that any agents inactive against leukemia, but potentially active against solid tumours would be missed. Secondly, the assay system was murine in nature, and thus any compounds targeting human-specific pathways would also be overlooked. However the assay was a good indicator of cytotoxicity, and many useful drugs were identified, most notably paclitaxel (Taxol) (35). In 1985, the NCI started a new program screening extracts against a wide range of human cell lines, covering leukemia, colon, skin, breast, ovary, brain, kidney and prostate. This allows the identification of agents active against a range of different cancers, as well as yielding patterns of sensitivity/resistance of the different cell lines, that will give clues as to the

mechanism of action of a certain compound when compared to the patterns obtained from compounds with known mechanisms (34;36).

Screening against cell lines has advantages over single molecule screens as factors such as the metabolism of the compound within the cell can be accounted for. There is also the advantage that a specific target does not have to have been identified for a particular cancer in order to identify agents that are active against that cancer.

This approach is also favourable in comparison to screening in a whole animal system. However, compounds identified in a cell line screening system still need to be verified in a whole animal model, since compounds that are active against a cell line may be metabolized so rapidly in a whole organism that they would not be effective, and potential side effects such as nephro- or cardio-toxicity would not be detected until the compound is administered to a whole organism (33).

An ideal chemotherapeutic agent would kill only cancer cells, and have little or no effect on normal cells. However, most chemotherapies cause severe side effects owing to the fact that they are not specific against cancer cells, and so normal cells die during the treatment as well. Thus there is an important distinction between cytotoxic compounds – that will kill all cells indiscriminately, and targeted therapies, that exploit some feature of the cancer cells to selectively kill only the cancer cells.

The identification of differentially active compounds is hampered by the lack of normal control cell lines. Most normal human cells are extremely hard to culture, and only modification of normal cells (for example with telomerase or viral proteins) allows them to propagate in culture. However, the modifications made that allow the cells to divide in culture alter their behaviour from normal towards a cancerous phenotype. Thus matching a tumour type with a corresponding normal to determine differential activity is extremely difficult.

1.4. Natural Products

1.4.1. Introduction

The source of compounds to be tested for activity in various screening programs varies. Many companies have large libraries of synthetic compounds for sale, and for the sake of sheer volume this can be a good option. However, chemical synthesis cannot match the complexity of natural products (representing the end point of millions of years of chemical evolution). Thus natural products (secondary metabolites) still remain an extremely promising reservoir of chemotherapeutic lead compounds, with over 60% of currently used chemotherapeutic agents derived or developed from natural sources (37;38).

The diversity of chemical structures found in nature is the key reason behind the popularity, and effectiveness of natural products as chemotherapeutic agents. Millions of years of evolution have supplied chemical diversity that cannot be matched by combinatorial chemical libraries.

1.4.2. Current natural product based anti-cancer agents

The predominant source of natural products are plants and microorganisms. In the last 30 years, with the advent of better diving equipment, the potential of the marine environment as a source of natural products has begun to be tapped (39).

Taxol or docetaxel is probably one of the most recognised chemotherapeutic agents from a natural source. In addition, the vinca alkaloids (most notably vincristine and vinblastine), isolated from the Madagascan rosy periwinkle (formerly *Vinca roseus*, now *Catharanthus roseus*) are another example of a plant-derived natural product used in cancer therapy. Their main mechanism of action is inhibition of microtubule assembly, causing tubulin to form self-aggregates (40). Other sources of natural products are microorganisms. The most well known examples from this group are probably the anthracyclines and bleomycins (41).

Taxol, from the bark of the Pacific Yew tree has presented a model for the development of a natural product from identification, through drug trials and to the clinic (35). The development process of Taxol highlights many of the problems experienced by scientists working with natural compounds – identifying the active

compound in extracts of the yew tree took several years. Following the successful identification of Taxol, supply became a problem. With an extremely complex structure, synthesis in the early years was close to impossible, and promised to be extremely expensive. Supply from the trees themselves was limited, as harvesting the bark in most cases destroyed the tree, and for the initial trials a great number of trees were destroyed for a small quantity of drug. However, a few years later it was found that a semi-synthetic analogue (docetaxel) had similar activity, and could be synthesized from the leaves of the yew tree, allowing sustainable harvesting (35).

1.4.3. Marine natural products

The marine environment is an extremely promising area for the identification of novel, biologically active compounds. More than 70% of the world's surface is covered by sea, and the biodiversity present in coastal waters is often many times higher than that found on land. One estimate is that the marine biodiversity more than equals that of Amazonian rain forests (41). This biodiversity is accompanied by an equal chemical diversity, and, to date, more than 14000 unique compounds have been identified from marine organisms (41).

Many marine organisms (invertebrates, algae and micro-organisms) produce natural products as a chemical defence against predation or in a response to inter-species competition for limited resources (e.g. space on a reef or nutrients) (42). Interestingly, the isolation and identification of marine natural products by chemists, working in tandem with pharmacologists, over the last three decades has provided important lead compounds for the pharmaceutical industry, especially in the field of new anti-cancer drug discovery (43-45). Marine biota are a unique reservoir of biomolecular diversity, not only because of the large number of species present in the oceans but also because the marine environment presents very different physiological and ecological challenges compared to those experienced by terrestrial species (46). As a consequence of the differences between terrestrial and marine habitats the initial expectation that marine organisms utilize unique biosynthetic pathways, or exploit variations on established biosynthetic pathways, to biosynthesize structurally unusual natural products has been validated by the complexity and novelty of the plethora of marine natural products isolated over the last thirty years (42;47).

Blunt *et al.* 2006 have recently shown that sponges closely followed by micro-organisms, coelenterates and tunicates (ascidians) are the primary source of bioactive metabolites in the marine environment. Interestingly, anti-cancer activity dominates the bioactivity reported for the secondary metabolites isolated from all four of these phyla and there are currently 21 sponge and tunicate metabolites in pre-clinical or clinical trials as potential anti-cancer treatments (Figure 1.7.) (46).

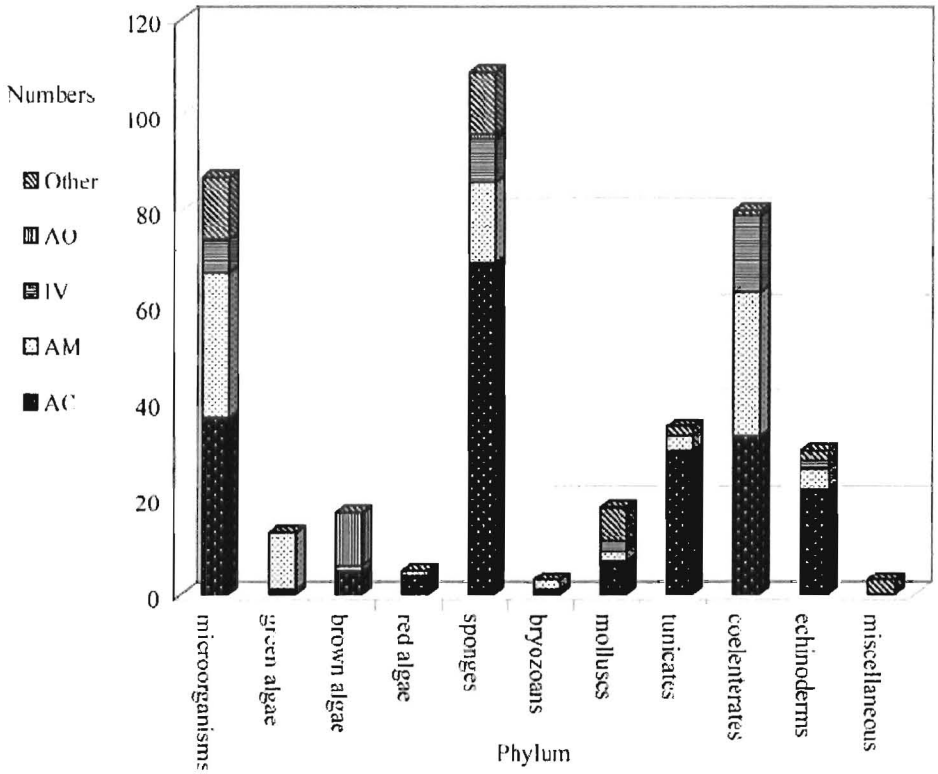

Figure 1.7. Bioactive marine compounds.

The activity of marine compounds identified in 2003 from various phyla. Activity includes antimicrobial (**AM**), antioxidant (**AO**), *in vivo* (**IV**) – including assays against brine shrimp and sea urchin eggs, anticancer (**AC**) including a range of assays including cytotoxicity, antimitotic, kinase and DNA binding assays, and other activity (**Other**) including antiviral, antifouling, feeding deterrant and ion channel assays. (Figure from Blunt *et al.* (47))

However, despite the promising results obtained in preliminary screens, very few marine compounds have reached the market, or even clinical trials, due to several problems. Chief among these is the issue of supply. The source organism may be extremely sparse, and yield of the active compound is often low (46;48). An obvious solution to this problem is mariculture, but many marine organisms grow slowly, and thus this approach would not be feasible for production of the large quantities of

compound that would be needed for clinical trials and later commercialisation. Recent identification of symbiotic organisms as the source of several bioactive compounds offers the option of fermentation to produce active compounds. Many marine organisms are filter feeders, and thus concentrate large numbers of bacteria. Recent studies have shown a huge genetic diversity present in the sea – especially the deep sea – this presents a potential source of new microorganisms that may in turn have huge numbers of unique compounds (49). However, identification of the source microorganisms, and optimization of culture conditions to produce the compound of interest present their own challenges.

Despite these challenges, more compounds of marine origin are entering clinical trials, with a total of 44 marine compounds in clinical trials in 2004 (38). At present Ziconotide, a conotoxin identified from cone snail venom, is the only licenced marine compound (for the treatment of chronic pain), but many other compounds are in trials, with 13 new compounds entering trials in the last 6 years (2000 – 2005), all for cancer treatment (50), and 21 sponge and tunicate metabolites currently in pre-clinical or clinical trials as potential anti-cancer treatments (46).

Didemnin B was the first marine-sourced compound to enter clinical trials. It is a cyclic depsipeptide isolated from the tunicate *Tridemnum solidum*, and acts by inhibiting protein synthesis and introducing a cell cycle block in G1 phase. However, severe neuromuscular toxicity was observed, and trials were discontinued. More recently a related depsipeptide (aplidine) has been evaluated, and shows activity against a range of tumour types, and does not display as severe side effects (51).

One of the most promising drug candidates from a marine organism is ET-743. This is a member of a class of compounds called ecteinascidins, all isolated from the tunicate *Ecteinascidia turbinate*. ET-743 has activity against most tumour cell lines in the nanomolar and sub-nanomolar ranges. Activity is related to its ability to selectively alkylate guanine residues in the minor groove, and also interact with DNA-binding proteins, and this compound has been tested against a range of tumours (52-54).

Another highly promising group of marine compounds are the dolostatins. These are peptidic compounds which have cytotoxic activity. The most active of the group – dolosatin 10 has entered clinical trials, but has failed to show significant activity, despite high *in vitro* activity. Currently research is focusing on identifying analogues

that may have higher activity *in vivo*, and two of these – soblidotin and synthadotin – are also in clinical trials (50).

Regardless of the source of their material, researchers developing novel chemotherapeutic agents to treat cancer have a particular interest in understanding the mechanism of action of their active agents. This understanding can facilitate the design of more effective agents, and the knowledge of a molecular target can assist the clinical trial process.

1.5. General principles of chemotherapy

Over the years anti-cancer agents have been classed into several major categories, based on their mechanism of action. These include tubulin interactive antimitotics, DNA damaging agents, antimetabolites, alkylating agents, topoisomerase inhibitors and DNA binders. 5-fluorouracil, discussed above, is a member of the antimetabolite class of anti-cancer agents. Discussed briefly below are the mechanisms of action of a few of these classes, with examples of these agents.

1.5.1. Tubulin and actin inhibitors

Tubulin and actin are the main cytoskeletal proteins in the cell, and both play important roles in cellular structure, motility and division. Tubulin plays a particularly important role in mitosis, forming the mitotic spindle along which the condensed chromosomes migrate to opposite sides of the cell prior to cell division (55).

Both tubulin and actin are constantly remodeled. Both molecules form polymeric chains, that are continually restructured by the addition or removal of more tubulin or actin subunits. Molecules that inhibit either the polymerization, or the depolymerisation of tubulin generally cause cell cycle arrest in G2, at the metaphase/anaphase transition (40).

The vinca alkaloids were one of the first classes of compounds found to interact with tubulin. Taxol was also discovered to inhibit tubulin dynamics, but stabilizes tubulin in the polymerized form rather than the depolymerised form. Other tubulin-interacting agents include colchicine, nocodazole, cryptophycins, estramustine. A more recently discovered compound is the marine natural product discodermolide (56).

While the majority of antitumor molecules targeting the cytoskeleton interact with tubulin, actin also presents an attractive therapeutic target. Actin binding molecules include the cytochalasins, which were the first group of actin inhibiting compounds described. Many actin-inhibiting agents are being isolated from the marine environment, including the latrunculins (macrolides) (40), jasplakinolide (a cyclodepsipeptide) (57), and swinholide (a dilactone macrolide) (58).

1.5.2. DNA damaging agents

DNA damage is an event that on first examination would not seem to be selective against cancer cells. However, damage to DNA can have far more serious effects on cancer cells than on normal cells due to changes in cellular processes such as DNA repair, increased cycling, and increased transcription.

Many chemotherapeutic agents have been shown to interact with DNA, and there are many kinds of interactions that can cause cellular effects. Some agents simply bind to DNA, blocking the access of various proteins to DNA, thus preventing DNA transcription, unwinding by topoisomerases, and repair. Other agents directly modify DNA, causing mutations and damage. Types of alterations include alkylation, and crosslinking (59).

The earliest DNA targeting molecules were also the earliest anti-cancer agents – in World War 2, an accident that involved exposure to nitrogen mustard gas in oil-based solution led to a large number of soldiers exposed to this mixture developing lymphotoxic symptoms. This was later established to be due to the DNA alkylating activity of the nitrogen mustard gas, with the feature of targeting tissues with high proliferative indexes. This suggested a possible method of targeting rapidly dividing tumours, and was used to successfully treat lymphomas (59).

Other DNA interacting agents include cisplatin (discussed in detail above), doxorubicin, mitomycin C and ET743.

Some of the more recent agents targeting DNA are far more specific in their activity, and are a direct consequence of our increased understanding of DNA structure and function. The structure of DNA is far more complex than a simple double-stranded helix, and the secondary structures formed by DNA serve as highly selective targets for designed DNA interactive agents (60).

1.5.3. Reactive oxygen species production

Reactive oxygen species (ROS) are produced by a range of chemicals, exposure to radiation (UV etc.), as well as during normal cellular metabolism. ROS are a form of free radicals, and includes hydrogen peroxide, superoxide radical, hydroxyl radicals, and singlet oxygen, among others. There are also reactive nitrogen species and

reactive sulphur species. All free radicals include one or more unpaired electrons (61), and thus can react with biological molecules such as DNA, proteins and lipids. They can cause extensive damage to a cell, and cellular antioxidants such as superoxide dismutase (SOD) and catalase as well as the glutathione and thioredoxin systems exist specifically to deal with this stress.

ROS production has been shown to be a factor in the activity of a variety of chemotherapeutic agents, including doxorubicin (62;63), fenretinide (64) and paclitaxel (65). ROS generation by chemotherapeutic agents is a good strategy since many tumours are already under increased oxidative stress, with many tumours having been shown to have both lower levels of antioxidant enzymes and increased levels of reactive oxygen species (66). Thus a slight increase in ROS, that will be tolerated by normal cells (with the exception of some tissues that are also under oxidative stress), will have far greater effects on cancer cells and may lead to cell death (67).

ROS production by chemotherapeutic agents can also be the cause of side effects – for example, the cardiotoxicity associated with doxorubicin has been linked to ROS damage to the cardiac endothelium, a location which has low levels of antioxidant enzymes (68).

1.6. Cell death

The ultimate aim of any chemotherapy is to preferentially kill cancer cells. However, the consequences of cell death of a large number of cells in the body may be detrimental, especially if cell death is via the necrotic pathway. Necrotic cell death leads to inflammation and tissue injury, and thus the more desirable type of cell death for chemotherapeutic agents to cause is apoptosis.

1.6.1. Apoptosis

Apoptosis is also known as programmed cell death, reflecting the orderly chain of events that occurs leading to cell death. Apoptotis differs markedly to necrosis, where dying cells "explode", releasing cell contents into the surrounding environment. Apoptotic cell death neatly breaks down the constituents of the cell, and packages them into discreet apoptotic bodies, which are then phagocytosed (69;70).

The process of apoptosis is carried out by a group of caspases (cysteine proteases), and is tightly controlled. Several pathways can be activated leading to apoptosis, but the two most well characterized are the death receptor mediated pathway and the mitochondrial pathway (Figure 1.8.).

The death receptor mediated pathway is activated when a ligand for the death receptor binds. This then causes cleavage of caspase 8, which can then cleave (and activate) the effector caspase 3. An example of a death receptor ligand is TNFα (tumour necrosis factor α) which binds to the TNF receptor (TNFR) (71).

A key event in the mitochondrial pathway is the permeabilisation of the mitochondrial membrane, triggered by an alteration in the levels of the pro and antiapoptotic BCL2 molecules. This releases a number of proapoptotic factors into the cytoplasm including cytochrome c, which binds and alters the conformation of APAF1 (apoptotic protease activating factor 1). APAF1 binds and cleaves procaspase 9, and activated caspase 9 then activates caspase 3 (70).

Both the death receptor pathway and the mitochondrial pathway ultimately result in the activation of caspase 3, which plays an important role in the disassembly of the cell (71).

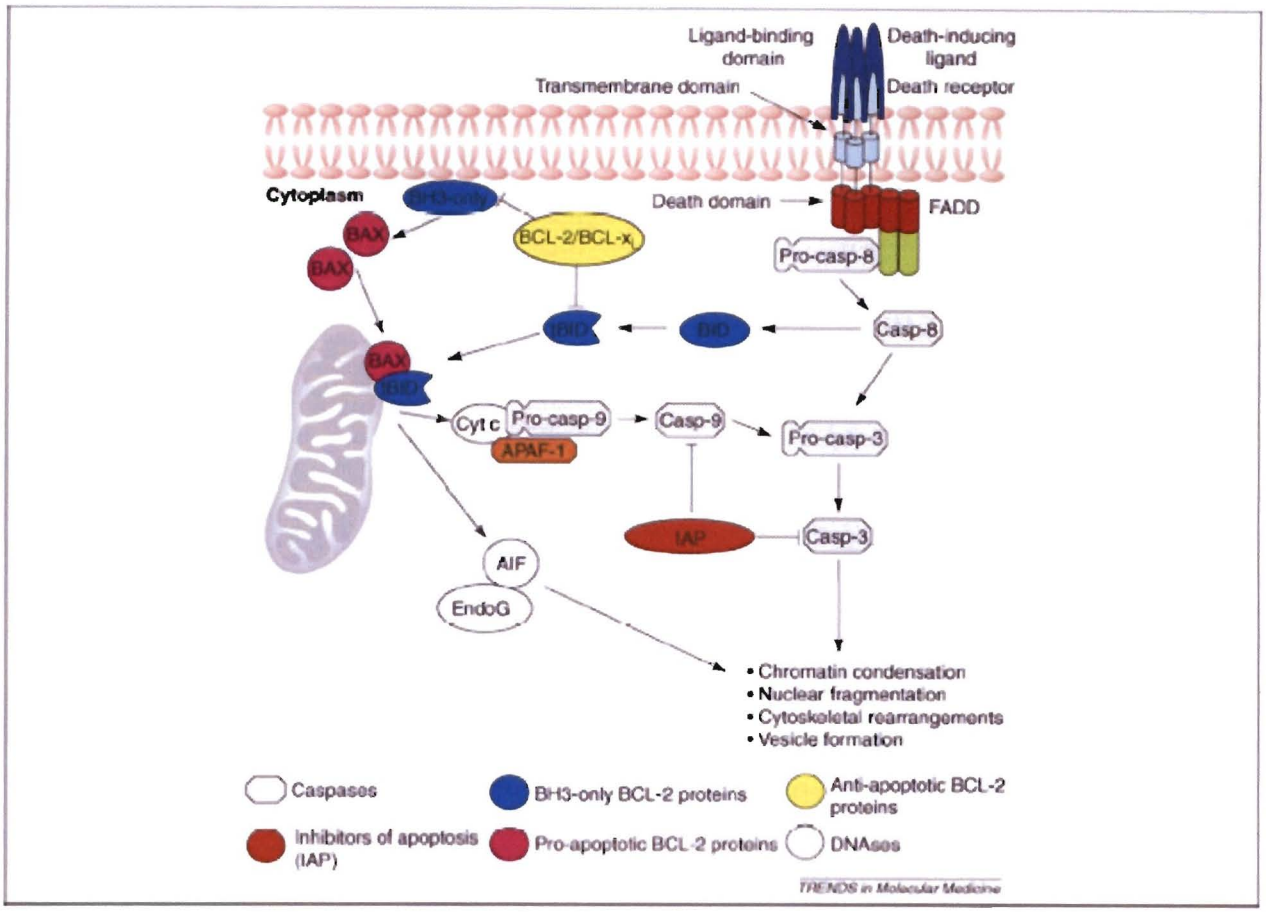

Figure 1.8. Apoptosis pathways.

Apoptosis can occur following signalling from either the death receptors or the mitochondria. The mitochondrial pathway involves release from the mitochondria of cytochrome c, following a complex interplay of pro- and –anti-apoptotic stimuli. Cytochrome c then binds APAF1, which leads to the cleavage of procaspase-9 to caspase-9, which in turn activates caspase-3. The death-receptor pathway involves binding of a death receptor ligand to the death receptor, which leads to activation of caspase-8. This in turn leads to activation of caspase-3. Caspase-3 is an effector caspase which mediates many of the cellular events observed in apoptosis. (Figure from Bremer *et al.* (71))

1.6.2. Necrosis

Necrosis is a form of cell death where cells swell, and eventually lyse. Necrosis can be caused by a variety of stimuli including hypoxia, infection with microorganisms and immune responses. Necrosis plays an important role in preventing reproduction of pathogens, and recruiting an immune response (72).

Evidence suggests that necrosis will also occur under conditions that would normally result in apoptosis if the cell has insufficient energy (ATP). Thus necrosis presents an alternative pathway to allow cell death.

1.6.3. Autophagy

Autophagy was originally described as a method of cell survival under starvation conditions, and is literally a process of cell autocannibalism, where autophagic vacuoles form in the cell to digest cellular components, releasing essential nutrients for cellular processes (70;73). As a starvation response, autophagy is only seen when cells are stressed, and thus there is great debate as to whether this is a survival pathway or a death pathway in mammalian cells. Theoretically, if nutrients are returned to cells undergoing autophagy, they should recover, but if starvation conditions continue, autophagy will eventually lead to death. Some evidence suggests that autophagy is another alternative to apoptosis under low energy conditions (74).

1.7. Project plan

There is obviously a need for new chemotherapeutic agents to treat oesophageal cancer. In this project we attempted to identify novel compounds that might serve as new drug leads for the treatment of this disease.

The objectives of this study were as follows :

1. Establish a screening program, similar in approach to the NCI 60-cell line screen, using oesophageal cancer cell lines to identify compounds that may be of use as chemotherapeutic agents for oesophageal cancer.

2. Screen marine extracts, and supply cytotoxicity data to assist with activity-directed fractionation of active compounds.

3. Identify novel compounds active against oesophageal cancer, and assess their mechanism of action.

CHAPTER 2

SCREENING OF MARINE SAMPLES FROM SOUTHERN AFRICAN WATERS

2.1. Introduction

As outlined in Chapter 1, the marine environment holds great promise as a source of novel natural products (secondary metabolites). In the southern African context the approximately 3000 km long coastline, stretching from Namibia in the west to southern Mozambique in the east, is inhabited by a rich diversity of natural product producing marine organisms (including invertebrates, algae, and marine microorganisms). This rich biodiversity stems from the three different biogeographical zones which characterize this stretch of coastline – the cool temperate west coast, the warm temperate southeast coast, and the subtropical east coast. (75). Each of these bio-geographical zones sustains distinct populations of marine flora and fauna and of the over 10 000 species of marine organisms recorded off the southern African coast, a large proportion (*ca* 12 %) are reported to be endemic to the region (75;76). Associated with high levels of marine invertebrate endemism are concomitant high levels of novel secondary metabolite chemical structural diversity which in turn suggests a high possibility of novel bioactivity (including biomedical potential) (77). The marine life of southern Africa and its associated natural product diversity therefore represents an as yet relatively untapped source of bioactive biomolecules.

This potential was recognized over three decades ago in a South African government report, entitled 'Drugs from the Sea', which stated, "very little attention has yet been paid in South Africa to the recovery of drugs from the sea. This field offers exciting and rewarding challenges to South African scientists. Once research brings down the unit cost, the sea may offer a vast potential for the production of drugs for South Africa." (78). Prior to this report, research into marine chemistry in South Africa had been limited to marine phospholipids, long chain fatty acids and alcohols, and marine algal polysaccharides (79-81).

In the 34 years since this report only limited South African research has been carried out to discover marine pharmaceuticals from South African organisms. However, since the early 1990's, the groups working on South African marine chemistry – Yoel

Kashman (in collaboration with Mike Schleyer at Durban's Oceanographic Research Institute) and Mike Davies-Coleman (working with John Faulkner of Scripps Institute of Oceanography, and Pat Colin of the Coral Reef Research Foundation) have driven exploration of South Africa's marine chemistry and biodiversity (82). The work presented in this chapter explores the feasibility of screening South African marine organisms to identify compounds of potential use against oesophageal cancer.

2.1.1. Marine compounds

As part of our program to identify novel compounds with potential activity against oesophageal cancer, we established a collaboration with the Chemistry Department at Rhodes University. This gave us access to a wide variety of marine extracts and compounds, as well as the expertise of the chemists working to identify novel compounds from marine organisms. Samples obtained from Rhodes include crude extracts from marine organisms, fractions from various purification and separation procedures, and pure compounds. At all stages, fractionation, purification and chemical characterization were carried out by the chemists at Rhodes University.

2.1.2. Overall strategy

The flow chart in Figure 2.1. provides an overview of the overall screening strategy followed. Marine organisms were collected from a number of locations (Figure 2.4. and Figure 2.5.). In most cases collection was carried out by SCUBA, except at Marion Island where samples were collected by dredging. A portion of each organism was set aside for identification by marine biologists (Dr. Toufiek Samaai, CSIR, Durban, and Dr. Shirley Parker-Nance, Nelson Mandela Metropolitan University, Port Elizabeth), while a second portion was retained as a voucher specimen. A large portion of each sample was stored at -20°C for later use, while a small amount was extracted into methanol and then freeze-dried to yield a crude extract. These extracts were screened for activity against the oesophageal cancer cell line WHCO1 as outlined in Materials and Methods, and active extracts identified in this way underwent an iterative bioassay guided fractionation process until pure compounds were obtained. At this stage the relative activity of the pure compounds was assessed by IC_{50} determination using the MTT assay. A group of related compounds were identified for further characterization and are discussed in Chapter 3. This chapter is based on the screening of marine extracts, bioassay-guided fractionation and IC_{50} determination of pure compounds identified during this collaboration. To

make the information more accessible to the reader, the results in this section have been presented in the context of the identity of the source organisms (identified by marine biologists) and the chemical fractionation and structural identification of the natural compounds (carried out by chemists at Rhodes University).

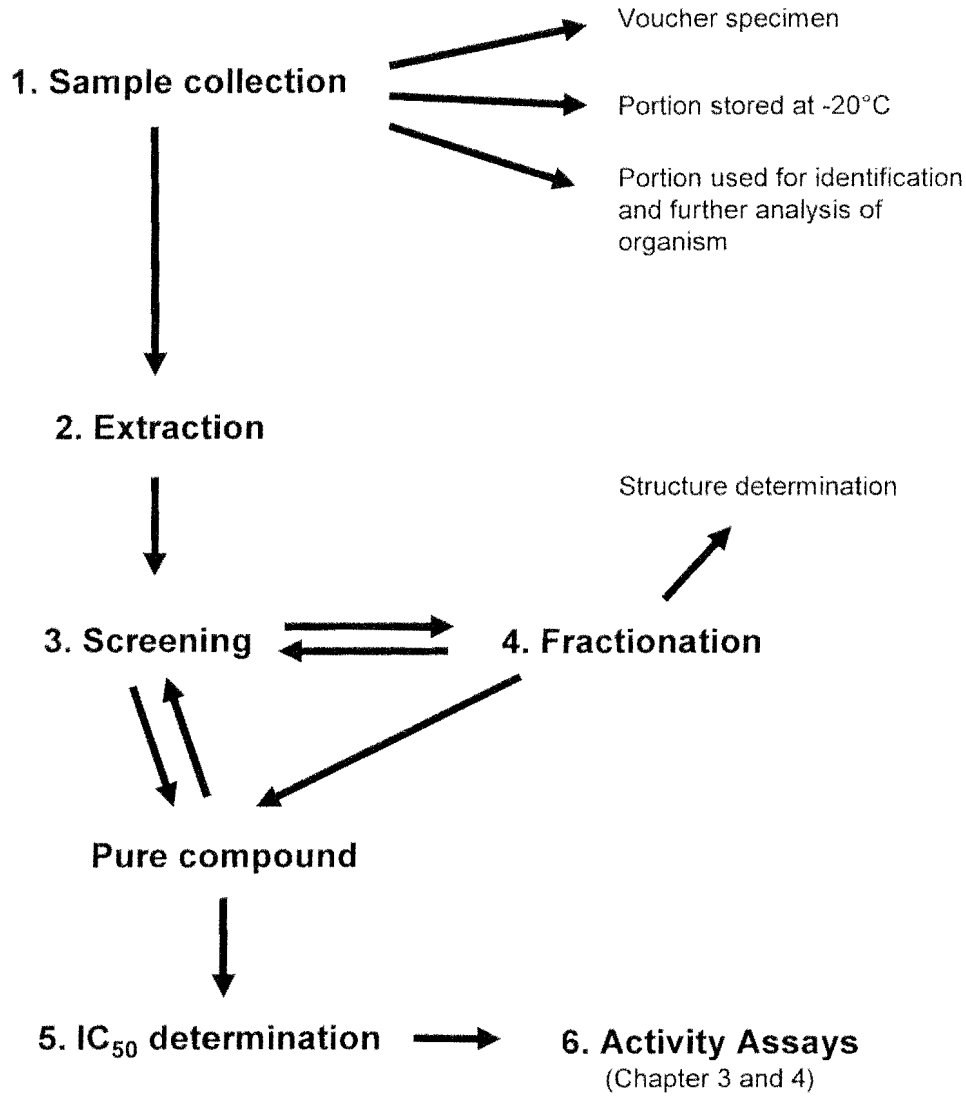

Figure 2.1. Overall Strategy for screening, bio-assay guided fractionation and activity determination.

All samples were processed in this manner. The sample was divided into 4 parts. The majority of each sample was stored at -20°C for later use if necessary. A voucher specimen and a portion for identification were retained by the marine biologists, while a final portion was extracted into methanol, to give a crude extract for screening. Extracts identified as active in our screening assay were fractionated, and each resulting fraction was tested for activity in the same screening assay, giving rise to an iterative bioassay guided fractionation process that eventually yielded pure compounds. The relative activity of these pure compounds was determined as an IC_{50} value derived from a dose response curve using MTT as an end point. A group of related compounds was identified for further study to determine their mode of action, and are discussed in detail in Chapters 3 and 4.

2.1.3. Screening

To measure the activity of extracts and compounds in this study, we determined the toxicity of these samples against an oesophageal cancer cell line derived from a South African patient (83). This was carried out using an assay similar in format to that of the NCI 60 cell line screen (84). Initial screening was performed using the WHCO1 oesophageal cancer cell line. This cell line was derived from a biopsy of an oesophageal squamous cell carcinoma from a South African patient (83), and has been shown to display characteristics typical of an oesophageal cancer (83;85-87), making it a useful first line screen.

The 60 cell line screen conducted by the NCI was established in 1990, and performs high-throughput screening against a panel of 60 cancer cell lines using a sulforhodamine B assay to assess the survival of cells after exposure to 5 concentrations of each test reagent (84). Researchers can submit compounds for testing by an online application, which is then assessed, and if sufficient evidence is supplied that the compound is novel, and may provide good results, the compound is tested.

Due to the logistical considerations of using the NCI 60 cell line screen, it was thus convenient to set up a similar assay in our laboratory. This allowed us to modify the approach for our particular circumstances, to allow screening not only of compounds, but also of extracts, allowing activity-directed fractionation. (The NCI assay generally only accepts pure compounds of known structure for their screen.) The rapid turnaround of a local screen enables faster bioassay-guided fractionation, and costs (and logistical considerations) are reduced as samples do not need to be processed internationally.

The NCI test each compound/extract at five concentrations, and assay for remaining cells using a sulforhodamine B assay which is a protein stain. The initial assay in our study quantitates the cells surviving after treatment with 3 concentrations of each sample by staining with crystal violet (also a protein stain) (88).

The NCI initially test compounds against a small range of cell lines, and then proceed to test compounds displaying activity against a panel of 60 cell lines. Our assay differs in the number and type of cell lines used. While the NCI is concerned with identifying active compounds for a wide range of cancers, and thus assays against

an initial panel of 3 cancer cell lines, and then the full panel of 60 cancer cell lines, we are interested in the predominant forms of cancer in South Africa. Currently our assay uses an oesophageal carcinoma cell line from a South African patient, which can easily be expanded to include a cervical cancer cell line. Since oesophageal cancer and cervical cancer are the main causes of cancer-related death among black South African males and females respectively, our program will hopefully provide a drug lead for these cancers.

An advantage of using a limited number of cell lines in our screening system is the volume of material required. NCI guidelines for screening are for 10-15mg of pure compound, (though in the case of limited supply they will accept 5mg). However, we have routinely tested samples with masses of 1mg or less. The small volumes required by our assay allows the chemists working on the project to retain a larger volume for further purification during activity-directed fractionation, which in turn increases the chances of identifying the active compound.

The extracts from a wide variety of marine organisms were tested. These include sponges, ascidians, microorganisms and soft corals. The locations for the collection of these organisms varied from Marion Island, Algoa Bay, Tsitsikamma, Cape Town, Aliwal Shoal and Mozambique (Figure 2.4. and Figure 2.9.).

2.1.4. Activity-directed fractionation

Crude extracts found to be active in our screening program were selected for activity-directed fractionation. These extracts are subjected to a variety of separation techniques which were all performed in the Chemistry Department at Rhodes University, and the resulting fractions then retested for activity in our assay. This process allows us to identify the active compound(s) in an extract through an iterative process between the collaborating laboratories at UCT and Rhodes University.

2.1.5. IC_{50} determination

Once a pure active compound has been isolated, it is possible to more accurately quantitate the activity using the MTT assay to perform a dose response curve, and measure IC_{50} values. It is then possible to compare the activity of different compounds against the same cell line, or the same compound against different cell lines.

An extremely desirable characteristic of a chemotherapeutic agent is differential activity, with high activity against cancer cells, and low activity against normal cells. The control cell line used during this study (to determine if any of the compounds tested displayed reduced activity against normal cells compared to tumour cells) was an epithelial cell line derived from a non-malignant breast tumour (MCF12A; ATCC# CRL10783) (89). This is not the most appropriate control since it is neither oesophageal nor completely normal. However, as mentioned in Chapter 1, it is very difficult to maintain normal oesophageal epithelial cells in culture, and very few model systems are available. Consequently the results obtained from testing compounds against the MCF12A cell line may provide an initial indication of specificity.

If a group of compounds is structurally related, comparing the activity of those compounds against one cell line may allow us to form a hypothesis regarding structure-activity relationships. We have made some conclusions of this nature with the group of quinone/hydroquinone structures discussed in Chapter 3, as well as several groups of compounds discussed below. These observations may help in the rational design of more effective chemotherapeutic agents.

The activities of the marine natural products were compared to cisplatin, a commonly used chemotherapeutic agent for oesophageal cancer, that displayed an IC_{50} of 13 μM against WHCO1 cells (90).

2.2. Results and Discussion

2.2.1. Preliminary Screening

A total of 479 samples were screened. Of these 175 were crude extracts, 278 were fractions from activity-directed fractionation steps, and 26 were pure compounds.

Samples were tested against WHCO1 cells at 3 different concentrations and the number of cells remaining after 48 hours of treatment was assessed using the crystal violet assay (88). All samples were resuspended at 30mg/ml (using mass/volume rather than molarity since most samples were extracts rather than pure compounds), then tested at final concentrations of 50, 10 and 1 µg/ml with control (untreated wells) receiving equal quantities of solvent (DMSO). Plates were processed using crystal violet staining, which is a protein stain – the number of cells remaining after treatment stain blue, and when the stain is solubilised in acetic acid, the absorbance gives a reading proportional to the number of remaining cells.

This method is not particularly accurate, and there are several shortcomings. False positives may occur, where a compound causes cells to detach, but does not cause cell death. Since the protocol involves discarding culture medium, floating cells are discarded and an artificially low reading is obtained. In this case samples which do not cause cell death will test positive. False negatives may also occur, where a compound or extract precipitates and contributes to the absorbance reading, thus giving an artificially elevated reading, masking the true cytotoxicity of the sample. Both false negatives and positives are controlled for by observing cells prior to processing, and correlating the readings with the observations.

Samples were scored according to the proportion of cells remaining at each concentration of treatment, compared to untreated. The scoring system ranked samples on a scale from 0 (no activity) to 3 (high activity), as illustrated in Figure. 2.2. and described in Materials and Methods.

Of the 175 extracts tested, 54% (95/175) were inactive, 38% (67/175) had low to medium activity, and 7.4% (13/175) had high activity. Five of the active extracts were selected for activity-directed fractionation.

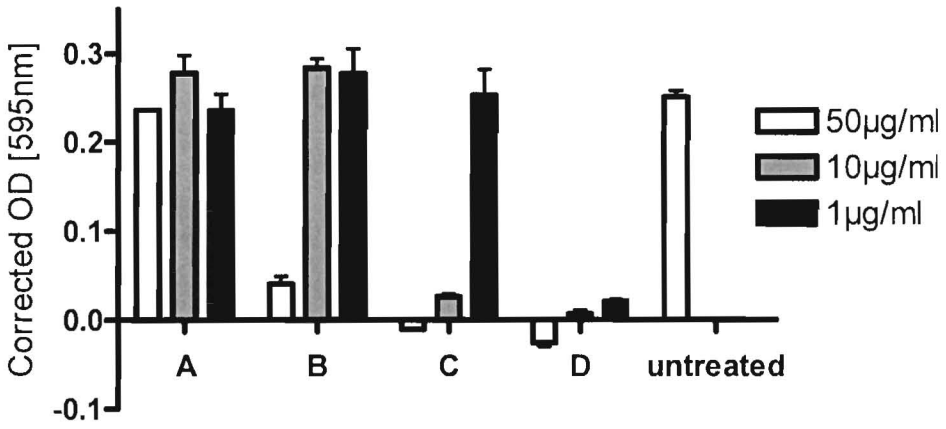

Figure 2.2. Example of screening data against the human oesophageal cancer cell line WHCO1.

Sample A, with no activity would be scored 0, Sample B, which decreased the number of cells to below 10% of untreated at only the highest concentration tested, would be scored 1. Sample C reduced cell number to below 10% at the highest and medium concentrations, but not the lowest concentration, and would be scored 2, while sample D, which reduced cell number to below 10% of untreated at all concentrations would be scored 3.

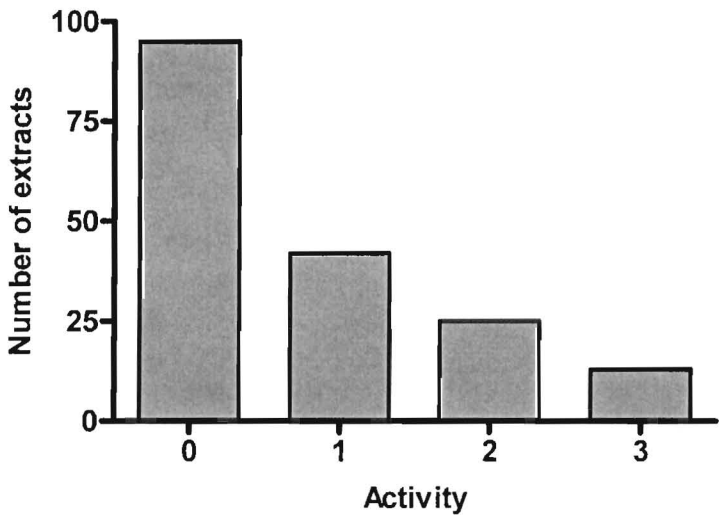

Figure 2.3. Activity scores for all extracts screened against WHCO1.

Slightly over half of all extracts tested had no activity (Score = 0), one quarter had low activity (Score = 1), 14% had moderate activity (score = 2), and 7.5% had high activity (score = 3).

2.2.1.1. Locations

The southern African coast spans three distinct biogeographical zones (Figure. 2.4.). The three regions are firstly the cool temperate West Coast north west of Cape Point (A), which is cooled by the Benguela current. Upwellings of nutrient rich water along this coast result in high biomass, though less biodiversity amongst natural product producing marine invertebrates like sponges. Between Cape Point (A) and East London (D) is a warm temperate zone, in which the water temperature, although generally warmer than the West Coast, is cooler than the East Coast. The Agulhas Bank forms a wide continental shelf here, and the shallow, temperate waters hold great biodiversity in terms of marine invertebrates. North of East London (D) is the warm, sub-tropical coastal area, and north of Durban (E) coral reefs (relatively common in warm tropical seas) are found. Both regions (D and E) support many non-endemic circumtropical marine invertebrate species.

The collections of marine invertebrates discussed in this thesis were made in the diverse, temperate zone (Tsitsikamma (B) and Algoa Bay (C)), the tropical zone (Aliwal Shoal (F) and Mozambique (G)) and Marion Island, a sub Antarctic island in southern African waters, over a ten year period (1994-2004) (Figure 2.5).

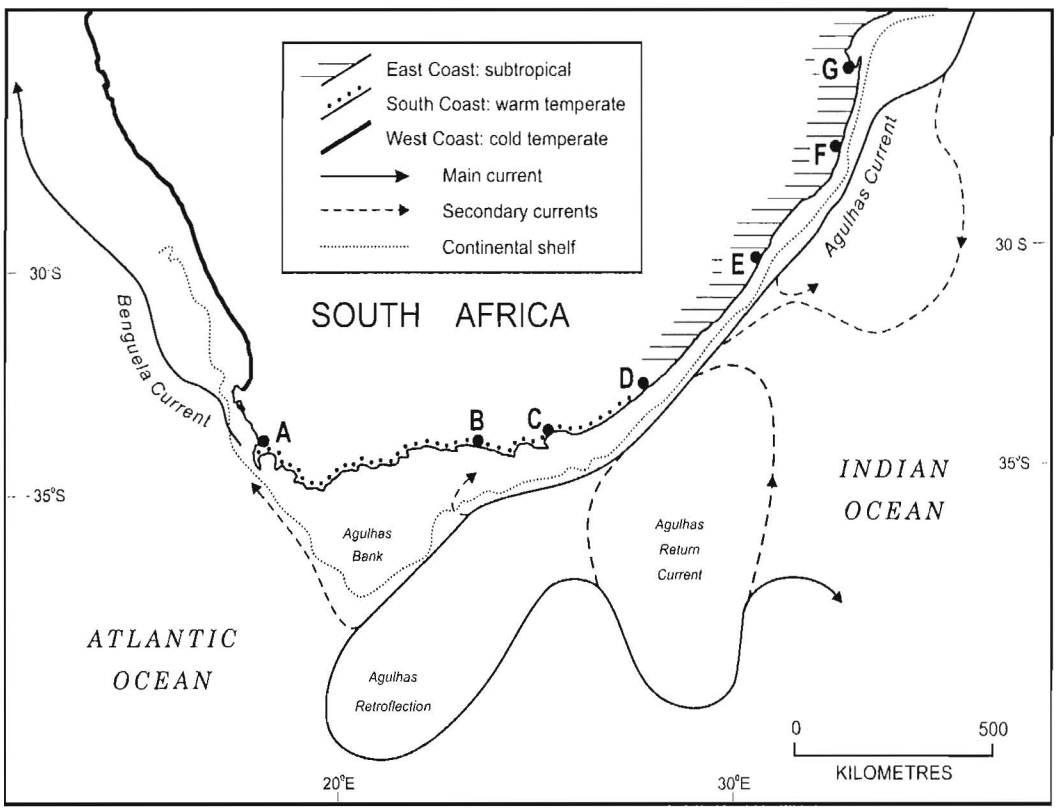

Figure 2.4. Biogeographical zones of the Southern African coastline, and collection sites. Thirteen samples were collected at Tsitsikamma (B), and 64 from Algoa Bay (C), both of which lie in the warm temperate zone (from Cape Point (A) to East London (D)). Thirty-nine samples were collected on the Aliwal Shoal (F), and 21 samples from Mozambique (G). (Image reproduced with permission from Davies-Coleman *et al* (82))

2.2.1.1.1. Tsitsikamma

The Tsitsikamma Marine Reserve and National Park is situated on the southern coast of South Africa in the diverse, temperate zone. As a protected area the marine life is relatively undisturbed. The collection took place in April 1995 and yielded a total of 13 extracts – 8 from sponges, 3 from ascidians and 2 from soft corals. The activity from these extracts was limited, with only 2 samples showing any activity at all, and that activity was the lowest category. The two samples with activity were isolated from a soft coral and a sponge. The low sample size from this location makes any statistical analysis of limited value, and it is difficult to draw any conclusion from these data. However, further collections at this location would be useful since the status of this area as a national park means that there are likely to be a number of species present that would not be found in other areas.

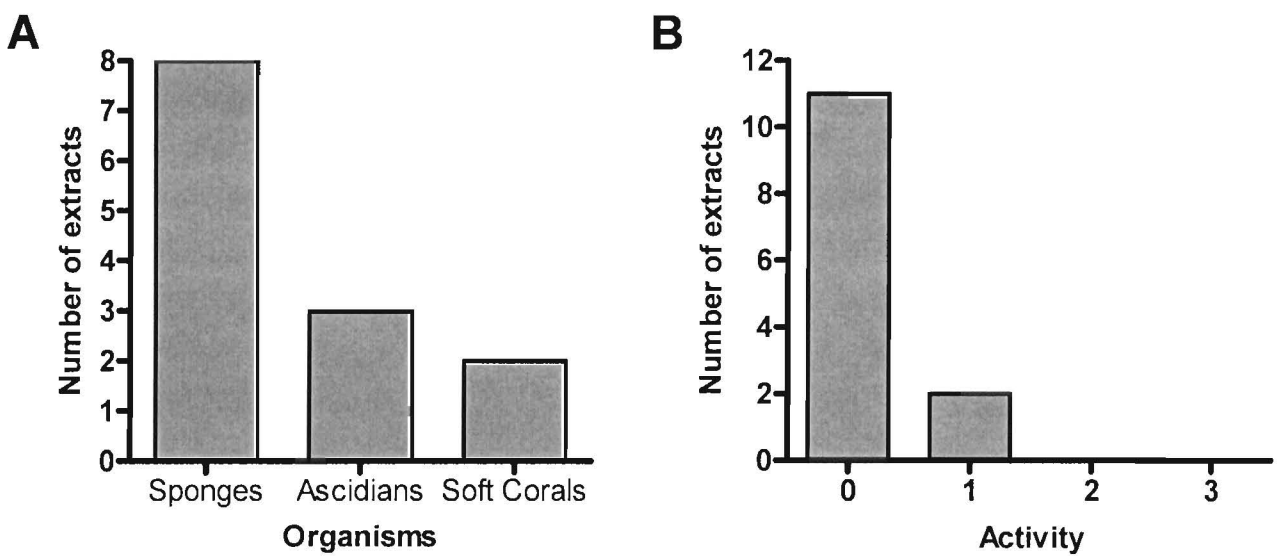

Figure 2.5. Number of organisms (A), and activity of extracts (B) collected from Tsitsikamma National Park.

A total of 13 samples were collected at Tsitsikamma National Park. Of these, 8 were sponges, 3 ascidians, and 2 soft corals. The majority of these samples were inactive (11/13), and the remaining 2 samples had low activity (Score = 1).

2.2.1.1.2. Algoa Bay

Algoa Bay is also located on the temperate south coast, and holds the harbour of Port Elizabeth. The collection at this location was carried out in July, 2004, and was a collection targeted to gather ascidian samples. Sixty-four extracts from this collection, all ascidian in origin, were tested. Of these samples the majority (79.7%) were completely inactive, while 11 (17.2%) had low activity, and only 2 (3.1%) had moderate activity in our assay.

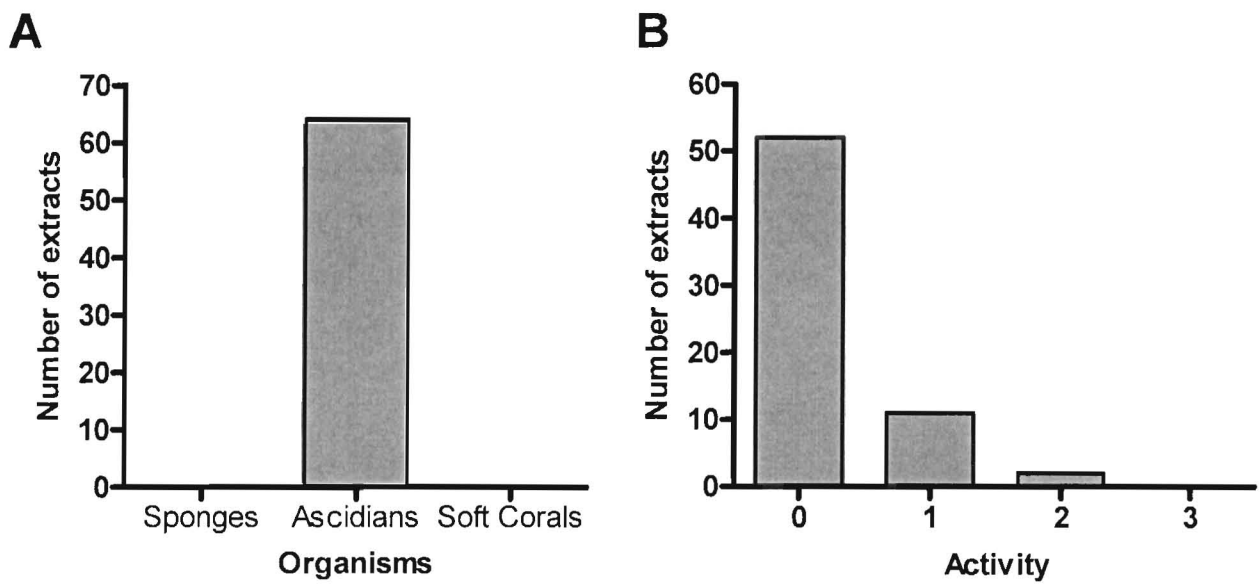

Figure 2.6. Number of organisms (A), and activity of extracts (B) collected from Algoa Bay. A total of 64 samples were collected at Algoa Bay. Since this was a directed collection, all samples were ascidians. The majority of these samples were inactive (52/64), 11 samples had low activity (score = 1), and the remaining 2 samples had moderate activity (score = 2).

2.2.1.1.3. Aliwal Shoal

The collection at the Aliwal Shoal was carried out in July 1994 and yielded 39 extracts with the majority (32) from sponges, 6 from soft coral and 1 ascidian extract. The samples from this collection were the only samples other than those from Marion Island to give high activity, with 3/39 having high activity. All the extracts with high activity were derived from sponges. The ascidian extract was moderately active, and 5 of the 6 soft coral extracts had some activity, though this was restricted to 3 with low activity and 2 with moderate activity.

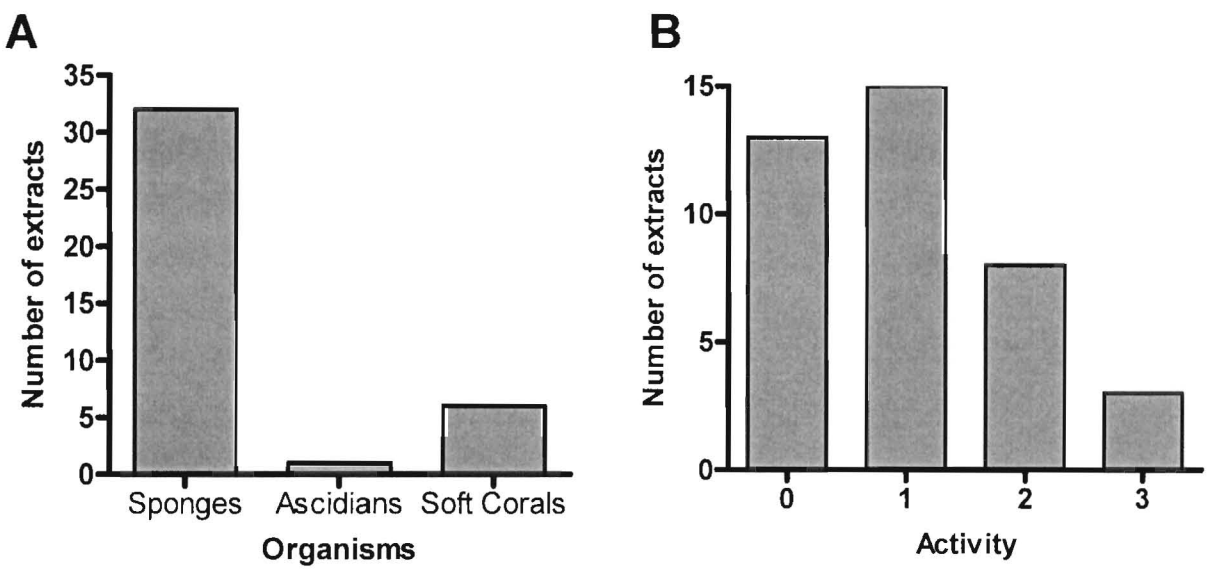

Figure 2.7. Number of organisms (A), and activity of extracts (B) collected from the Aliwal Shoal.

A total of 39 samples were collected from the Aliwal Shoal. This comprised of 32 sponge samples, 2 ascidian samples, and 6 soft coral samples. Approximately equal numbers of samples had no (score = 0) and low (score = 1) activity (13 and 15 samples respectively), while 8 samples had moderate activity (score = 2), and 3 samples had high activity (score = 3). All the highly active samples were derived from sponges.

2.2.1.1.4. Mozambique

Two collections were carried out in the Ponto do Ouro region of southern Mozambique in July, 1994 and October, 1995. Twenty-one extracts from this collection were tested with 15 sponge samples, 4 soft coral extracts and 2 ascidian extracts. None of the samples had high activity. Both ascidian samples were moderately active, while 2 of the soft coral samples were inactive and the other 2 showed only low activity. About a third of the sponge extracts had no activity, another third had low activity, and the final third had moderate activity.

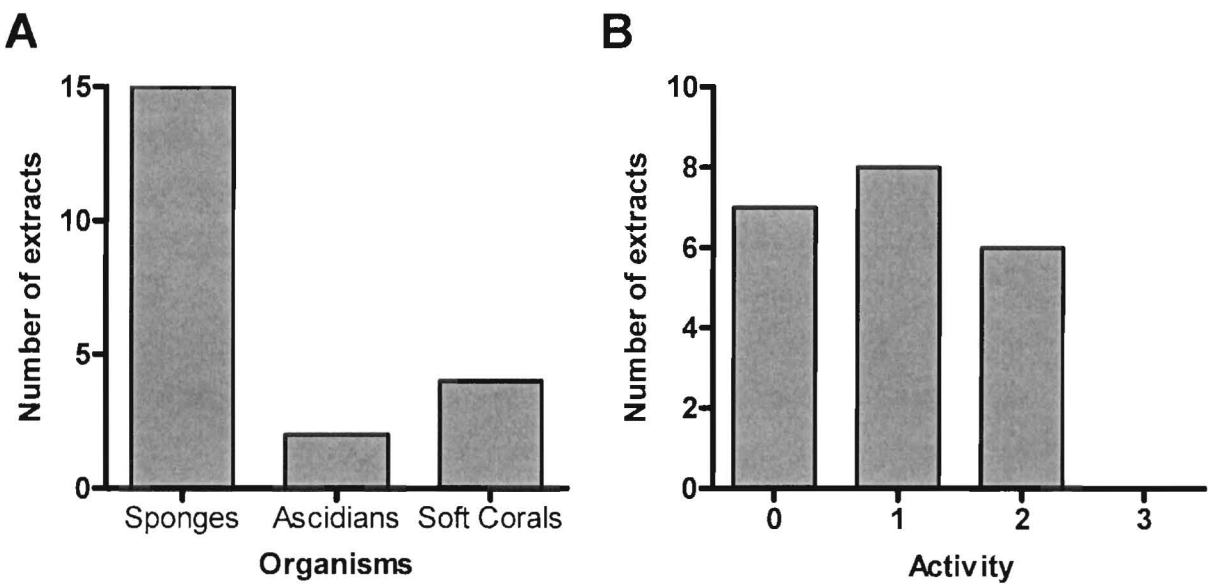

Figure 2.8. Number of organisms (A), and activity of extracts (B) collected from Mozambique.

A total of 21 samples were collected from Mozambique. This comprised of 15 sponge samples, 2 ascidian samples, and 4 soft coral samples. Approximately equal numbers of samples had no (score = 0), low (score = 1) and medium (score = 2) activity (7, 8 and 6 samples respectively), and there were no samples with high activity (score = 3).

2.2.1.1.5. Marion Island

Marion Island is a sub Antarctic island located about 1800 km south east of Port Elizabeth in the southern Ocean, and is the largest of the Prince Edward Islands group. The SA Agulhas – the Antarctic supply ship – travels to the island to deliver supplies, as well as transporting scientists to and from the island at biannual intervals, and carries out various scientific experiments during the time it is based in the region around Marion Island.

Two collections at Marion Island were carried out during April 2004 and April 2005. In contrast to collections at the other locations, where samples were collected by SCUBA, samples were collected by dredge from the SA Agulhas. Thirty-eight extracts from this collection were tested – 37 of which were sponge samples, while 1 was an ascidian. The samples from Marion Island had the highest hit rate of any of the locations tested, with more than 25% of the samples (10/37) having activity levels of 3, almost 50% (19/37) of the extracts with activity of 2 or higher, and only 35% (13/37) with no activity. Owing to the way in which these samples were collected (by dredge, and without a marine taxonomist) it is suspected that many of the samples are actually duplicates of the same organism. This would have the effect of lowering the sample size, and at the same time would explain the high number of active extracts (most from the same organism) (91). Even so, the high percentage of activity observed in these samples means it would be imperative to perform another collection at this location and obtain a larger number of samples, with accurate identification and in quantities sufficient for activity-directed isolation and identification of the active compounds.

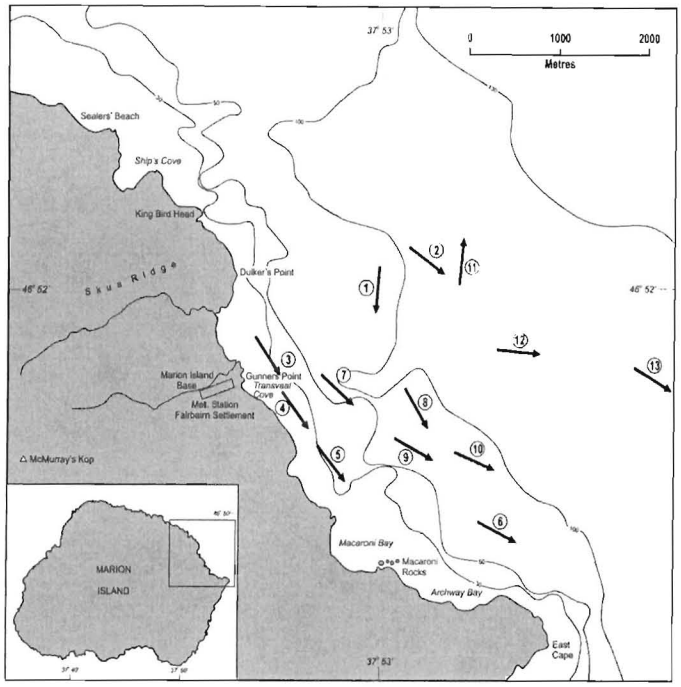

Figure 2.9. Collection areas around Marion Island.

Samples in this collection were collected by dredge off the SAS Agulhas. Dredge locations and directions are indicated by the arrows numbered 1-13. (Image reproduced with permission from Davies-Coleman *et al* (91))

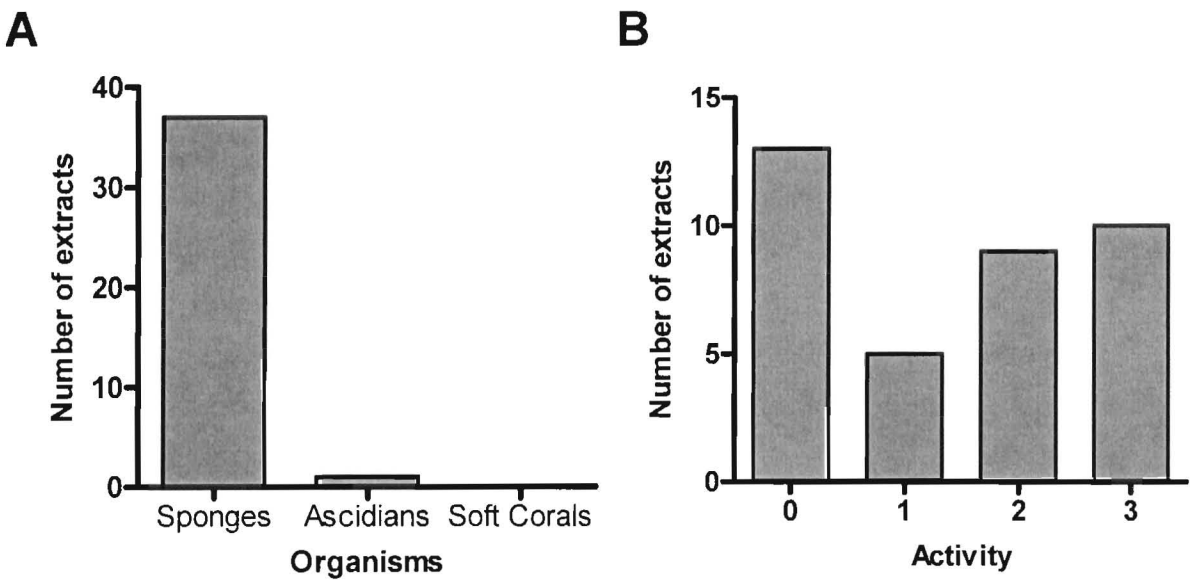

Figure 2.10. Number of organisms (A), and activity of extracts (B) collected from Marion Island.

A total of 38 samples were collected from Marion Island. Unlike the other collections, these samples were collected by dredge, rather than SCUBA. The collection comprised of 37 sponges and 1 ascidian sample. 13 samples were inactive (score = 0), 5 samples had low activity (score = 1) and 9 samples had medium activity (score = 2). This collection had the highest percentage of highly active samples, with 26% (10/38) of the samples showing high activity. The single ascidian specimen in this collection had no activity.

2.2.1.2. Organisms

2.2.1.2.1. Sponges

Sponges are members of the Phylum Porifera in which three classes are recognized viz. Class Demospongia, Class Calcarea and Class Hexactinellida. Over 15000 sponge species are known, the majority of which are marine (48;89). Sponges are sessile, and rely on filter feeding for nutrition. Although sponges are the simplest multicellular organisms, they lack any true organs, and each cell can give rise to an entire organism.

Sponges were the predominant organism from which extracts were obtained, with a total of 92 samples. Sponges yielded the most active extracts, with 13 extracts (14%) with high activity, 18 (20%) with moderate activity and 25 (26%) with low activity. This suggests that sponges represent an important source of bioactive metabolites, supporting observations made elsewhere (47). Faulkner has suggested that because marine natural product chemists generally require a taxonomic identification of the source organisms before they can publish their results in the chemistry literature their investigations are often biased towards groups of marine invertebrates which are taxonomically well-studied *e.g.* sponges (92).

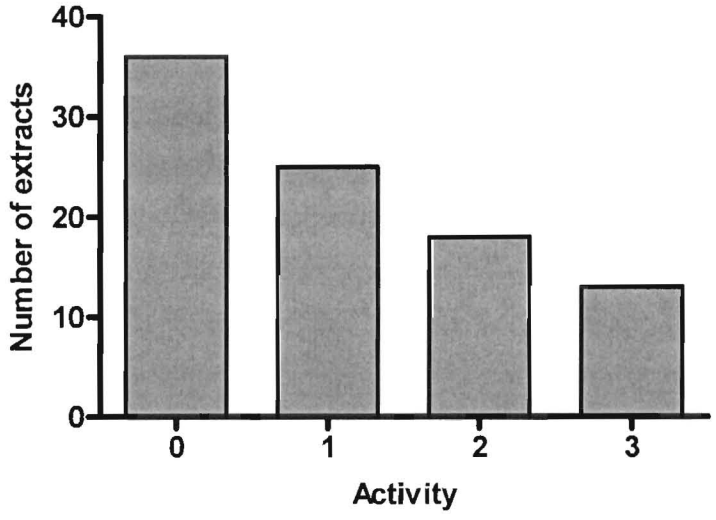

Figure 2.11. Activity of sponge extracts.

A total of 92 extracts from sponges were tested. This group of extracts displayed the highest activity, with 14% (13/92) with a score of 3. 40% (36/92) of the samples had no activity (score = 0), 27% (25/92) had low activity (score = 1) and 20% (18/92) had moderate activity (score = 2).

2.2.1.2.2. Ascidians

Ascidians belong to the Phylum Chordata, Subphylum Tunicata, Class Ascidacea and are commonly referred to as tunicates. Tunicates are filter feeders, siphoning water through one opening and out another. Although they may exist as single organisms, many species are colonial and over 2500 species of ascidians are known.

Ascidians were the second most common source organism for our studies, with 71 ascidian extracts tested for activity. Extracts derived from ascidians had the lowest levels of activity with only 5 (7%) with moderate activity and 11 (14%) with low activity. None of the extracts isolated from ascidians displayed high activity. Since ascidians were the third most common source of bioactive compounds (47), we were surprised by the low activity observed in these samples. However, since the majority of these samples were collected at one location, this may reflect a site-specific lack of activity. It is also possible that bioactive compounds exist in these samples, but at such low concentrations that their activity was not detectable in our assay.

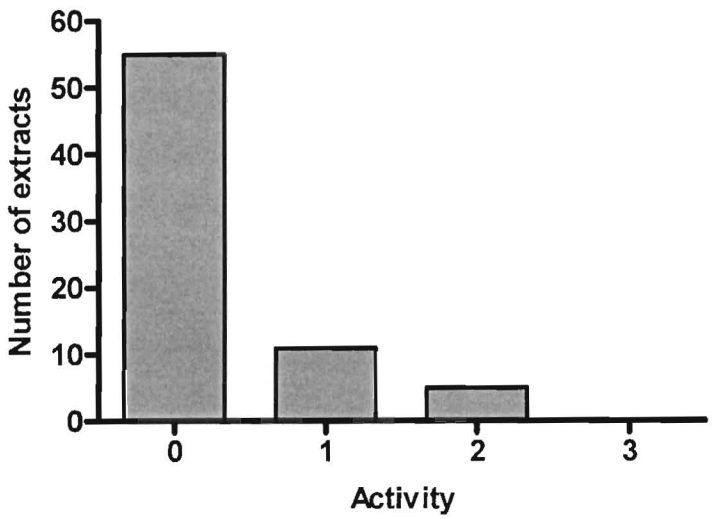

Figure 2.12. Activity of ascidian extracts.

A total of 71 extracts from ascidians were tested. No extracts had high activity (score = 3). More than ¾ of the samples had no activity (55/71), 15% (11/71) had low activity (score = 1) and only 7% (5/71) had moderate activity (score = 2).

2.2.1.2.3. Soft Corals

Soft corals (also known as octocorals) belong to Phylum Cnidaria, Class Anthozoa, Order Alcyonaria. They are colonial organisms made up of multiple polyps, each with eightfold symmetry.

There were only a very limited number of soft coral extracts – 12 in total. None of these had high activity, but 2 extracts (17%) had moderate activity, 6 extracts (50%) had low activity and 4 extracts (33%) had no activity. This indicates that there may be interesting active metabolites in soft corals and these organisms may be worthy of further investigation at a later point.

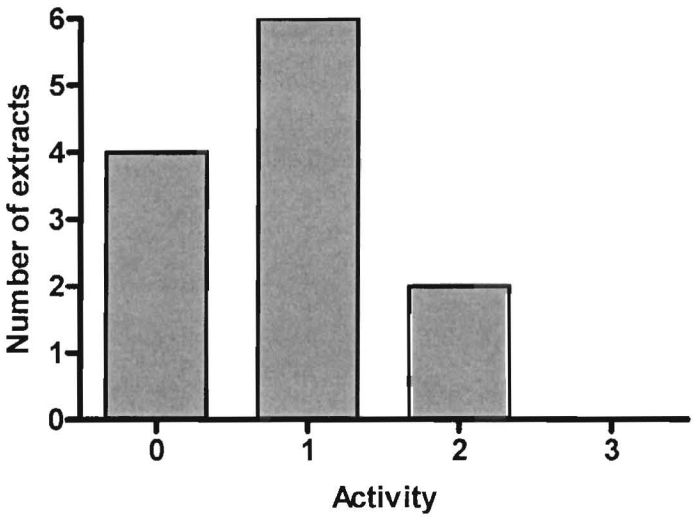

Figure 2.13. Activity of soft coral extracts.

Only a very limited number of soft coral samples were collected and tested. Of the 12 samples, none had high activity (score = 3). However only 4 of the samples had no activity (score = 0), half had low activity (score = 1) and 2 had moderate activity (score = 2).

2.2.2. Bioassay guided fractionation

16 pure compounds were identified from 5 active extracts via activity-directed fractionation. Several other compounds were isolated based on interesting chemical properties prior to this project. In the discussion below the compounds isolated via activity directed fractionation are discussed under the source organism. In some cases pure compounds from other sources are discussed when a structural similarity exists.

2.2.2.1. *Leptogorgia gilchristii*

The gorgonian *Leptogorgia gilchristii* is an octocoral (sea fan or gorgonian) that was collected in Mozambique off Ponto Malongan. The moderately active methanolic extract was considered a good candidate for bioassay guided fractionation due to its large volume and the interesting NMR spectra obtained.

2.2.2.1.1. Bioassay guided fractionation

Fractionation involved non silica-based chromatography (Polymeric reversed-phase separation – HP-20 column), followed by normal-phase flash- and HPLC using diol solid supports. This resulted in the isolation of 3 pure compounds, malonganenones A, B and C (Figure 2.14.) (93).

2.2.2.1.2. IC_{50} determination

The malonganenones are tetraprenylated alkaloids. Many polyprenylated quinone and purine metabolites have been previously isolated from southern African octocorals. Our collaborators have previously isolated the triprenyl hydroquinone rietone (Figure 2.14.) from the soft coral *Alcyonium fauri* (94), as well as a series of triprenylated quinones and hydroquinones from the Arminacean nudibranch *Leminda millecra* (95) (Figure 3.1.). These are quite likely to be octocoral in origin as the nudibranch feeds on various octocorals (96). The series of triprenylated hydroquinones and quinones from *Leminda millecra* are discussed in detail in Chapter 3, and so this section focuses on the activity observed for the malonganenones and rietone.

Malonganenones A, B and C are interesting from a biochemical perspective since examples of purine, rearranged purine and formamide secondary metabolites from octocorals are rare. Malonganenone A is the first 3,7-disubstituted hypoxanthine from a marine source, and malonganenones B and C are the first formamide structures isolated from gorgonians (93). The bioactivity of the malonganenones was assessed in comparison to the previously described triprenyl hydroquinone rietone for comparison purposes.

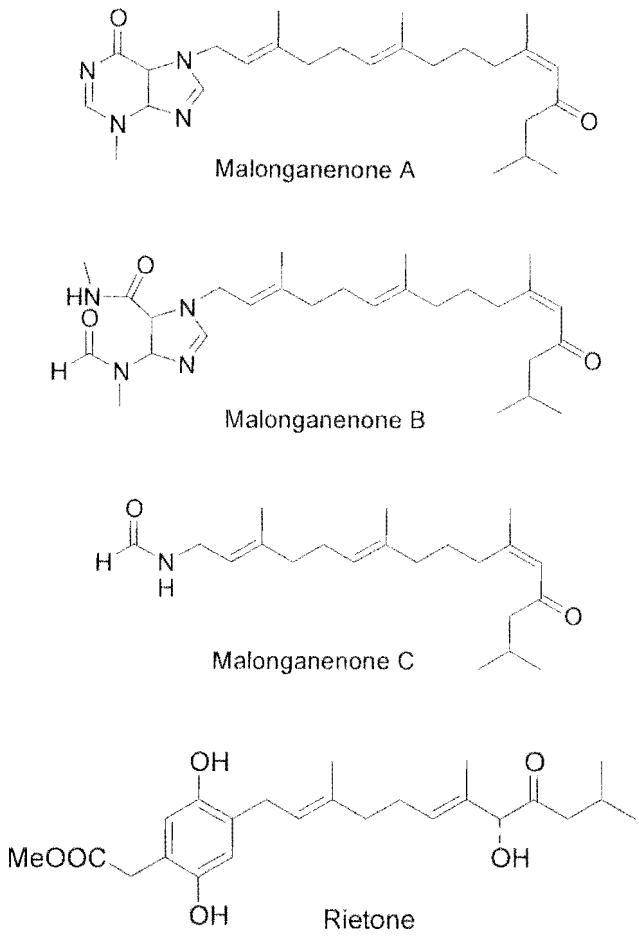

Figure 2.14. Structures of the compounds identified from *Leptogorgia gilchristii* by activity directed fractionation.

Also shown is the structure of a related compound, rietone, identified in a previous project from the soft coral *Alcyonium fauri* (94).

The malonganenones and rietone were assayed against a number of cell lines, following initial fairly positive results in our primary screen against WHCO1, with activity (IC_{50}) varying from 17 μM to 57 μM. The cell lines tested were 6 oesophageal cell lines of either South African (WHCO) or Japanese (KYSE) origin, and one control cell line, the benign breast epithelial cell line MCF12A.

The activity among the malonganenones against the different cell lines was fairly consistent, with the closed ring structure of malonganenone A conferring similar activity than the open ring structure of malonganenone B in all cell lines. Together these two compounds (malonganenone A and malonganenone B) appeared more active than the acyclic formamide (malonganenone C). The only exception to this case was the decreased activity of malonganenone B observed against WHCO5. The activity of rietone was similar to that of malonganenone C in most of the cell lines.

	IC_{50} values in μM (95% CI)			
	Malonganenone A	**Malonganenone B**	**Malonganenone C**	**Rietone**
WHCO1	16.6 (11.0-25.2)	14.6 (10.9-19.6)	57.7 (52.9-63.0)	54.0 (46.0-63.5)
WHCO5	4.9 (2.4-10.0)	2.2 (1.4-3.3)	27.9 (18.0-43.2)	32.2 (23.4-44.4)
WHCO6	51.2 (46.2-56.7)	26.8 (19.5-36.6)	77.5 (66.9-89.7)	> 100*
KYSE70	25.9 (16.5-40.7)	33.4 (25.8-43.3)	> 100*	> 100*
KYSE180	14.5 (8.6-24.3)	11.6 (7.3-18.2)	19.4 (13.6-27.6)	> 100*
KYSE520	16.4 (9.2-29.2)	12.8 (7.6-21.7)	> 100*	> 100*
MCF12A	13.0 (6.1-27.5)	13.0 (7.0-24.0)	15.3 (8.8-26.7)	7.4 (6.2-8.9)

Table 2.1. Anti-oesophageal cancer activity of the malonganenones and rietone. .

The IC_{50} values (and 95% confidence intervals) obtained for the malonganenones and rietone against 6 oesophageal cancer cell lines, and the non-malignant breast epithelial cell line MCF12. (* - IC_{50} values lay above the maximum tested concentration.)

Malonganenones A and B displayed similar activity against the normal cell line (MCF12A) as against the oesophageal cancer cell lines. However rietone was surprisingly 4-6 fold more active against MCF12A than against the oesophageal cancer cell lines. This was observed in 2 independent IC_{50} determinations, and may reflect the routine alteration of pathways associated with tumorigenesis conferring resistance against rietone.

Rietone was previously assayed for its anti-HIV properties in the NCI *in vitro* anti-HIV bioassay, but the activity displayed was inadequate to prompt further work (IC_{50} = 9.32 μM) (94). Our results suggest a potential use for this compound as an anti-cancer agent, but further testing against a wider range of tumours is recommended in light of the increased toxicity of this agent against the control cell line.

Malonganenone C showed increased toxicity against the normal cell line MCF12A when compared to the oesophageal cancer cells (with the exception of KYSE520). This observation should be confirmed by testing this compound on a broader panel of cancer and normal cell lines.

2.2.2.2. *Strongylodesma aliwaliensis*

The Latrunculid sponge *Strongylodesma aliwaliensis* (Family Latrunculidae) was first identified by our collaborators in 2004 (97). (Figure 2.15.A)

2.2.2.2.1. Bioassay guided fractionation

The aqueous MeOH partition of the sponge *Strongylodesma aliwaliensis* was found to possess high activity (score = 3) in our assay. A portion of this extract was dissolved in MeOH and was fractionated using a variety of techniques including HP-20, C18 Sep-Pak (columns) C18-RP-HPLC to give the known compounds damirone C, makaluvamines I and M (98), and four novel compounds *N*-1-β-D-ribofuranosyldamirone C and *N*-1-β-D-ribofuranosylmakaluvamine I (99), makaluvic acid C and *N*-1-β-D-ribofuranosylmakaluvic acid C (100). The structures of all these compounds are shown in Figure 2.15.B.

2.2.2.2.2. IC_{50} determination

The low yield of makaluvamine I isolated from the extract precluded activity determination. All the other compounds isolated from *S. aliwaliensis* were evaluated for anti-oesophageal cancer activity, and were evaluated against 3 oesophageal cancer cell lines (Table 2.2.).

A

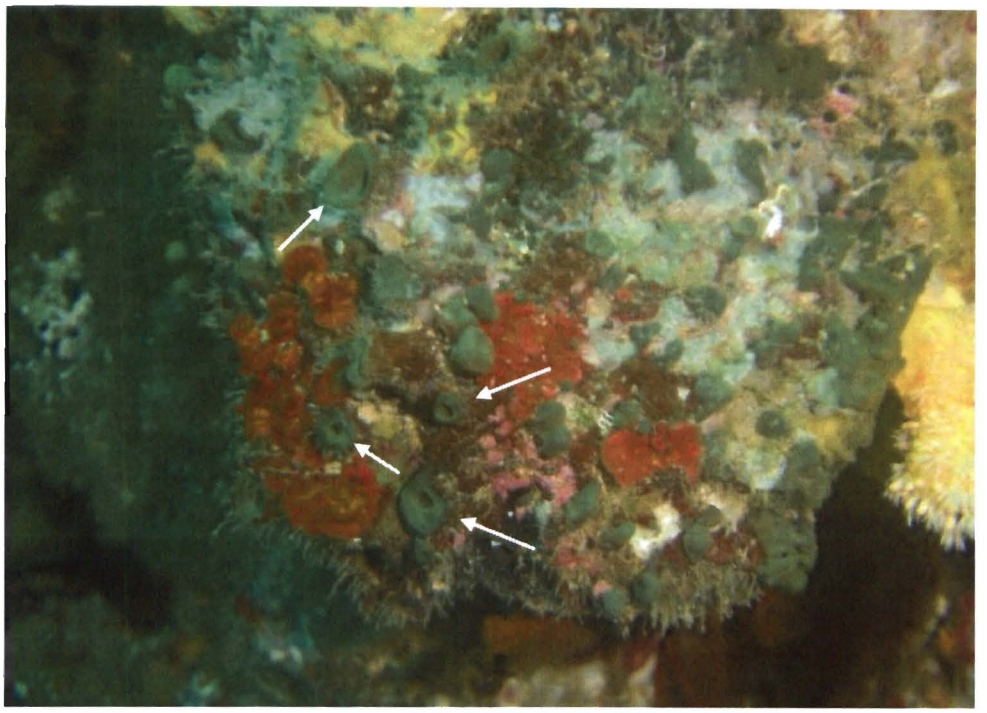

B

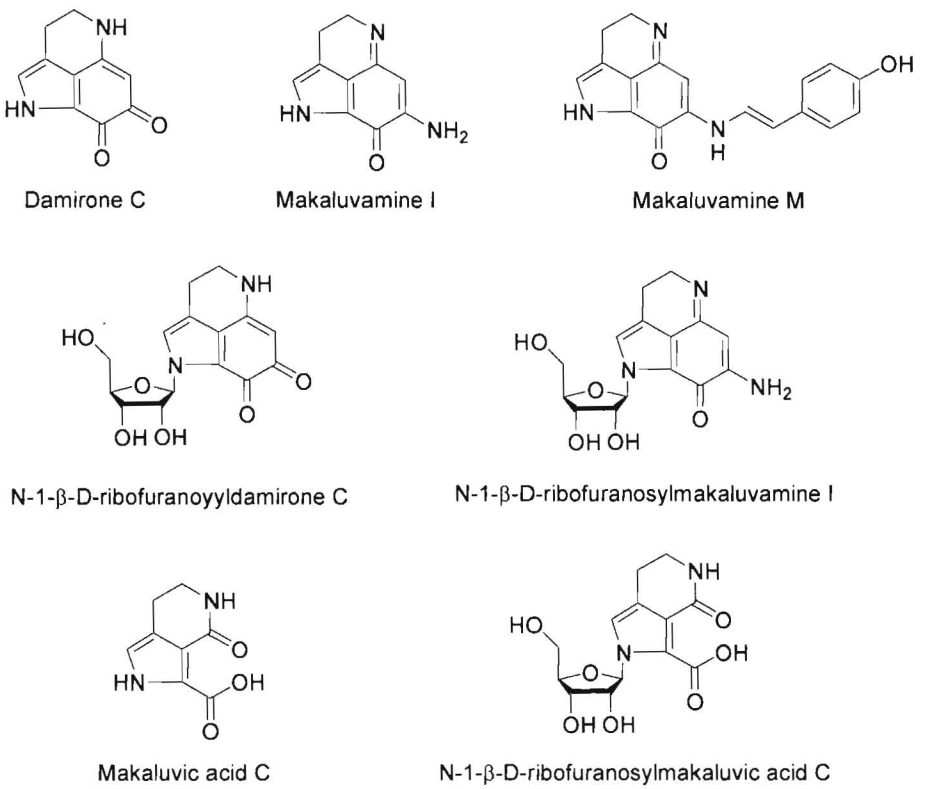

Figure 2.15. *Strongylodesma aliwaliensis* (A), and the compounds identified from this sponge by activity diirected fractionation (B).

Strongylodesma aliwaliensis is a green, ball shaped sponge. In this picture, it is covered in symbiotes, though green oscules protruding from the surface can be observed (arrows).

	IC_{50} values in μM (95% CI)		
	WHCO1	**WHCO6**	**KYSE30**
Damirone C	55.7 (51.2-60.5)	78.3 (69.8-87.9)	77.9 (72.7-83.4)
Makaluvamine M	0.19 (0.17-0.21)	6.8 (3.0-13.2)	3.2 (2.7-3.9)
N-1-β-D-ribofuranosyl damirone C	37.9 (32.9-43.7)	75.7 (68.5-83.6)	71.6 (59.0-87.0)
N-1-β-D-ribofuranosyl makaluvamine I	1.45 (1.44-1.46)	5.6 (4.2-7.4)	3.2 (2.8-3.7)
Makaluvic acid C	>150*	>150*	>150*
N-1-β-D-ribofuranosyl makaluvic acid C	60.6 (52.5-70.0)	>200*	>200*

Table 2.2. Anti-oesophageal cancer activity of the compounds isolated from the sponge *Strongylodesma aliwaliensis*.

These compounds were tested against three oesophageal cancer cell lines.

(* IC_{50} values lay above the maximum tested concentrations.)

The IC_{50} values suggest that the addition of the sugar moiety improves activity slightly (comparing N-1-β-D-ribofuranosyldamirone C to damirone C, and N-1-β-D-ribofuranosylmakaluvic acid C to makaluvic acid C). The alteration of the pyrroloiminoquinone nucleus in N-1-β-D-ribofuranosylmakaluvamine I to the ortho quinone structure in N-1-β-D-ribofuranosyldamirone C results in a significant loss of activity, confirming the important role played by the pyrroloiminoquinone moiety in determining the anticancer activity of these compounds (101).

Interestingly, we had also had access to two compounds with similar structures isolated by our collaborators in a previous project. These were tsitsikammamine B and discorhabdin A (Figure 2.16.).

Tsitsikammamine B was isolated with tsitsikammamine A and two novel pyrroloiminoquinone alkaloids (14-bromodiscorhabdin C and 14-bromodihydrodiscorhabdin C) from *Tsitsikamma favus* from the Tsitsikamma Marine Reserve (102).

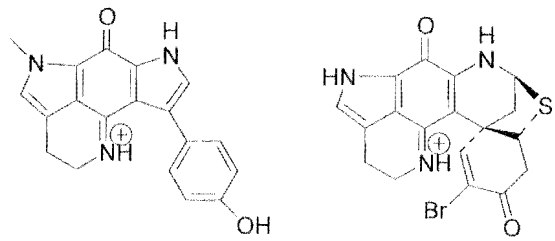

Tsitsikammamine B Discorhabdin A

Figure 2.16. Tsitsikammamine B and discorhabdin A.

These compounds are similar to those isolated from *Strongylodesma aliwaliensis*, and this chemical similarity reflects the phylogenetic relationship between these organisms.

Discorhabdins are found predominantly in the genera *Latrunculia*, while makaluvamines are generally isolated from the genera *Zyzzya* (99). The source sponge for tsitsikammamine B was found to share morphological characteristics between these two genera, and this resemblance was expected to extend to the secondary metabolites isolated from it. This was the case, with the compounds isolated having similarity to both the discorhabdins and the makaluvamines (102). A number of the discorhabdins have been shown to have potent antitumour activity (103-105), while tsitsikammamine B has been shown to intercalate into DNA and cause cleavage by inhibiting topoisomerase I (103). Our results show similar levels of activity of discorhabdin A and tsitsikammamine B against an oesophageal cancer cell line, and a cervical cell line (Table 2.3.) to that seen in a previous study (103), where discorhabdin A showed an IC_{50} of 0.007 μM, and tsitsikammamine B an IC_{50} of 2.38 μM against the HCT116 cell line.

	IC_{50} values in μM (95% CI)		
	WHCO1	**ME180**	**MCF12A**
Tsitsikammamine B	1.3 μM (0.9-1.8)	1.0 μM (0.8-1.1)	0.9 μM (0.9-1.0)
Discorhabdin A	6.3 nM (1.1-34.9)	13.7 nM (12.4-15.2)	9.0*

Table 2.3. Anti-oesophageal cancer activity of tsitsikammamine B and discorhabdin A against several cell lines.

These compounds were tested against the oesophageal cancer cell line WHCO1, the cervical cancer cell line ME180 and the non-malignant breast epithelial cell line MCF12A. (* Insufficient compound was available to repeat the IC_{50}.)

2.2.2.3. *Axinella weltneri*

The sponge *Axinella weltneri* was collected by SCUBA from a reef off Ponto do Ouro in southern Mozambique in July 1994 (Figure 2.17.A.).

2.2.2.3.1. Bioassay guided fractionation

The EtOAc partitioned fraction from the sponge *Axinella weltneri* had moderate activity in our assay, and was fractionated on a silica gel column. The most active of these fractions was subjected to semi-preparative HPLC purification. One of the resulting fractions exhibited significant activity against WHCO1 and was determined by NMR to be the triterpene sodwanone A (Figure 2.17.B.).

2.2.2.3.2. IC_{50} determination

Sodwanone has previously been identified from *Axinella weltneri* (106), and its anticancer activity against a lung carcinoma cell line reported (107). However, its identification by activity-directed fractionation in this project validates the potential of our system to identify compounds of interest.

In addition, sodwanone A displayed substantial activity (IC_{50} of 1.2 – 1.7 μM) (Table 2.4.) against 3 oesophageal cancer cell lines, which compares favourably to the results reported for the lung carcinoma cell line mentioned above (IC_{50} = 12 μM) (107).

Current work by our collaborators has focused on producing synthetic analogues of sodwanone A, and two analogues have been tested to date. Unfortunately both of these analogues were extremely insoluble, making it difficult to measure activity.

A

B

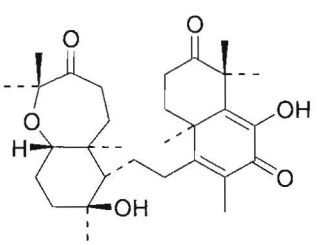

Sodwanone A

Figure 2.17. *Axinella weltneri* (A), and sodwanone A (B), isolated by an activity-directed fractionation process.

A. weltneri is the red sponge in the foreground.

2.2.2.4. *Aplysilla sulphurea*

The sponge *Aplysilla sulphurea* was also collected by SCUBA from a reef at Ponto do Ouro in southern Mozambique in July, 1994.

2.2.2.4.1. Bioassay guided fractionation

Four compounds were isolated from the EtOAc extract of the sponge *Aplysilla sulphurea* collected in Mozambique, which exhibited moderate anti-oesophageal cancer activity (score = 2) in our screening system. Fractionation on an HP-20 column led to the isolation of (+)-curcudiol, reported concurrently from the sponge *Didiscus flavus* (108) and from *Epipolasis* sp.(109). The known compound aplysulphurin, a common metabolite of the spongian diterpene class originally isolated from an Australian collection of *A. sulphurea* (110) was eventually purified by crystallization. The supernatant mother liquor from the recrystallization was chromatographed using first silica gel and then silica HPLC to yield 9,11-dihydrogracilin A which was originally isolated from the Antarctic sponge *Dendrilla membranosa* (111). An inactive peroxy-steroid was also isolated and identified from an active fraction. The structures of all these compounds are shown in Figure 2.18.

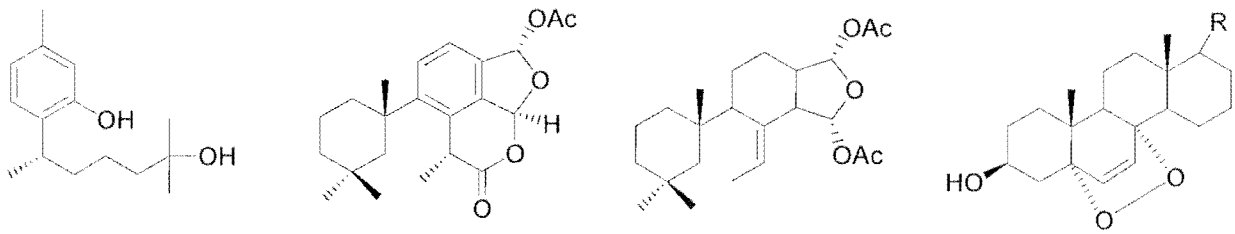

(+)-curcudiol Aplysulphurin 9,11-dihydrogracillin peroxy-steroid (R=?)

Figure 2.18. The compounds identified from *Aplysilla sulphurea* by activity directed fractionation.

2.2.2.4.2. IC_{50} determination

Both of the diterpenes (aplysulphurin and 9, 11-dihydrogracillin) displayed high activity against all three cell lines tested. This activity was greater than that of cisplatin against the oesophageal cancer cell line WHCO1 (IC_{50} = 13 μM). Curcudiol had very low activity in our system, with slight activity against WHCO1, and no activity against the other cell lines, and the peroxysteroid was completely inactive (Table 2.4.).

	IC_{50} values in μM (95% CI)		
	WHCO1	**WHCO6**	**KYSE30**
Sodwanone A	1.3 (0.9-1.7)	1.7 (1.4-2.2)	1.4 (0.4-4.6)
(+)-Curcudiol	89.2 (71.7-111.0)	>200*	>200*
Aplysulphurin	3.5 (1.7-7.0)	10.0 (7.7-13.1)	7.0 (4.7-10.5)
9,11-Dihydrogracillin A	1.1 (0.7-1.8)	1.0 (0.7-1.4)	1.5 (1.3-1.6)

Table 2.4. Anti-oesophageal cancer activity of sodwanone A, and the compounds isolated by activity-directed fractionation from *A. sulphurea.*

The IC_{50} values for these compounds was determined against three oesophageal cancer cell lines. (* IC_{50} values lay above the maximum tested concentrations.)

2.2.3. *Lyngbya majuscula* (Homodolastatin 16)

Homodolastatin 16 is a cyclic depsipeptide that was isolated from a Kenyan collection of the cyanobacterium *Lyngbya majuscula* (112). This compound was isolated prior to the start of the collaboration as part of an NMR (Nuclear Magnetic Resonance) based targeted search for bioactive depsipeptides from East African marine cyanobacteria. This compound was submitted for screening because of the well-documented anti-cancer activity of dolastatin 16 (112). Homodolastatin 16 is a higher homologue of dolastatin 16 and differs from the latter compound by possessing an extra methylene group.

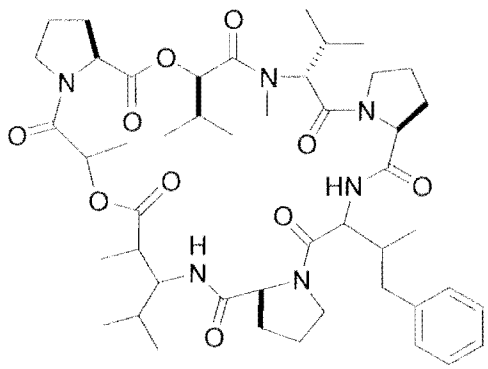

Dolostatin 16

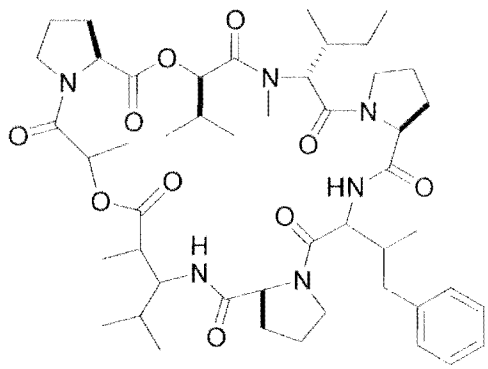

Homodolostatin 16

Figure 2.19. Dolostatin 16 and homodolostatin 16.
Homodolostatin 16 was isolated from the cyanobacterium *Lyngbya majuscula*. It differs from dolostatin 16 by the presence of an additional methyl group.

The dolastatins are a group of depsipeptides with similarity to the original member of this group, dolastatin 10. Dolastatin 10 was originally isolated from the sea hare *Dolabella auricularia* by Pettit *et al.* in the 1970's, but owing to exceptionally low yield, the active portion of the highly active extracts was only identified almost 15 years later (113). Dolastatin 10 has high antiproliferative activity (ED_{50} of $4.6x10^{-5}$ µg/ml against murine PS leukemia cells), and was found to bind to tubulin, strongly affecting microtubule assembly (114). Dolastatin 10 has been tested in Phase I and II trials, but trials were discontinued as it exhibited peripheral neuropathy in 40% of patients, and was not effective in patients with hormone-refractory metastatic adenocarcinoma and recurrent platinum sensitive ovarian carcinoma. However, it has been used as the starting point for the synthesis of a wide variety of analogues.

Dolastatin 16, was originally isolated from the same sea hare, *Dolabella auricularia*, and later from a Madagascan collection of *L. majuscula*. It has been reported to be cytotoxic against a variety of cancer cell lines, including lung (NCI-H460 : GI_{50} 0.00096 µg/ml), colon (KM20L2 : GI_{50} 0.0012 µg/ml), brain (SF-295 : GI_{50} 0.0052 µg/ml) and melanoma (SK-MEL5 : GI_{50} 0.0033 µg/ml) (GI_{50} – concentration resulting in a 50% inhibition of growth) (112). We thus tested homodolastatin 16 against two oesophageal cancer cell lines (WHCO1 and WHCO6), as well as the cervical cancer cell line ME180. While there was significant activity against these cell lines (WHCO1 : IC_{50} 4.3 µg/ml, WHCO6 : IC_{50} 10.1, ME180 : IC_{50} 8.3 µg/ml), the activity observed was substantially lower than that reported for dolastatin 16 (112). In this case I have converted the IC_{50} values of homodolastatin from µM to µg/ml to facilitate the comparison between our results and that of Pettit *et al.* Regrettably no dolastatin 16 was available for screening as a control in our assays.

2.3. Conclusion

In the course of this project, a cheap, relatively rapid screening program was established. Currently the cell line utilized for this screen is the oesophageal cancer cell line WHCO1, but this could be expanded to include other cell lines of interest. Oesophageal and cervical cancer are the 2 most common causes of cancer related death among men and women in southern Africa respectively. Thus identifying agents that may be used as chemotherapeutic agents for these cancers is an extremely important objective.

This screening program can be used to test samples from any source, but during the course of this project we have focused on screening marine natural products. A total of 479 samples were processed. These included 175 extracts from marine organisms. After identifying a number of extracts as good candidates, we proceeded with activity-directed fractionation, testing a total of 278 fractions, of the extracts of interest. These gave rise to a number of compounds. In addition several compounds identified in earlier projects were also tested.

In the course of screening, a large number of primary extracts were tested. Since we know the source organisms of these extracts, we are able to draw some conclusions regarding the most likely organisms to yield active compounds. According to Blunt *et al.* (2006) sponges are the primary source of bioactive metabolites in the marine environment, closely followed by micro-organisms, coelenterates and tunicates (ascidians) (46). Our results support this observation with the highest activity samples being derived from sponges. The few soft coral samples tested were on average more active than the ascidian samples, but our numbers are too low to draw a conclusion from this.

The compounds identified by bioassay-guided fractionation show the potential of our screening program and close collaboration between chemists, biochemists and taxonomists to yield bioactive compounds from southern African marine sources. Identification of the known compound sodwanone A by activity-guided fractionation shows the potential of our system to identify viable drug leads, and the number of unique, cytotoxic compounds identified from a relatively small number of organisms and fractions, at minimal cost shows the viability of a screening program of this sort carried out in South Africa

CHAPTER 3

CYTOTOXIC EFFECT OF KLMs ON OESOPHAGEAL CANCER CELLS

3.1. Introduction

In our search for novel cancer therapies from the marine environment, we identified a group of related compounds with activity against our screening cell line. These compounds had been identified prior to our collaboration by chemical methods in an investigation of the sequestered chemistry of the Arminacean nudibranch *Leminda millecra*. This investigation yielded a variety of novel chemical structures as well as the previously identified millecrones A and B, isofuranodiene and (+)-8-hydroxycalamenene (96). The novel compounds identified included a group of related triprenylquinones and triprenylhydroquinones (95).

3.1.1. Source and isolation of compounds

Leminda millecra (Griffiths, 1985) (Figure 3.1.) is an Arminacean nudibranch, a marine gastropod that lacks a shell (hence nudi – naked, branch – gills). Nudibranchs are members of the Phylum Mollusca, Class Gastropoda, Subclass Opisthobranchia, Order Nudibranchia, Suborder Arminina. *L. millecra* is the only member of the Lemindidae family of nudibranchs, and is endemic to the South African coastline, occurring between the Cape Peninsula and Kwazulu Natal. This nudibranch has previously been shown to feed on octocorals, and both octocoral spicules and metabolites were identified in samples of *L. millecra* from the Transkei coast (96).

Figure 3.1. The Arminacean nudibranch *Leminda millecra*.
The nudibranch is pictured feeding on an octocoral.

An abundance of *L. millecra* in the waters of Algoa Bay provided a source for further elucidation of the sequestered chemistry of this organism (95), and the subsequent biological assays described in this thesis. Two collections of L. millecra (a total of 32 specimens collected in Algoa Bay in October 1998 and February 1999) were processed through a series of purification steps, including silica gel chromatography and HPLC to yield the hydroquinones and quinones discussed in this chapter (Figure 3.2.). The reader is referred to McPhail *et al.* (95) where a more detailed description of the isolation and characterization of these compounds is provided.

Previously, similar structures have been isolated from the marine fungus *Penicillium* sp. and were found to be active against a variety of cancer cell lines (115;116) .

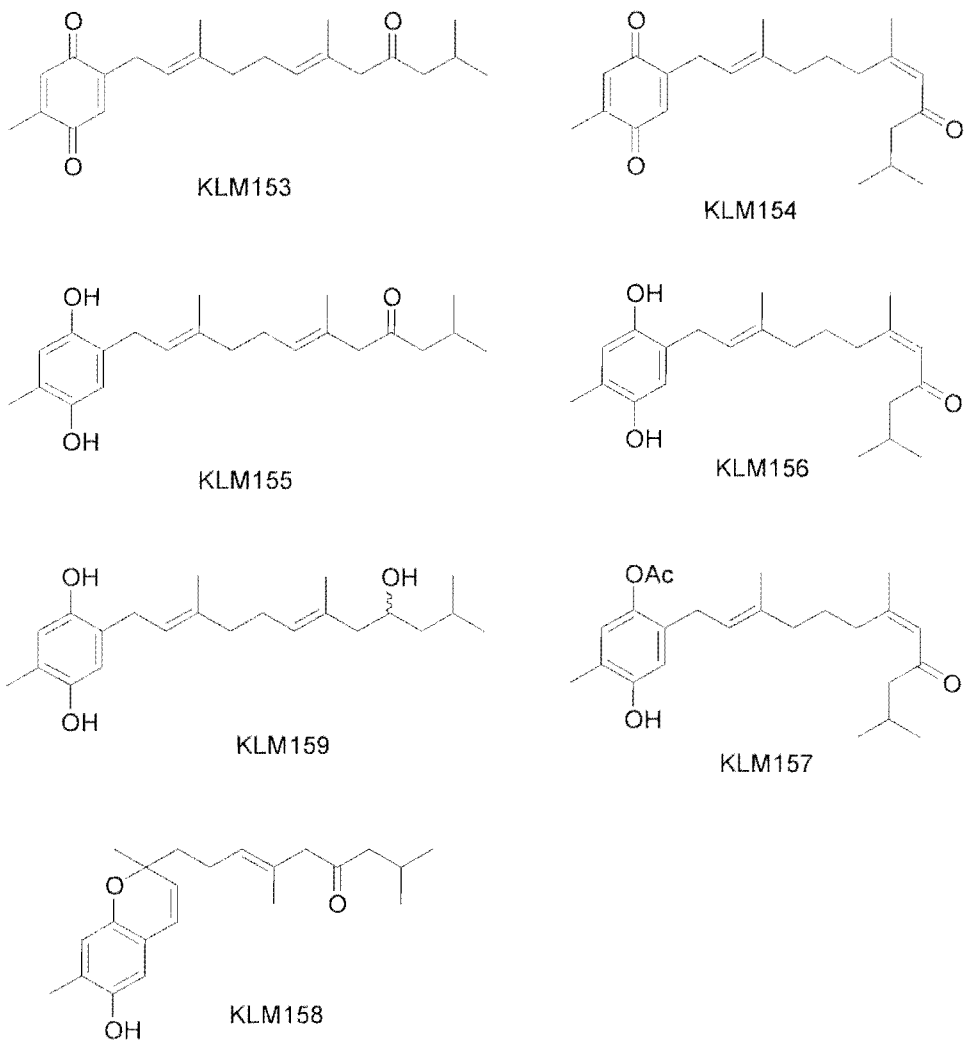

Figure 3.2. Triprenylquinones and hydroquinones isolated from the Arminacean nudibrach *L. millecra*.

The nomenclature is that originally used by the chemist isolating these compounds, and has been retained for consistency.

3.1.2. Quinones as chemotherapeutic agents

Many biologically active quinones exist, and are in use as therapies for a variety of diseases, and are widely used in the treatment of malignancies. The quinoid anthracycline antibiotics are amongst the most utilized anticancer agents ever developed (68;117). Quinones in clinical use include doxorubicin, streptonigrin, mitomycin c and diaziquone, while EO9 and the aziridinylbenzoquinones DZQ (diaziridinylbenzylquinone) and RH1 are currently in clinical trials (118) (Figure 3.3.). Despite the fact that over a thousand quinone compounds have been tested for anticancer activity, and the widespread use of many quinones as anticancer agents, the mechanism of action of these compounds, and the contribution of the quinone structure to the activity of these compounds remains uncertain. This is due to the fact that antitumour quinones generally consist not only of a quinone moiety, but also other structures that may contribute to toxicity (117). General mechanisms that have been described for quinone reactivity include quinone redox cycling and conjugation reactions with bionucleophiles such as DNA (117).

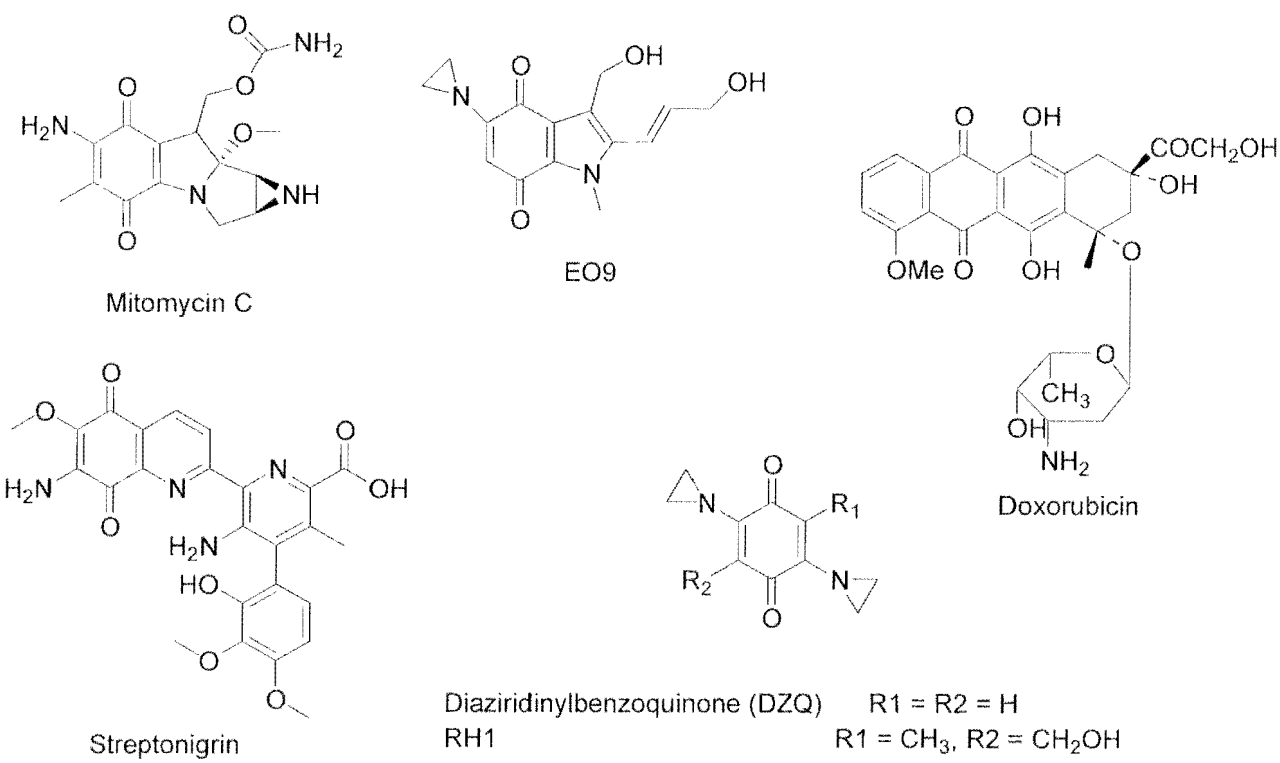

Figure 3.3. Quinones of clinical significance.

Mitomycin C, doxorubicin and streptonigrin are agents in clinical use, while EO9 and the aziridinylbenzoquinones DZQ and RH1 are in clinical trials.

3.1.3. Experimental approach

The compounds isolated from *L. millecra* were evaluated for activity against the oesophageal cancer cell line WHCO1 as a model system, and once activity was identified, the activity of the most abundant (and most active) compounds was tested against a wider panel of cell lines. We then determined the involvement of apoptosis, necrosis and cell cycle perturbations in the cellular response to treatment with these agents.

In Chapter 4, the mode of action of these compounds is explored.

Unfortunately, one of the major problems associated with compounds extracted from marine organisms is a scarcity of supply. There was a limited amount of each of the KLM compounds available, and thus it was necessary to limit mechanistic studies to only one, and in some cases two of the most abundant (and most active) compounds. In some cases, the activity of the entire group of compounds was examined to explore the relationship between structure and activity.

3.2. Results

3.2.1. Effect of KLMs on cell viability

Initial screening of compounds KLM153 – KLM159 on the viability of WHCO1 cells was performed using the crystal violet assay (Figure 3.4.). All these compounds caused almost complete cell death at the highest concentration tested (50 µg/ml). Most (except KLM157) reduced the cell number to less than 50% of untreated at 10 µg/ml. At 1 µg/ml, most of the compounds increased the cell number slightly. The only exception to this was KLM153. Cell numbers increased significantly in the case of several compounds – e.g. KLM154 and KLM159 which increased cell number to almost 150%. This increase was confirmed by visual observation of the cells prior to processing for screening, and was not associated with any form of precipitate.

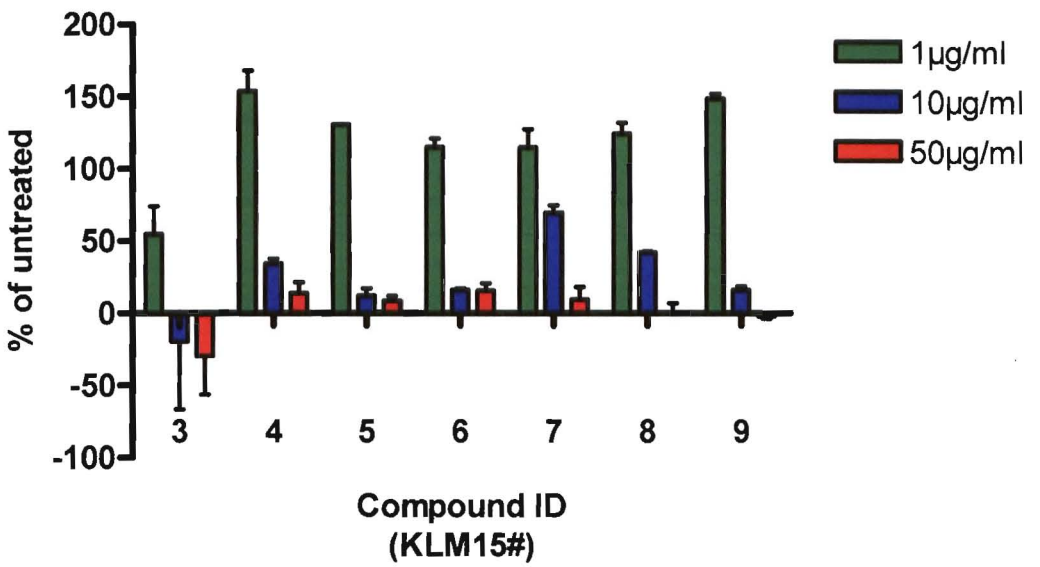

Figure 3.4. Effect of the KLMs on cell viability in our initial screening assay.
Initial screening of these compounds was carried out as outlined in Materials and Methods. Compounds were diluted and added to wells in duplicate at three concentrations, and following a 48 hour incubation, the plate was processed using the crystal violet stain. Values are expressed as the % of untreated cells (as measured by absorbance at 595nm). Error bars indicate the standard deviation.

3.2.2. IC_{50} determination

Following the promising results of the initial screening assay, these compounds were evaluated for their cytotoxic activity using the MTT assay to determine IC_{50} values against the oesophageal cancer cell line WHCO1.

The compounds showed varying activity against these cells (Table 3.1.), and their close structural similarity allowed us to make some tentative structure/activity observations. Changes in the substitution pattern at the 1 and 4 positions yield varying activity, with the most active compounds being those with a non-esterified hydroquinone nucleus (e.g. KLM155 and KLM156). The quinone nucleus of KLM153 and KLM154 is the least active of the three variants, while the acetyl substitution of KLM157 is less active than the hydroquinones, but more active than the quinones (Figure 3.5.). Changes in the geometry of the double bonds in the side chain also affect activity – KLM153 and KLM155 (all trans) are more active than KLM154 and KLM156 (trans,cis) (Figure 3.6.). KLM159 (which differs from KLM155 only in the substitution of a hydroxyl group for a carbonyl group on the triprenyl side chain) is less active than KLM155. There were insufficient quantities of KLM158 to repeat the IC_{50} determination for this compound.

Compound	IC_{50} [μM]	CI (95%)
KLM153	37.9	37.7 – 38.0
KLM154	83.3	82.1 – 84.5
KLM155	9.4	9.4 – 9.5
KLM156	12.9	12.5 – 13.3
KLM157	42.6	42.6 – 42.7
KLM158	19.4*	
KLM159	32.7	32.5 – 33.0

Table 3.1. IC_{50} values (and 95% confidence interval) for KLM's against the oesophageal cancer cell line WHCO1.

Dose response curves for each KLM were performed against the oesophageal cancer cell line WHCO1 as outlined in Materials and Methods. Each experiment was performed in quadruplicate and repeated at least twice. (* Insufficient compound was available to repeat the IC_{50})

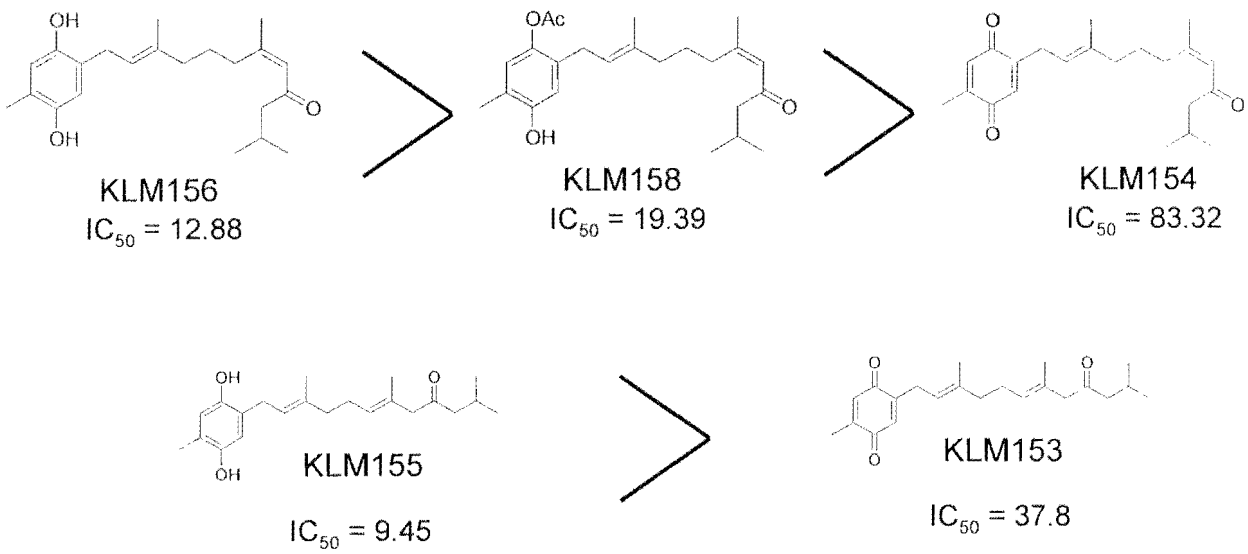

Figure 3.5. Changes in activity based on the substitution of the ring

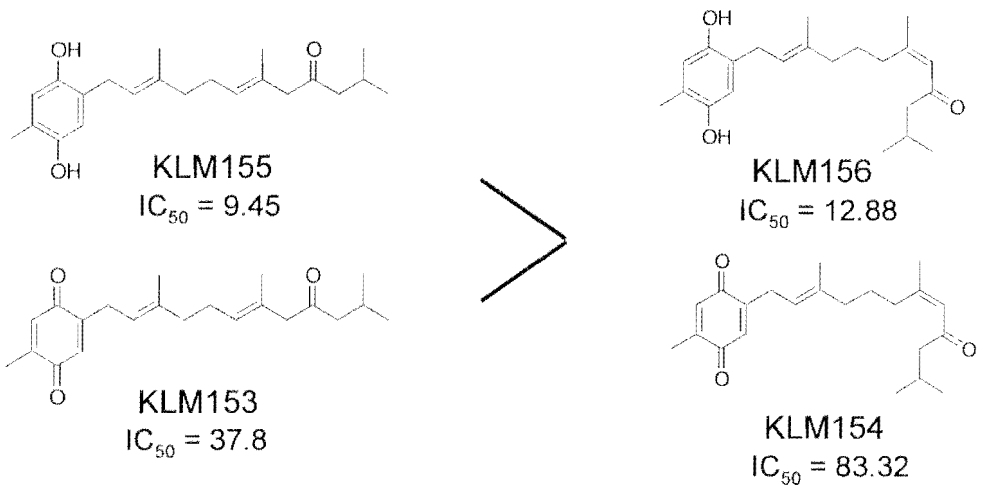

Figure 3.6. Changes in activity based on structure of the side chain.

The triprenyl hydroquinone rietone discussed in Chapter 2 (Section 2.2.2.1), was isolated from the soft coral *Alcyonium fauri* (94), and has moderate activity against the oesophageal cancer cell lines tested, with activity in a similar range to that of KLM157 against WHCO1 (Table 2.1).

The most active compound (KLM155) was evaluated against a range of cell lines, including oesophageal cancer cell lines WHCO1 and 6, cervical cancer cell lines ME180 and SiHa and the benign breast epithelial line MCF12A, as a control (Table 3.2.). KLM155 displayed cytotoxicity against most of the cell lines tested, with the exception of the cervical cancer cell line SiHa, which was resistant up to the highest concentration of KLM155 tested (150 μM).

Cell line	IC_{50} [μM]	CI (95%)
WHCO1	9.4	9.4 – 9.5
WHCO6	5.8	5.6 – 6.0
MCF12A	31.9	31.6 – 32.3
ME180	33.9	33.7 – 34.1
SiHa	>150	

Table 3.2. IC_{50} values (and 95% confidence interval) for KLM155 against a variety of cell lines.

Dose response curves for KLM155 were performed against WHCO1 and WHCO6 (oesophageal cancer cell lines), ME180 and SiHa (cervical cancer cell lines) and MCF12A, a benign breast epithelial cell line. Each experiment was performed in quadruplicate and repeated at least twice.

3.2.3. The effect of KLM155 on cell growth and survival

A growth curve of cells with and without various concentrations of KLM155 was carried out to determine whether the reduction in cell number was due to a cytotoxic or cytostatic effect (Figure 3.7.). A low number of cells (1500/well) was seeded in quadruplicate in 96 well plates (with replicate plates for each time point), and allowed to settle overnight before various concentrations of KLM155 were added. MTT was added to replicate plates at each time point and the OD_{595nm} measured as a surrogate of cell number.

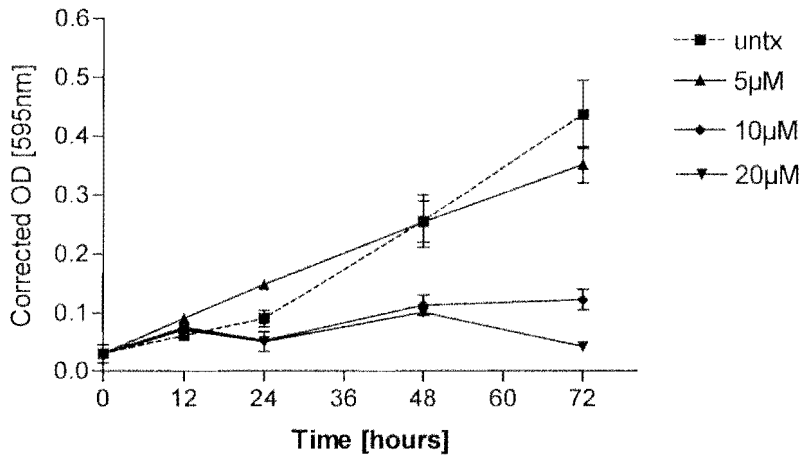

Figure 3.7. Growth curve of WHCO1 cells treated with varying concentrations of KLM155. Cells were plated at 1500 cells per well and allowed to settle overnight. They were then treated with varying concentrations of KLM155 and MTT reagent was added at the relevant time points. Each point represents the mean of 4 wells, with standard deviation, and this is representative of at least two independent experiments.

At the lowest concentration tested (5 μM), very little effect on WHCO1 cell growth was observed, though cell number was slightly higher than untreated cells at 12 and 24 hours. This may be a correlation with the increase in cell number seen at low concentration in the initial screening experiments (Figure 3.4.). At the higher concentrations tested (10 μM and 20 μM), cell number (or rather absorbance) remained very close to baseline, increasing only slightly at 72 hours for 10 μM treated cells. However, the readings were so close to the readings at time 0 that it was difficult to determine whether the effect of KLM155 at these concentrations was cytotoxic or cytostatic.

We thus performed a dose response curve plating a much higher number of cells (5000 per well) (Figure 3.8.). After allowing cells to settle overnight, KLM155 was added to quadruplicate wells at various concentrations. MTT was added to one set of untreated wells at this point to serve as a time 0 (indicated on the graph by a dotted line). After 24 hours both 5 and 10 μM KLM155 significantly decreased cell number below that of untreated, but cellular proliferation had still occurred, since the readings were higher than those at time 0. However both 20 μM and 50 μM KLM155 had decreased cell number below that at time 0, indicating a cytotoxic effect at these higher concentrations, and a cytostatic (perhaps combined with cytotoxic) effect at the lower concentrations.

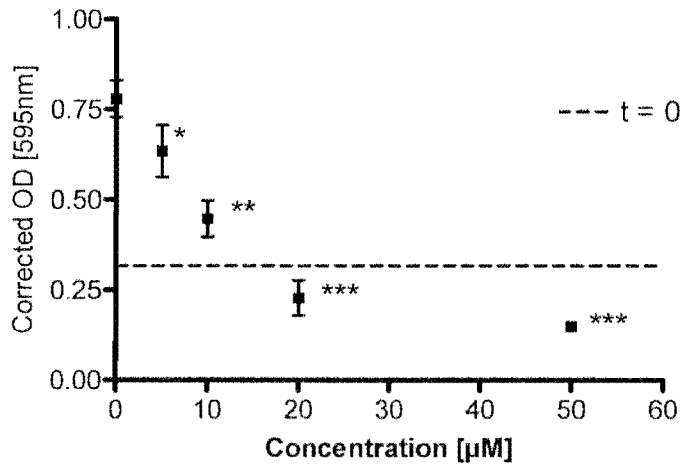

Figure 3.8. Death curve. WHCO1 cells treated with varying concentrations of KLM155. Cells were plated at 5000 cells/well and allowed to settle overnight. They were then treated with varying concentrations of KLM155 and grown for another 24 hours. MTT reagent was then added. The dotted line represents the absorbance reading at time zero. Each point represents the mean of 4 wells, with standard deviation, and this is representative of at least two independent experiments. (* $p<0.01$, ** $p< 0.005$, *** $p<0.001$ compared to untreated)

3.2.4. Effects of KLM155 and KLM156 on cell morphology

To observe the effect of the two most active KLMs (KLM155 and KLM156) on cell morphology, treated cells were viewed under light microscopy, and images captured using a Zeiss Axiovert 200 with an Axiocam camera and Axiovision 4.1 image software. Several morphological features were noted (Figure 3.9.).

The morphology of cells treated with 20 µM KLM155 for 24 hours is distinctly different to that of untreated cells. Cells are shrunken and rounded, and apoptotic bodies displaying typical membrane blebbing were observed (Figure 3.9.E).

Cells treated with 20 µM KLM156 were not as obviously affected as cells treated with KLM155, but on closer examination the morphology of adherent cells was slightly altered, while there were more floating cells than in untreated. Floating cells appeared intact in most cases, with very few apoptotic cells observed, but a large proportion of the floating cells appeared as doublets (Figure 3.9.F, inset), which indicated that there may be a cell cycle arrest in G2/M phase.

These morphological features were observed to a lesser extent after 6 hours of treatment.

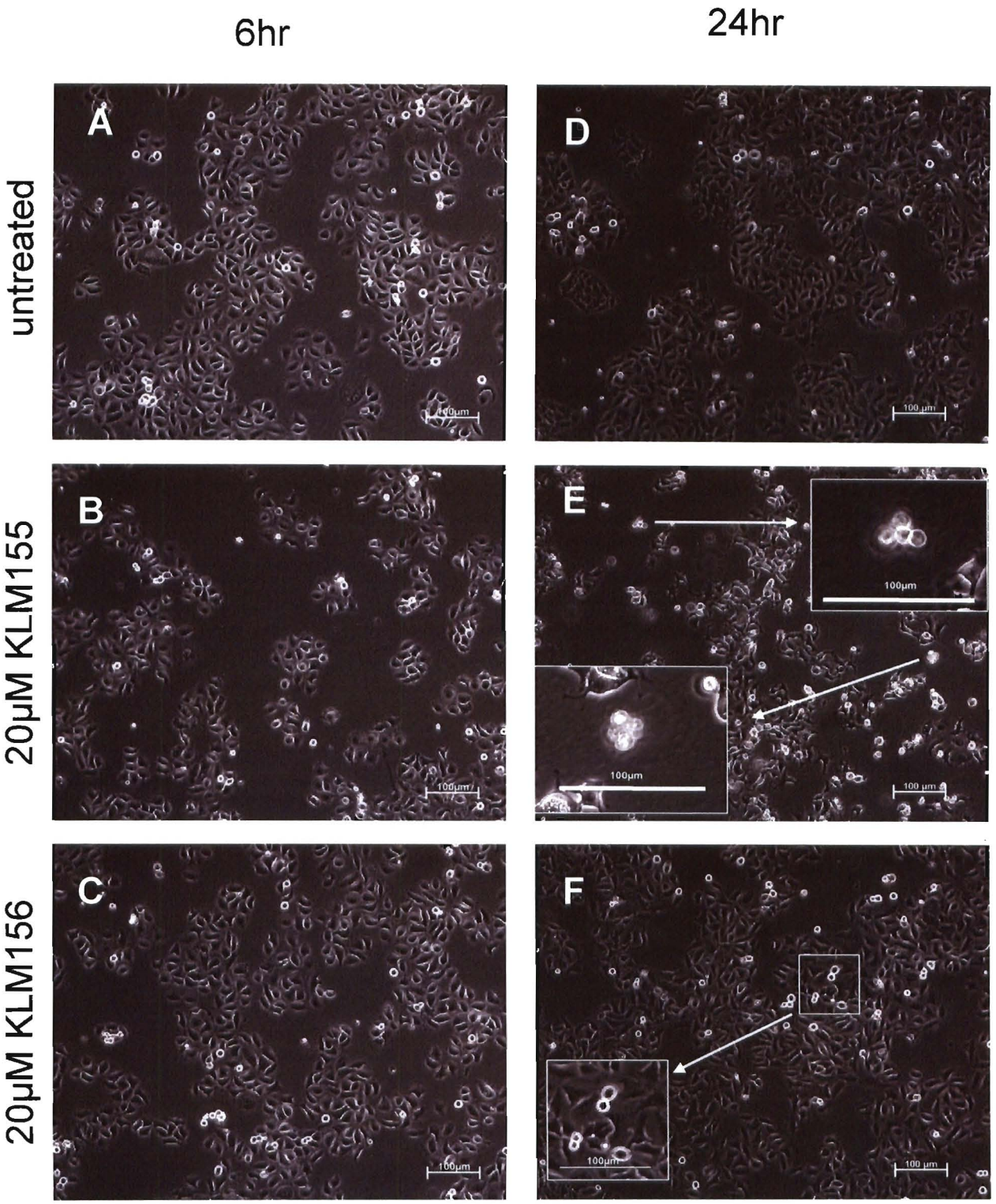

Figure 3.9. Morphological changes of cells untreated, or treated with 20μM KLM155 or KLM156 for 6 and 24 hours.

Cells were plated in 60mm dishes and after an overnight incubation to allow settling, KLM155 and KLM156 were added at 20μM. Photographs of the cells were captured using a Zeiss Axiovert 200 with an Axiocam camera and Axiovision 4.1 image software after 6 and 24 hours. Cells with membrane blebbing were observed in cells treated with KLM155 (inset in E) and cell doublets were observed in cells treated with KLM156 (inset in F).

3.2.5. Effects of treatment with KLM155 and KLM156 on the cell cycle

Cell cycle analysis was performed on cells treated with KLM155 and KLM156 to determine the effect these compounds might have on the cell cycle. Since we had observed an accumulation of cells with doublet morphology following treatment with KLM156, a G2/M cell cycle block was anticipated for this compound.

At the lowest concentration of KLM155 and KLM156 (2 μM and 10 μM), cell number remained similar (KLM155), or was slightly elevated (KLM156) compared to untreated, and the cell cycle profiles remained unchanged. However, at 20 μM both compounds caused substantial changes in cell cycle dynamics with a 26% increase in the G2 phase observed after treatment with both compounds (Figure 3.10). This was accompanied by a decrease in cell number to almost a third of untreated cells. At 50 μM the cell cycle in cells treated with KLM156 was completely dysregulated, while cells treated with KLM155 retained a G2 block.

The decrease in cell number seen at 10 μM in the death response curve (Figure 3.8.) was not observed in the cell cycle analysis. Several explanations for this can be considered. The first is the techniques used to measure cell number for the two assays differed. Cell number in the dose response curve was measured indirectly by MTT (reflecting metabolically active cells), while for cell cycle analysis cells were harvested by trypsinisation and counted using a haemocytometer. The processes of trypsinisation and centrifugation may have introduced some error in the cell counts, however this is unlikely to explain the large difference observed. The second, and more likely explanation for the lack of cell killing effect seen with 10 μM KLM155 in the cell cycle experiment, is the change in cell density as a result of scaling the experiment up to 60 mm dishes. For the MTT experiments, cells are plated at 1500 (or 5000) cells per well in a final volume of 100 μl giving a density of 3750 (or 12500) cells/cm^2 and 15 (or 50) cells/μl. However, for cell cycle analysis, cells are plated at 0.5x10^6 cells in a 6 cm dish in a final volume of 3 ml, which gives a density of 23809 cells/cm^2 and 166 cells/μl. Thus the final concentration of compound per cell, and the density of the cells are different. Similar effects of cell density (and indeed, even parental culture density) have been shown to affect the toxicity of tamoxifen and vinblastine in culture (119). However, we can consider 20 μM, which decreases cell number to half that of untreated cultures, to be equivalent to the IC_{50} concentration, and thus the cell cycle effects seen at this concentration to be indicative of those at IC_{50} concentrations in other formats (e.g. 96 well plate experiments).

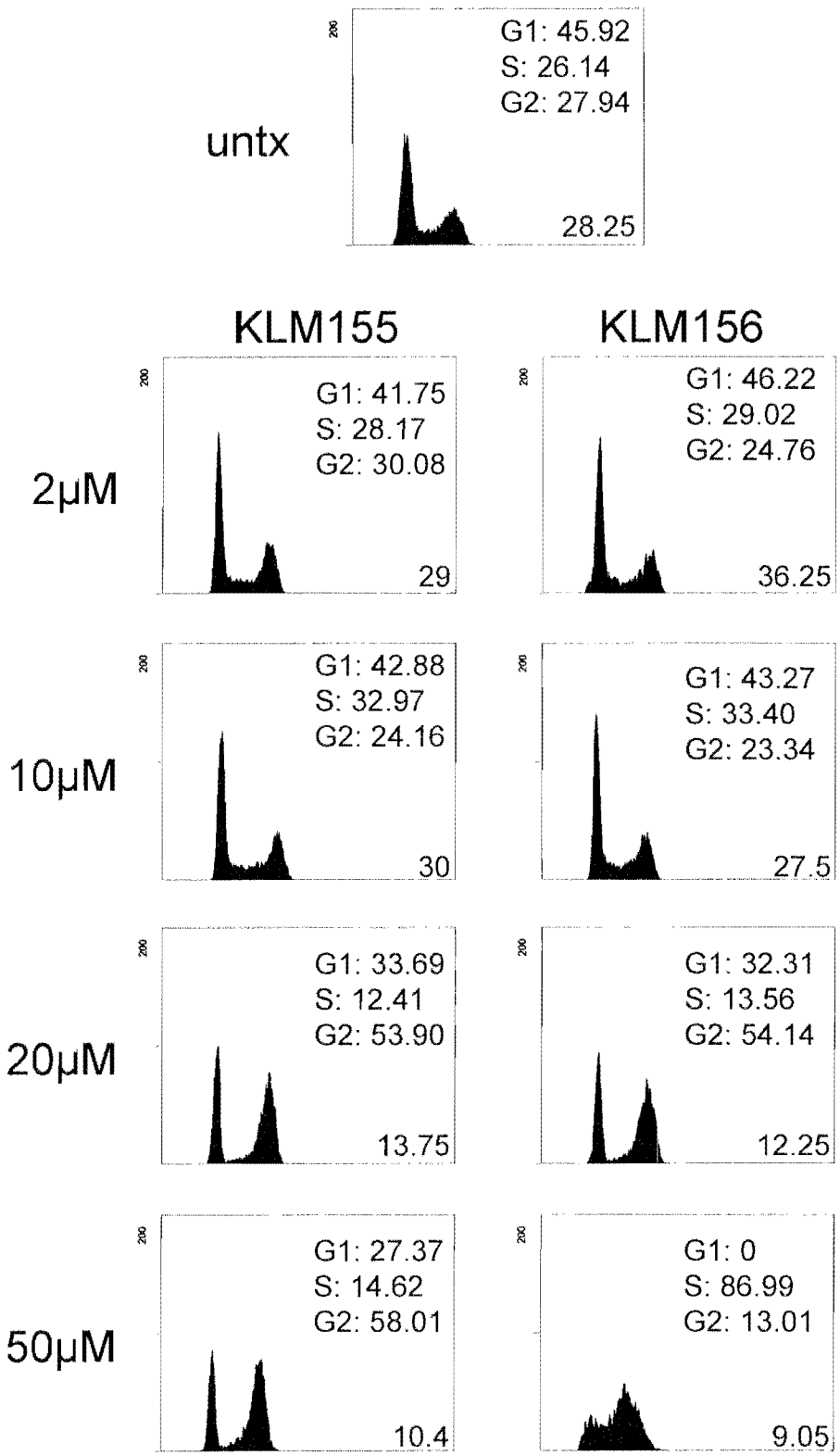

Figure 3.10. Cell cycle profiles for compounds treated with KLM155 or KLM156.

Cells were treated for 24 hours with the indicated concentrations of KLM155 and KLM156. They were then trypsinised, counted (numbers in the bottom right of each plot show the number of surviving cells $x10^5$ for that treatment condition), and then processed for cell cycle analysis as described in Materials and Methods. The x-axis indicates the amount of fluorescence, and the y-axis the number of cells. Results are representative of at least two independent experiments.

3.2.6. Determining the mode of cell death induced by KLM155 (apoptosis or necrosis)

It was important to determine the mode of cell death induced by the KLMs. Apoptosis is the preferred mechanism of cell death for chemotherapeutic agents so that inflammatory reactions are minimized.

Induction of apoptosis by KLM155 was assessed using a variety of techniques, all based on detecting the activation of the effector caspase 3. Initially an antibody against activated caspase 3, conjugated to a fluorescent molecule (FITC) was used to label cells, and fluorescence was detected by flow cytometry. Results using this technique indicated that 61% of cells treated with 25 μM KLM155 at 12 hours were undergoing apoptosis. These levels are similar to those induced by treatment with the positive control doxorubicin, while treatment with 30 μM KLM156 resulted in 35% of cells undergoing apoptosis (Figure 3.11.).

However, this technique involves considerable processing of the sample, and was not suitable for the large numbers of experimental conditions that would be required to test various time points, different concentrations or treatments with inhibitors.

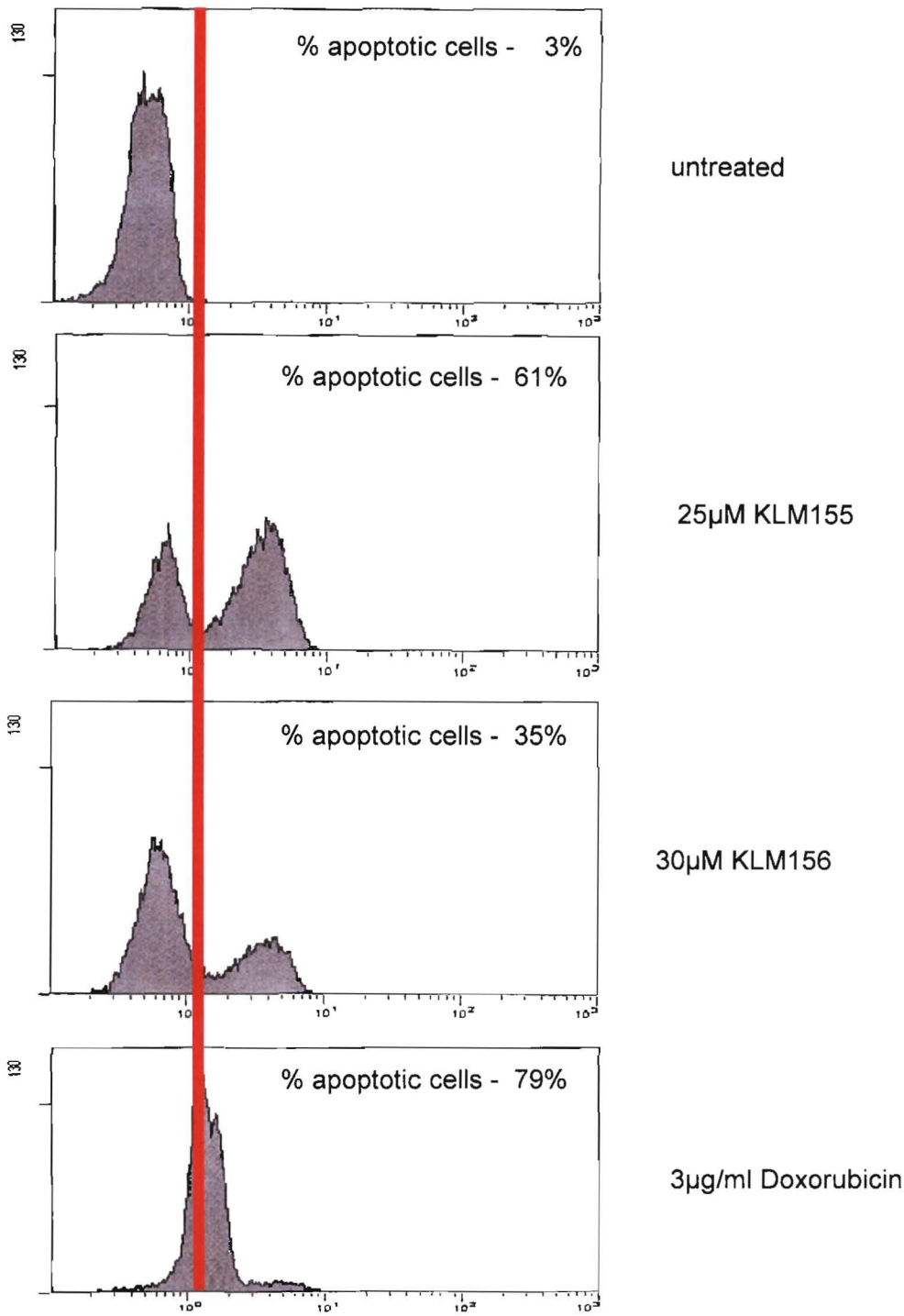

Figure 3.11. Apoptosis induction by KLM155 and KLM156 as measured using a fluorescent antibody to activated caspase-3.

Induction of apoptosis following 12 hours treatment with KLM155, KLM156 and 3μg/ml doxorubicin was measured using the Active Caspase-3 FITC Mab Apoptosis Kit (BD Biosciences) as described in Materials and Methods. Fluorescence was detected using flow cytometry. The x-axis represents fluorescence on a log scale, and the y-axis represents the number of cells.

We considered several approaches to measuring apoptosis in KLM155 treated cells, including DNA fragmentation, cleavage of a synthetic substrate (DEVD-AMC) to release a fluorescent molecule, and detection of PARP and procaspase 3 cleavage by Western Blot.

The assay we eventually used to measure apoptosis was the Caspase-Glo™ 3/7 Assay kit (Promega Cat#G8090), which relies on detection of luminescence after cleavage of a substrate by activated caspase 3 or caspase 7. Since the assay is designed for microplate format, it was suitable for a large number of sample conditions.

In a time course experiment apoptosis following treatment with 20 µM KLM155 was observed at 9 and 24 hours, but not at 3 hours, indicating that apoptosis induction occurs between 3 and 9 hours after treatment (Figure 3.12.).

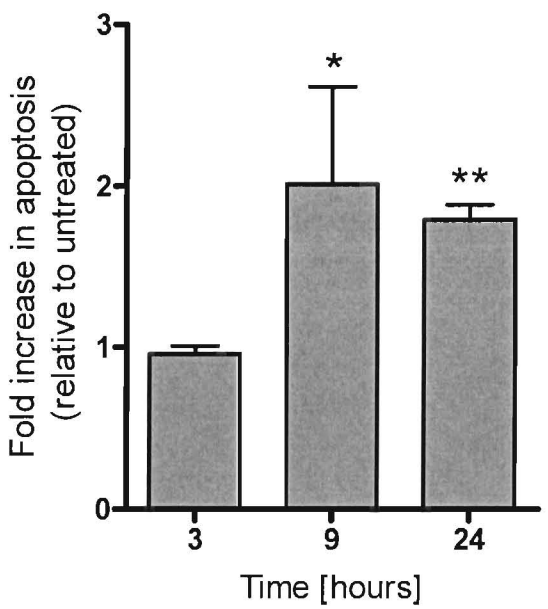

Figure 3.12. Time course of apoptosis induction by KLM155 measured using the Caspase-GloTM 3/7 Assay.

Cells were treated with KLM155 at 20µM in triplicate, and at the indicated times Caspase-Glo reagent was added, and the luminescence read on a Lumoscan plate reader. Values are the mean of triplicate wells, with standard deviation indicated by the error bars. (* $p < 0.05$; ** $p < 0.01$). Results are representative of at least two independent experiments.

Secondly we evaluated the effect of concentration on apoptosis induction. Cells were treated (in triplicate) with varying doses of KLM155, and after 9 hours, Caspase-Glo reagent was added, and the resulting luminescence measured (Figure 3.13). This indicated that lower concentrations of KLM155 (5 and 10 μM) did not induce apoptosis after 9 hours of treatment, but that the highest concentration tested (20 μM) did induce apoptosis.

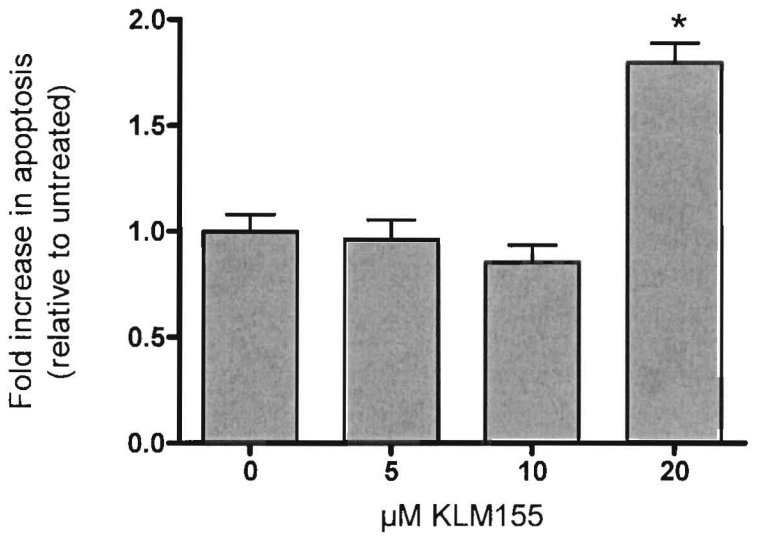

Figure 3.13. Apoptosis induction by KLM155 at varying concentrations.
The ability of differing concentrations of KLM155 were evaluated. Cells were treated in triplicate with the indicated concentrations of KLM155 for 9 hours. Caspase-Glo reagent was added, and the luminescence read on a Lumoscan plate reader. Values are the mean of triplicate wells, with standard deviation indicated by the error bars. (* $p < 0.001$). Results are representative of at least two independent experiments.

In order to confirm that cell death occurred only via the apoptotic pathway, and not by necrosis, we performed a necrosis assay using the CytoTox-ONE Homogeneous Membrane Integrity assay (Promega Cat#G7891). This kit contains a reagent cleaved by lactate dehydrogenase, which is released when cell membrane disruption occurs during necrosis, but not during early apoptosis. Thus fluorescence is a direct measure of the number of necrotic cells present. Cells were treated (in triplicate) with varying concentrations of KLM155, and at the indicated time points, CytotoxONE assay reagent was added to each well. A positive control using lysis buffer supplied with the kit was performed at each time point, and results are expressed as the percentage of fluorescent signal obtained for the control (Figure 3.14.). No significant increase in LDH activity was observed between untreated and treated cells at various time points.

We also established the integrity of the plasma membrane of KLM155 treated cells by examining the ability of cells to exclude trypan blue. Necrotic cells, with disrupted membranes would be unable to exclude trypan blue, as would cells in late apoptosis. Cells were treated, and at several time points, replicate wells were stained with trypan blue and examined for the presence of dead cells. None were observed (data not shown), confirming our observations that cell death is via apoptosis and not necrosis.

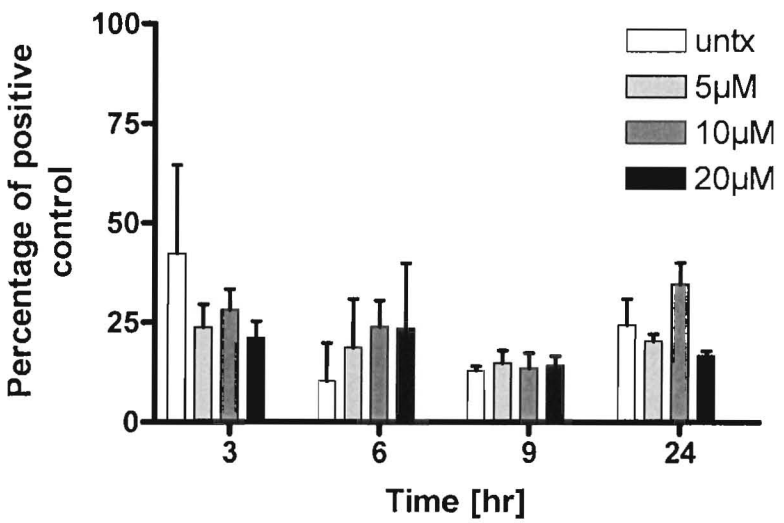

Figure 3.14. Necrosis induction by KLM155 at varying concentrations and times. The ability of differing concentrations of KLM155 to induce necrosis were evaluated. Triplicate wells were treated, and at the indicated time points CytotoxONE reagent was added. Fluorescence was then measured using a fluorescence plate reader. Values are the mean of triplicate wells, with standard deviation indicated by the error bars. This result is representative of at least two independent experiments.

3.3. Discussion

All the KLMs tested were soluble in aqueous solution and cytotoxic to the cell line used for screening (WHCO1) with IC_{50} concentrations below 100 μM. Compounds KLM155 and KLM156 of this family displayed considerable activity against cultured oesophageal cancer cells, with IC_{50} values of 9.8 μM and 12.9 μM, respectively. This compares favourably to the commonly used chemotherapeutic agent cisplatin, which has an IC_{50} value of 13 μM against WHCO1 (90).

Further IC_{50} experiments were performed with the most active compound (KLM155) against a range of cell lines, including another oesophageal cancer cell line (WHCO6), two cervical cancer cell lines (SiHa and ME180), and the breast epithelial line (MCF12A). KLM155 shows similar activity for the two oesophageal cancer cell lines, while the cervical cell line, ME180, and the breast epithelial line, MCF12A, were slightly less sensitive. The cervical cancer cell line, SiHa, was resistant to KLM155 up to the highest concentration tested (150 μM).

We showed that these compounds induce apoptosis, and this is consistent with other reports that quinone and hydroquinone compounds induce apoptosis in cancer cell lines. The natural anthroquinone derivative, emodin, has been shown to induce apoptosis in human lung adenocarcinoma cells (120), 4-hydroxyestradiol was found to induce apoptosis in human mammary epithelial cells (121) and two marine quinones, isolated from the Mediterranean ascidian *Aplidium conicum* were also shown to induce apoptosis in a lymphoma cell line (122). All these compounds induced apoptosis via the mitochondrial pathway following the production of reactive oxygen species.

Considering all our results obtained in the 96-well plate format (IC_{50} data, growth and death curves, and apoptosis and necrosis data) it appears that at low doses (5 and 10 μM) KLM155 reduces cell number in comparison to untreated by causing a decrease in cell proliferation, rather than cell death. At higher concentrations (20 μM), KLM155 clearly decreases cell number below that plated initially, and apoptosis is detected at these concentrations.

In cell cycle analysis, a larger format was used, and due to scaling of the experiment, a greater density of cells was used. Previous work has shown that plating density affects the sensitivity of cells to various agents (119), and we assume this accounts

for the different sensitivity of these cells (as measured using cell counting) to KLM155 in this format. If we consider the concentration of KLM155 that reduces cell number in the 60 mm dish by 50% to be roughly equivalent to the IC_{50} concentration, then we can equate the cell cycle changes (accumulation of cells in G2) at 20 μM KLM155 to the results obtained in 96-well plate format at 10 μM.

The comparative simplicity of these compounds, and the close structural relationships between them allowed us to make some tentative conclusions regarding the contribution of the different chemical moieties to the toxicity of these compounds. The central quinone/hydroquinone structure plays a key, consistent role in activity, which is consistent with previous observations of similar compounds (116). While the cell lines used in this paper differ from those used by Li *et al.* (116), this observation may be of use in rational drug design, and is likely to be linked to either the potential of these compounds to produce reactive oxygen species, or to the rearrangement of these compounds into alkylating agents.

The configuration and substitutions on the triprenyl side chain were also important, as evidenced by the superior activity of the all trans chain (KLM155) over the trans,cis chain (KLM156), and the hydroxyl substitution over the carbonyl (KLM159 vs KLM155). These differences in activity may be due to altered stability of the molecules, or due to altered specificity for enzymes.

Considering that KLM155 clearly induced apoptosis in oesophageal cancer cells, and that sufficient quantities of this compound were available, we embarked on another study to examine the mode of action of KLM155.

CHAPTER 4

ROLE OF OXIDATIVE STRESS IN THE ACTIVITY OF THE KLMs

4.1. Introduction

Having determined that the KLMs induce apoptosis in oesophageal cancer cells, we investigated the role of oxidative stress in the activity of these compounds. Current evidence suggests that the commonly used chemotherapeutic agents doxorubicin (which contains both quinone and hydroquinone moieties) and paclitaxel induce cell death at least in part through the production of reactive oxygen species (62;63;65). The potential of the KLMs to be involved in redox type reactions was confirmed when the literature was examined for similar compounds (120-125).

Despite the widespread use of quinone compounds in cancer chemotherapy, the contribution of the quinone moiety to the activity of these compounds remains to be fully elucidated, since most of these compounds contain other structural moeitiesthat may also contribute to the biological activity (117). We hoped that by elucidating the action of the KLMs, which are relatively simple compounds, we could determine the contributions of the quinone and the side chain to ROS generation and activity.

4.1.1. Experimental approach

We tested the ability of the KLM155 to produce ROS, using the fluorescent probe DCF-DA. Having confirmed production of ROS by this compound, we evaluated the levels of ROS produced by all the compounds, and correlated this to the activity measured in Chapter 3. To evaluate the contribution of ROS production to cell death, we treated cells with KLM155 in the presence and absence of the ROS scavengers BHA and Trolox, and assessed cell survival and apoptosis.

As a further confirmation that the KLMs induced oxidative stress, we performed microarray analysis in KLM155 treated cells. The majority of the genes we identified as being upregulated were involved in antioxidant response pathways or repair of DNA and protein damage.

To establish the pathways by which these genes are upregulated, and by which apoptosis occur, we examined the signaling of various stress response pathways in response to KLM treatment and identified c-Jun as being upregulated. Further experiments inhibiting signaling via the JNK stress signaling pathway were performed to establish the importance of this response in KLM induced cell death.

4.2. Results

4.2.1. Production of reactive oxygen species in response to KLM treatment

We used the ROS sensitive probe 2',7'-dichloro-fluorescein diacetate (DCF-DA) to measure ROS generation in KLM treated cells. This compound is a cell-permeant indicator for reactive oxygen species that is nonfluorescent until the acetate groups are removed by intracellular esterases and oxidation occurs within the cell(126;127). It detects the presence of hydrogen peroxide and multiple radicals – the peroxyl and hydroxyl in particular. Experiments were carried out by pretreating WHCO1 cells with DCF-DA, then treating with KLM155, and visualizing fluorescence using a fluorescent microscope. A dose dependant generation of reactive oxygen species could be observed (Figure 4.1.). Cells treated with higher concentrations of KLM155 and KLM156 had more cells fluorescing, and brighter fluorescence than cells treated with lower concentrations, or untreated cells. However this protocol is very sensitive to temperature, pH and light, and the results were hard to quantitate and reproduce, and thus other approaches were explored to determine ROS production.

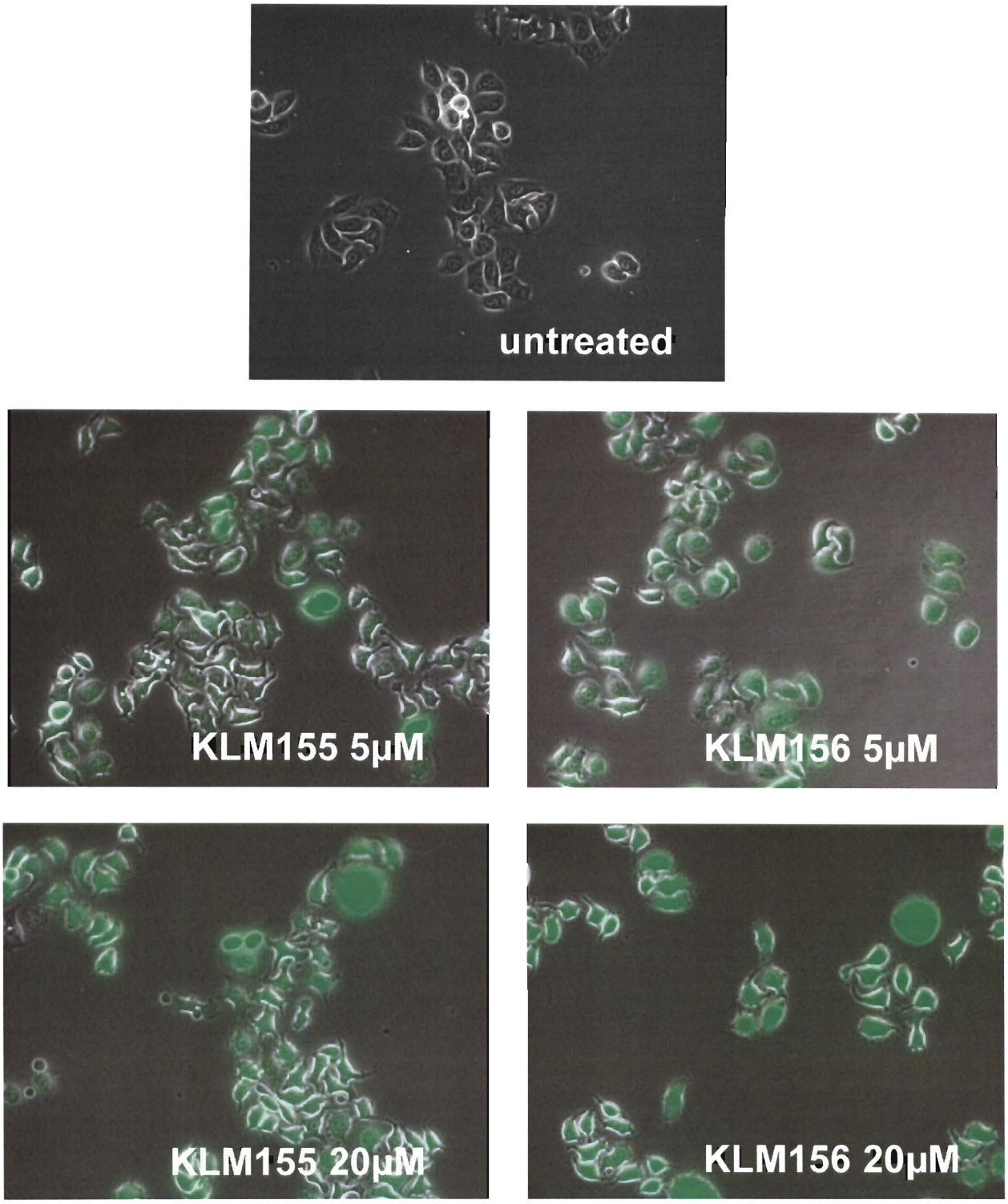

Figure 4.1. ROS production in cells treated with KLM155 and KLM156.

To determine if treatment of WHCO1 cells with KLM155 and KLM156 induces ROS production, cells were pretreated for 15 minutes with the fluorescent probe DCF-DA (25μM). They were then incubated with KLM155 or KLM156 at 5 or 20μM for 30 minutes, and fluorescence observed using a Zeiss Axiovert 200 with an Axiocam camera and Axiovision 4.1 image software. The fluorescence and phase contrast images were overlaid to give the pictures above.

A similar protocol was established where cells were pretreated for 15 min with DCF-DA and the resulting fluorescence following treatment with KLMs was measured using a flow cytometer. This allowed quantification of the levels of fluorescence (and thus reactive oxygen species) in each cell. This approach has been used previously to measure ROS production in cancer cells following treatment with a range of chemicals (121;128).

Initial experiments to measure the levels of ROS in cells treated with KLM155 indicated generation of reactive oxygen species at higher concentrations, with ROS generation at 20 μM three fold higher than that of untreated cells (Figure 4.2.). ROS generation at 5 μM was not significantly different from that of untreated cells, while a slight increase (1.3 fold) was noted at 10 μM ($p<0.05$). Of particular interest, this pattern of ROS production resembled the pattern of apoptosis induction at the same concentrations (Figure 3.13.).

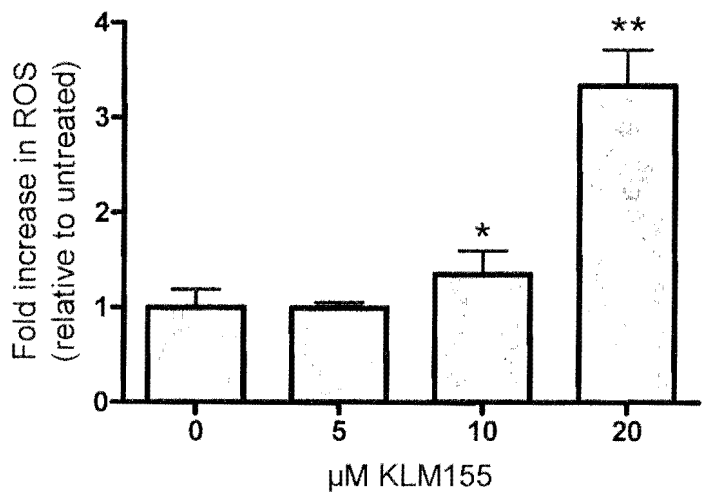

Figure 4.2. ROS generation by KLM155 in WHCO1 cells.

Cells were pretreated with 25μM DCF-DA for 15 minutes, and then treated with the indicated concentrations of KLM155. After 1 hour, cells were harvested by trypsinisation, and fluorescence was assessed by flow cytometry. Values are the mean of three replicates with standard deviation. (* $p<0.05$, ** $p<0.001$). This result is representative of at least two independent experiments.

A time course of ROS production, using 20 μM KLM155 revealed that reactive oxygen species were generated as early as 15 min after treatment, and increased up to 2 hours (the limit of the experiment) (Figure 4.3.).

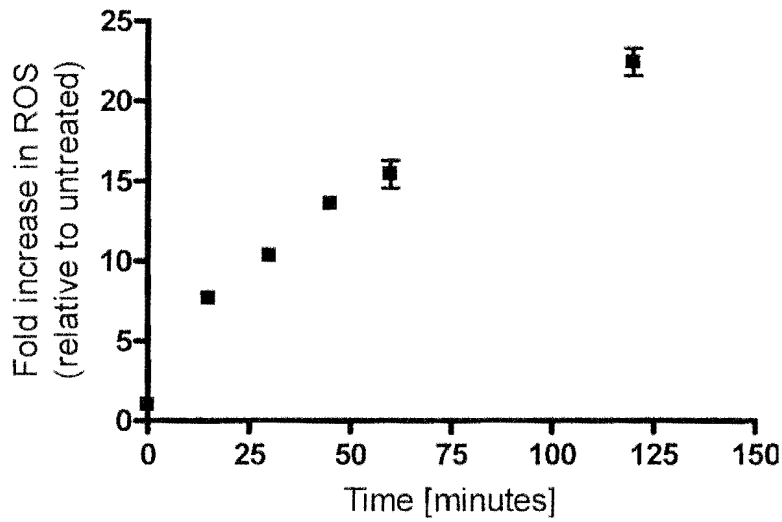

Figure 4.3. Time course of ROS generation by 20μM KLM155 in WHCO1 cells. Cells were pretreated with 25μM DCF-DA for 15 minutes, then treated with 20μM KLM155 for the indicated times. Pretreatment and treatment were staggered to allow harvesting (by trypsinisation) at the same time. Fluorescence was assessed by flow cytometry. Values are the mean of 3 replicates with standard deviation. This result is representative of at least two independent experiments.

We proceeded to test whether the other KLM compounds produce ROS, by testing the levels of ROS generated by each compound at 20 μM. Not only did all the KLM compounds generate reactive oxygen species to a greater or lesser extent, we also observed a correlation between the levels of ROS and the activity of each compound. The correlation showed that the more active compounds generated more ROS than less active compounds. A plot of the IC_{50} values for each compound against the levels of ROS generated at 20 μM showed a direct correlation between ROS generation and activity (Figure 4.4.) with an R^2 value of 0.67. If we consider KM158 as an outlier (since its structure differs substantially from the other compounds), and exclude it from the analysis, the R^2 value improves to 0.83. This indicates a strong correlation between activity (as measured by IC_{50} values) and ROS production.

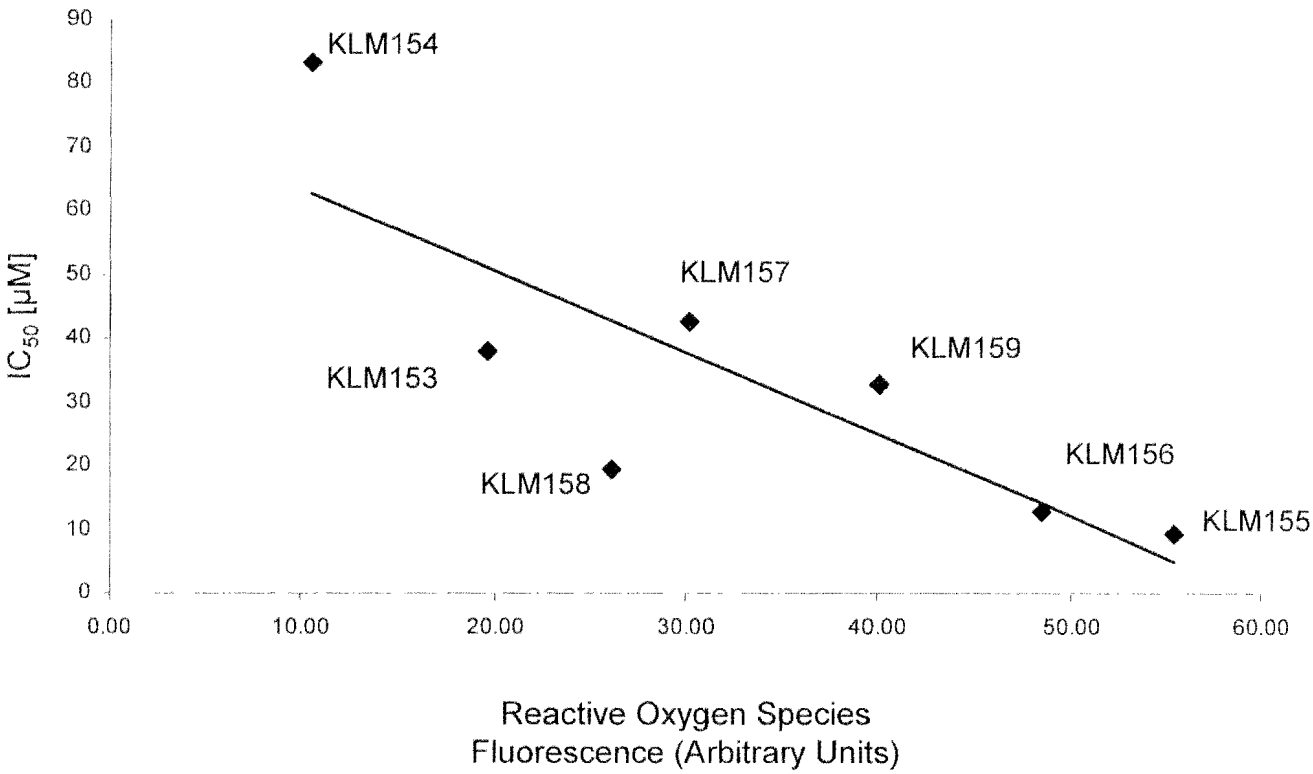

Figure 4.4. Correlation of IC_{50} concentration with ROS generation.

The IC_{50} for each compound (as determined by dose response curves, Table 3.2) was correlated with the level of ROS produced by that compound at 20μM (measured using DCF-DA and flow cytometry as outlined in Materials and Methods). A linear relationship between the two exists, with an R^2 value of 0.67. If the outlier KLM158 is excluded from the analysis, the R^2 value improves to 0.83, indicating a strong correlation between IC_{50} and ROS production. The determination of ROS production was performed in at least two independent experiments.

4.2.2. Inhibition of ROS production by the scavengers Trolox and BHA

To confirm whether the cell death observed was mediated via production of ROS, we treated cells in the presence and absence of the ROS scavengers Trolox (100 µM) and BHA (100 µM) and assessed the cells for apoptosis and survival.

When ROS scavengers were added to cells prior to treatment with KLM155, a reduction in caspase 3 activity was observed, with BHA decreasing activity by 73% ($p<0.01$) and Trolox decreasing caspase 3 activity by 66% ($p<0.05$) (Figure 4.5.). (This analysis uses treated as 100% and untreated as 0%).

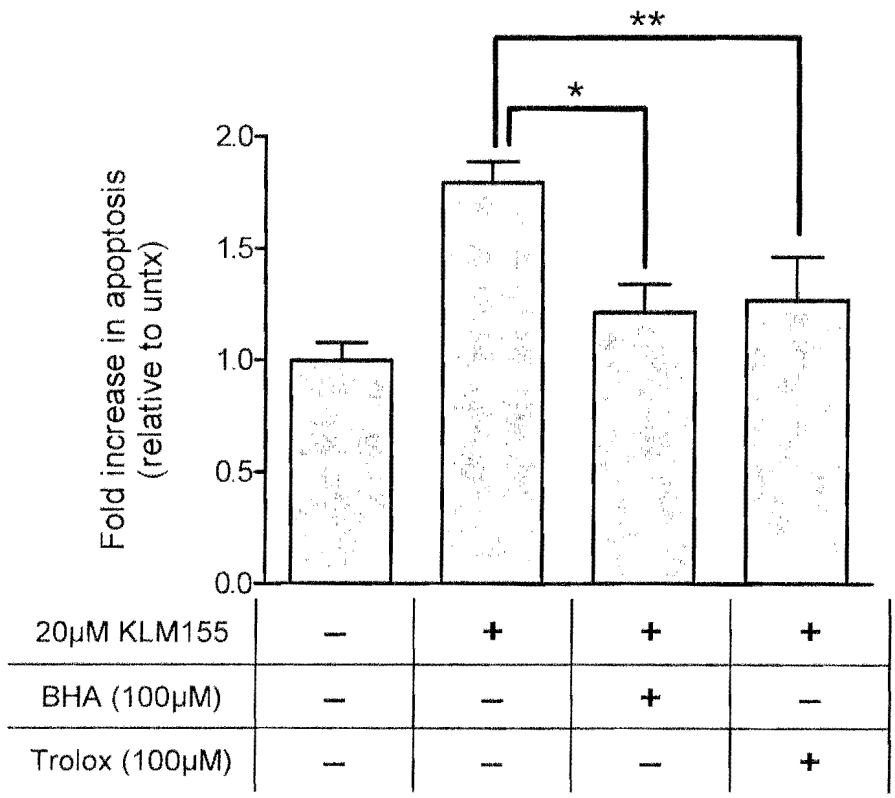

Figure 4.5. Inhibition of KLM155 induced apoptosis by addition of ROS scavengers. Cells were pretreated with the ROS scavengers Trolox or BHA, and then treated with KLM155 at 20µM. For each condition of scavenger, one set of wells (in quadruplicate) were treated, and one set used as control. Apoptosis was assessed using the Caspase-Glo kit after 24 hours of treatment, and values were expressed as fold increase in apoptosis relative to the KLM-untreated control for each scavenger. Values are the mean of triplicate wells, and error bars indicate standard deviation. (* $p<0.01$, ** $p<0.05$). This result is representative of at least two independent experiments.

A significant increase ($p<0.01$) in the survival of cells treated with the ROS scavenger Trolox and KLM155 was observed, compared to cells treated with KLM155 alone (Figure 4.6). While a similar trend was observed with BHA, this effect was not significant ($p=0.1$) The lack of correlation between decrease in apoptosis and increase in cell number for BHA treated cells needs to be explored further. The effect of BHA and Trolox on KLM155 mediated cell death was tested in at least two separate experiments with similar results to those reported in Figure 4.6.

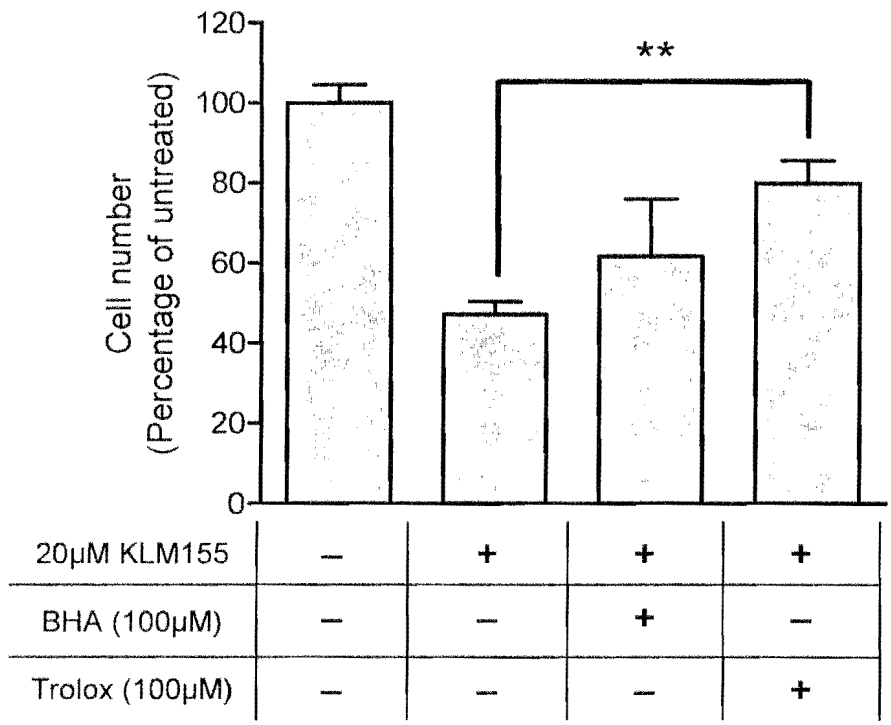

Figure 4.6. Prevention of KLM155 induced cell death by the addition of ROS scavengers. Cells were pretreated with the ROS scavengers Trolox or BHA, and then treated with KLM155 at 20μM. For each condition of scavenger, one set of wells (in quadruplicate) were treated, and one set used as control. The number of remaining cells was assesed using the MTT assay after 24 hours, and these values expressed as percentage of the KLM untreated control for each condition. Values are the mean of quadruplicate wells, and error bars indicate standard deviation. (** $p<0.001$) This result is representative of two independent experiments.

4.2.3. Transcriptional changes following treatment with KLM155

Our findings that KLM155 mediates cell death by producing ROS, suggested that a number of antioxidant mechanisms might be activated in order to respond to the oxidative stress. To further confirm that KLM treatment induced oxidative stress, we performed microarray analysis to evaluate the transcriptional response of WHCO1 cells to KLM155 treatment. This could provide information about a variety of antioxidant response and repair systems that may be induced by KLM155 treatment.

RNA for gene expression analysis was prepared from three replicate dishes of WHCO1 cells treated with 20 μM KLM155. Untreated controls in triplicate served as controls. After treatment, each dish was harvested separately using Trizol reagent to isolate total RNA. mRNA was amplified, labeled with Cy5 dye, and used in microarray analysis. An array was performed for each sample, with a human reference RNA sample (labeled with Cy3 dye) consistant across the arrays. Arrays were scanned and results generated in GenePix Pro uploaded into the NCI microarray database (MaDB) for further analysis.

Comparisons of genes with altered expression between the untreated and KLM155 treated groups revealed a number of genes at a p value of 0.05.

A total of 179 genes were identified as having altered expression in KLM155 treated cells compared to untreated cells. Restriction of the list to genes that were either 1.5 fold upregulated or 1.5 fold downregulated, limited the number to 23 genes of which 20 are known. Of these 23 genes, 13 were upregulated and 10 downregulated (Table 4.1.).

Gene	Description	Fold up	Fold down	p-Value
HO1	heme oxygenase (decycling) 1	8.13	0.12	0.00465
TXNRD1	Thioredoxin reductase 1	2.69	0.37	0.018
	Human DNA sequence from clone RP5-1103G7 on chromosome 20p12.2-13.	3.66	0.27	0.01846
FTH1	Ferritin, heavy polypeptide 1	1.64	0.61	0.02137
UQCRQ	Ubiquinol-cytochrome c reductase, complex III subunit VII, 9.5kDa	1.76	0.57	0.0373
ATP5C1	ATP synthase, H+ transporting, mitochondrial F1 complex, gamma polypeptide 1	1.61	0.62	0.03665
SGCB	Sarcoglycan, beta (43kDa dystrophin-associated glycoprotein)	1.65	0.61	0.00786
	ATP synthase, H+ transporting, mitochondrial F1 complex, alpha subunit, isoform 1, cardiac muscle	1.64	0.61	0.02647
DSTN	Destrin (actin depolymerizing factor)	1.53	0.65	0.02278
ELMO1	Engulfment and cell motility 1	1.61	0.62	0.04964
PAX3	Paired box gene 3 (Waardenburg syndrome 1)	1.62	0.62	0.02833
UBE2L3	Ubiquitin-conjugating enzyme E2L 3	1.63	0.61	0.00437
WFS1	Wolfram syndrome 1 (wolframin)	1.56	0.64	0.03453
FLJ38973	Hypothetical protein FLJ38973	0.65	1.53	0.00038
FABP7	Fatty acid binding protein 7, brain	0.6	1.66	0.03449
SSR1	Signal sequence receptor, alpha (translocon-associated protein alpha)	0.6	1.67	0.0429
	Unknown	0.61	1.63	0.04346
TTRAP	TRAF and TNF receptor associated protein	0.6	1.66	0.01011
RPS6KA1	Ribosomal protein S6 kinase, 90kDa, polypeptide 1	0.52	1.94	0.01314
PTN	Pleiotrophin (heparin binding growth factor 8, neurite growth-promoting factor 1)	0.6	1.66	0.02898
	ESTs	0.56	1.78	0.01804
RPL7	Ribosomal protein L7	0.55	1.82	0.04828
HSP90B1	Heat shock protein 90kDa beta (Grp94), member 1	0.47	2.11	0.04695
DDIT3	DNA-damage-inducible transcript 3	1.32	0.76	0.00655

Table 4.1. Genes up or down regulated in response to KLM155 treatment.
Microarray analysis was performed on triplicate untreated and treated (20μM KLM155 for 8 hours) samples, and data were analysed using MaDB software. This table presents the genes identified to be differentially expressed between treated and untreated samples, with a significant ($p<0.05$) increase or decrease in expression greater than 1.5 fold. The fold difference has been presented as both fold up (treated/untreated) and fold down (untreated/treated) in treated samples. The final gene identified (DNA-damage-inducible transcript 3) was included despite a lower fold upregulation because of its extremely high significance value.

Of these 23 genes, we selected four that were considered to be of most interest to validate using quantitative real-time RT-PCR. We chose genes that are involved in cellular stress responses, and were highly (>2 fold) up- or down-regulated in our array results. These were heme oxygenase 1, thioredoxin reductase, GADD34 (DNA damage inducible transcript 3) and HSP90. We also decided to evaluate the expression of two antioxidant genes (MnSOD and glutathione reductase), the quinone metabolizing enzyme, NQO1, and the molecular chaperone HSP70 (since another molecular chaperone, HSP90, was downregulated). GAPDH was used as the housekeeping gene for normalization.

Sequence and PCR conditions for each gene are in Table 6.3. in Materials and Methods. Real time PCR was carried out using the LightCycler FastStart DNA Master SYBR Green I reaction mix (Roche) on a LightCycler Instrument (Roche), and results were normalized using the $2^{-\Delta\Delta CT}$ method (129).

Heme oxygenase 1 is involved in the breakdown of heme, which is released from heme-containing enzymes when they are damaged by ROS (130). The gene for heme oxygenase showed the most upregulation on the array, with an 8 fold increase in treated compared to untreated cells ($p = 0.005$). Real time RT-PCR confirmed this upregulation (Figure 4.7.). In fact, the level of upregulation was much higher than that initially indicated by the microarray data with an upregulation of 102.7 fold ($p = 0.002$) over untreated.

The thioredoxin system is an antioxidant defense system. Thioredoxin is easily oxidized by ROS, and is then reduced by thioredoxin reductase, with NADPH as a cofactor (131). The gene for thioredoxin reductase was upregulated 2.7 fold in our array data ($p = 0.018$), and real time RT-PCR confirmed this upregulation, with a 2.6 fold induction in cells treated with KLM155 compared to untreated cells ($p = 0.029$) (Figure 4.8.).

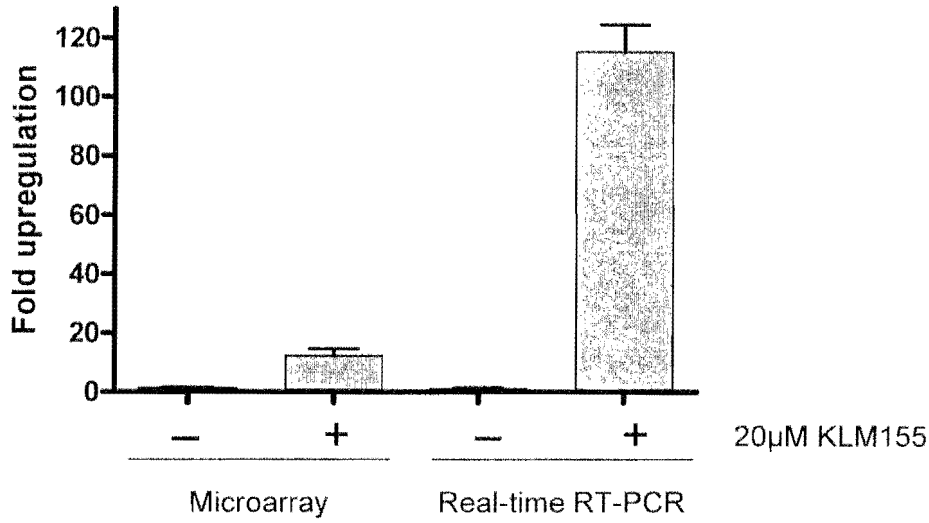

Figure 4.7. Microarray and Real time RT-PCR analysis for Heme oxygenase.

RNA from untreated and treated (20μM KLM155 for 8 hours) cells was analysed by microarray or quantitative real-time RT-PCR for the gene encoding heme oxygenase. Each bar represents the mean of triplicate samples, and error bars indicate standard deviation.

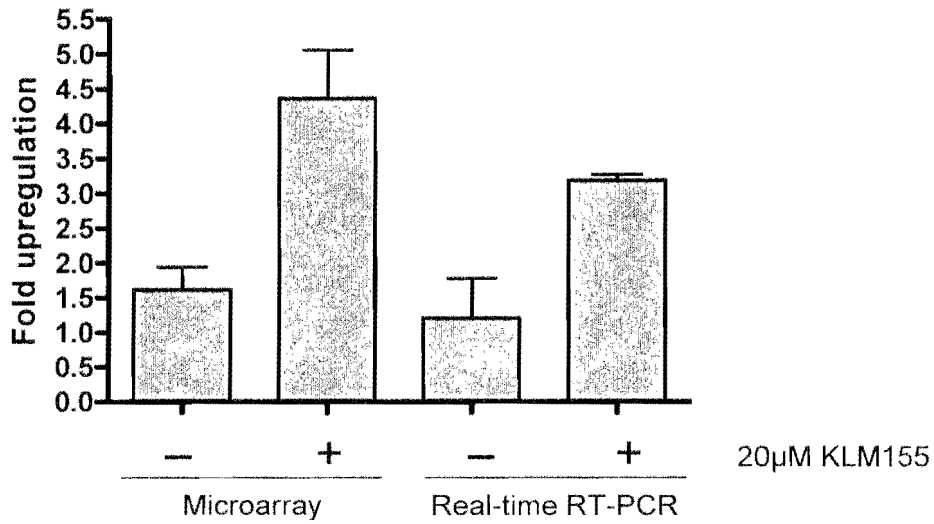

Figure 4.8. Microarray and Real time RT-PCR analysis for Thioredoxin reductase.

RNA from untreated and treated (20μM KLM155 for 8 hours) cells was analysed by microarray or quantitative real-time RT-PCR for the gene encoding thioredoxin reductase. Each bar represents the mean of triplicate samples, and error bars indicate standard deviation.

GADD34 (DNA damage inducible transcript 3) is induced in response to cell cycle arrest and DNA damage (ref 2 in Morton, 2006), plays a role in preventing protein synthesis under stress conditions, and can also suppress cell growth (132). Even though this gene was below the cut-off of 1.5 fold up or down regulated, we included it in the analysis because it was significantly upregulated ($p = 0.007$), and the biological action of the product of this gene may have some relevance in the action of the KLMs on cells. Real-time RT-PCR analysis showed much higher activation of this gene, with 6 fold upregulation, ($p = 0.004$) (Figure 4.9.).

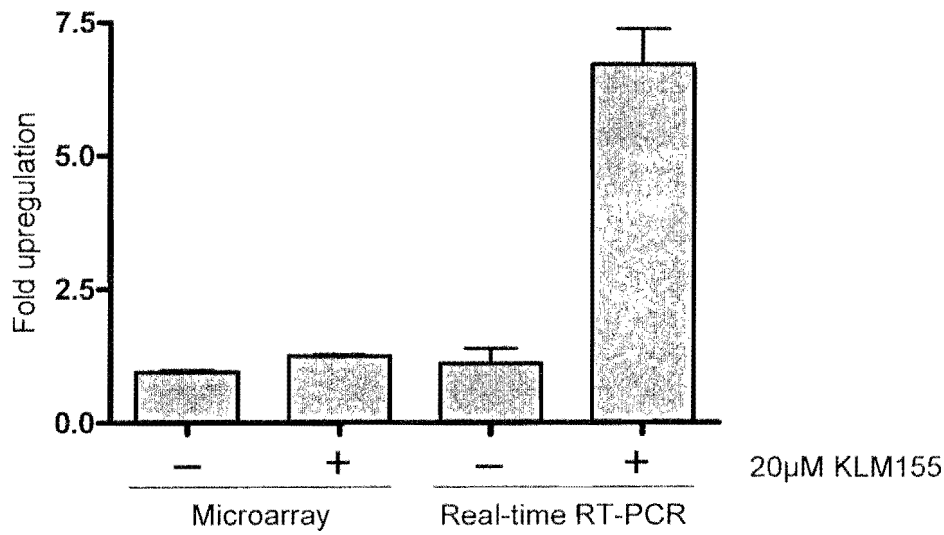

Figure 4.9. Microarray and Real time RT-PCR analysis for GADD34.

RNA from untreated and treated (20μM KLM155 for 8 hours) cells was analysed by microarray or quantitative real-time RT-PCR for the gene encoding DNA-damage-inducible transcript 3 (GADD34). Each bar represents the mean of triplicate samples, and error bars indicate standard deviation.

The heat shock proteins play key roles in protein folding and in stress responses, and prevent misfolding and aggregation of damaged proteins (133).The chaperone HSP90 was downregulated 2 fold ($p = 0.047$) in our microarray analysis, but real-time RT-PCR analysis did not show a significant difference between untreated and KLM155 treated cells. However, we also determined the expression of HSP70 in treated and untreated cells using real-time RT-PCR and determined that HSP70 expression was upregulated 2.8 fold ($p = 0.025$) (Figure 4.10.).

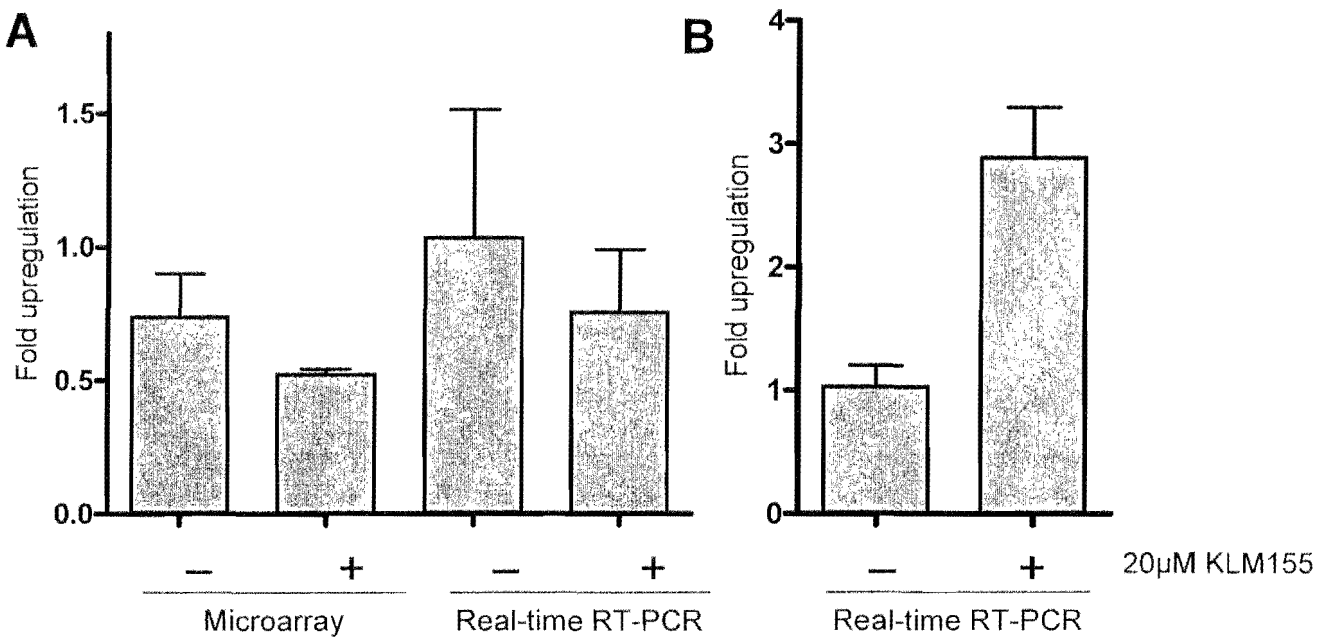

Figure 4.10. Microarray and Real-Time RT-PCR analysis for HSP90 (A) and Real-Time RT-PCR analysis for HSP70 (B).

RNA from untreated and treated (20μM KLM155 for 8 hours) cells was analysed by microarray or quantitative real-time RT-PCR for the genes encoding HSP90 and HSP70. Each bar represents the mean of triplicate samples, and error bars indicate standard deviation.

We evaluated the expression of two genes encoding antioxidant enzymes – manganese SOD (MnSOD) and glutathione reductase. We hypothesized that since the KLM155 causes the production of ROS, cells treated with this compound may increase levels of antioxidant proteins in order to combat this stress. However, neither of these genes showed any significant alteration in expression following KLM155 treatment, as measured using real time PCR (Figure 4.11).

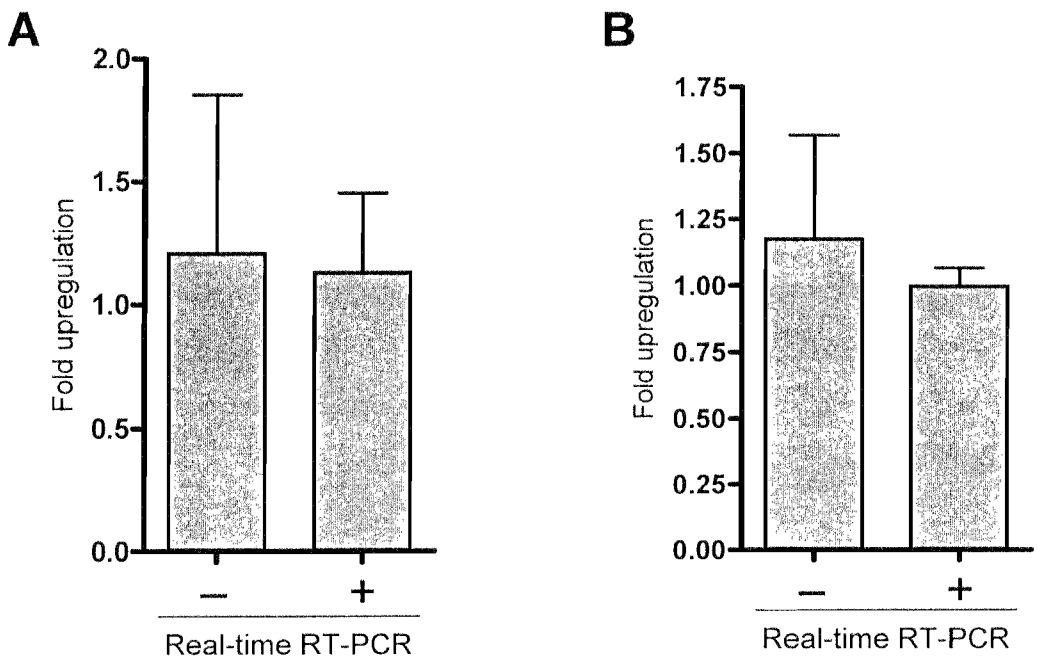

Figure 4.11. Real-Time RT-PCR analysis for MnSOD (A) and Glutathione reductase (B). RNA from untreated and treated (20μM KLM155 for 8 hours) cells was analysed by quantitative real-time RT-PCR for the genes encoding MnSOD and Glutathione reductase. Each bar represents the mean of triplicate samples, and error bars indicate standard deviation.

Finally we examined the levels of NQO1 in response to treatment with KLM155. NQO1 is a metabolic enzyme that metablises quinones via a two electron reduction into the corresponding hydroquinone. This is often a detoxifying step, but in some cases the hydroquinone is more toxic that the parent quinone. NQO1 was upregulated 7.6 fold in treated cells, compared to untreated cells ($p = 0.013$) (Figure 4.12.).

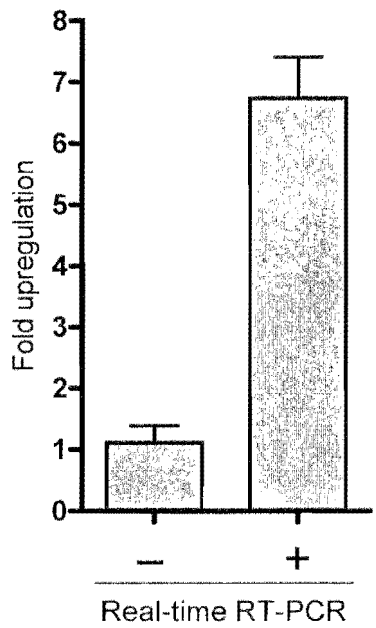

Figure 4.12. Real-Time RT-PCR analysis for NQO1.

RNA from untreated and treated (20μM KLM155 for 8 hours) cells was analysed by quantitative real-time RT-PCR for the gene encoding NQO1. Each bar represents the mean of triplicate samples, and error bars indicate standard deviation.

4.2.4. Effect of KLM treatment on signal transduction pathways

The previous sections have convincingly demonstrated that KLM155 treatment of cells is associated with the generation of ROS. The production of ROS in cells is often associated with the activation of stress signaling pathways like the MAPK kinase pathways, e.g. JNK or p38 (Figure 4.13.) (128;134-136). This can lead to the upregulation of antioxidant response genes, or to cell death, depending on the duration and intensity of ROS exposure (136). Since we had observed upregulation of a number of stress response genes, we determined whether the ROS production induced by KLM treatment leads to activation of the stress signaling pathways most commonly observed in ROS stress, namely the p38 and JNK pathways.

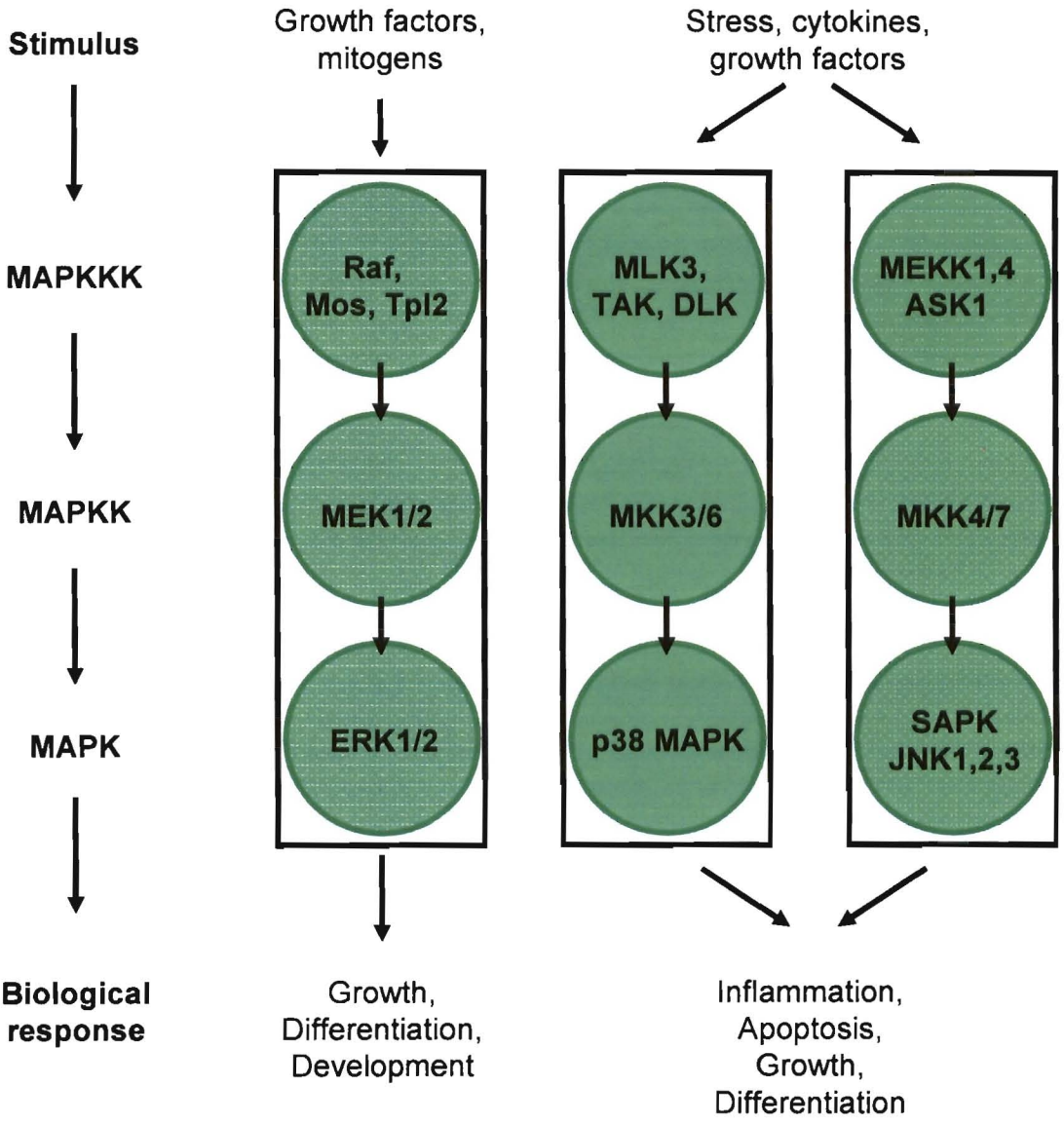

Figure 4.13. The ERK, p38 and JNK-MAPK signalling pathways.
Signal transduction through the MAPK pathways occurs by the sequential activation by phosphorylation of a series of kinases. The effector molecules (Mitogen activated protein kinases, or MAPKs) are activated by MAPKK (MAPK kinase), which in turn was activated by a MAPKKK (MAPKK kinase). (Figure adapted from http://www.cellsignal.com/)

Protein lysates from cells treated with varying concentrations of KLM155 were harvested at 6 and 24 hours after treatment. The levels of phosphorylated p38 (p-p38) and c-Jun in these lysates was evaluated using Western blot analysis (Figure 4.14.). c-Jun levels increased in treated cells in a concentration dependant manner at both 6 and 24 hours (Figure 4.14.A.). While p-p38 levels in KLM155 treated cells increased to almost 3 times as high as in untreated cells after 24 hours of treatment, levels in both treated and untreated cells were extremely low in comparison to a positive control of protein lysates from UV treated cells included on the blot (Figure 4.14.B., lane 9).

c-Jun is known to be both pro- and anti-apoptotic depending on the cellular environment and other signals, and regulates antioxidant genes among others, enabling the cell to deal with the damage caused by ROS. Upregulation of c-Jun was observed even at concentrations where ROS levels were low, and cell death did not occur, indicating that c-Jun may have different effects at low and high concentrations of KLMs. The effects of c-Jun are known to vary depending on the duration and intensity of the signaling via the JNK pathway under conditions of stress (136).

While we demonstrated increased levels of c-Jun, we did not examine levels of phosphorylated c-Jun since there is evidence in the literature to show that upregulation of c-Jun corresponds with an increase in activity (137;138), and our examination of the transcriptional profile of KLM155 treated cells had strongly indicated activation of either the JNK or p38 signaling pathway.

We used total ERK1/2 as a loading control since levels of other housekeeping genes (tubulin, actin) are known to vary during the cell cycle, and would thus be altered in treated cells undergoing a cell cycle block. We also confirmed equal protein loading by staining both the gels and the membrane after transfer.

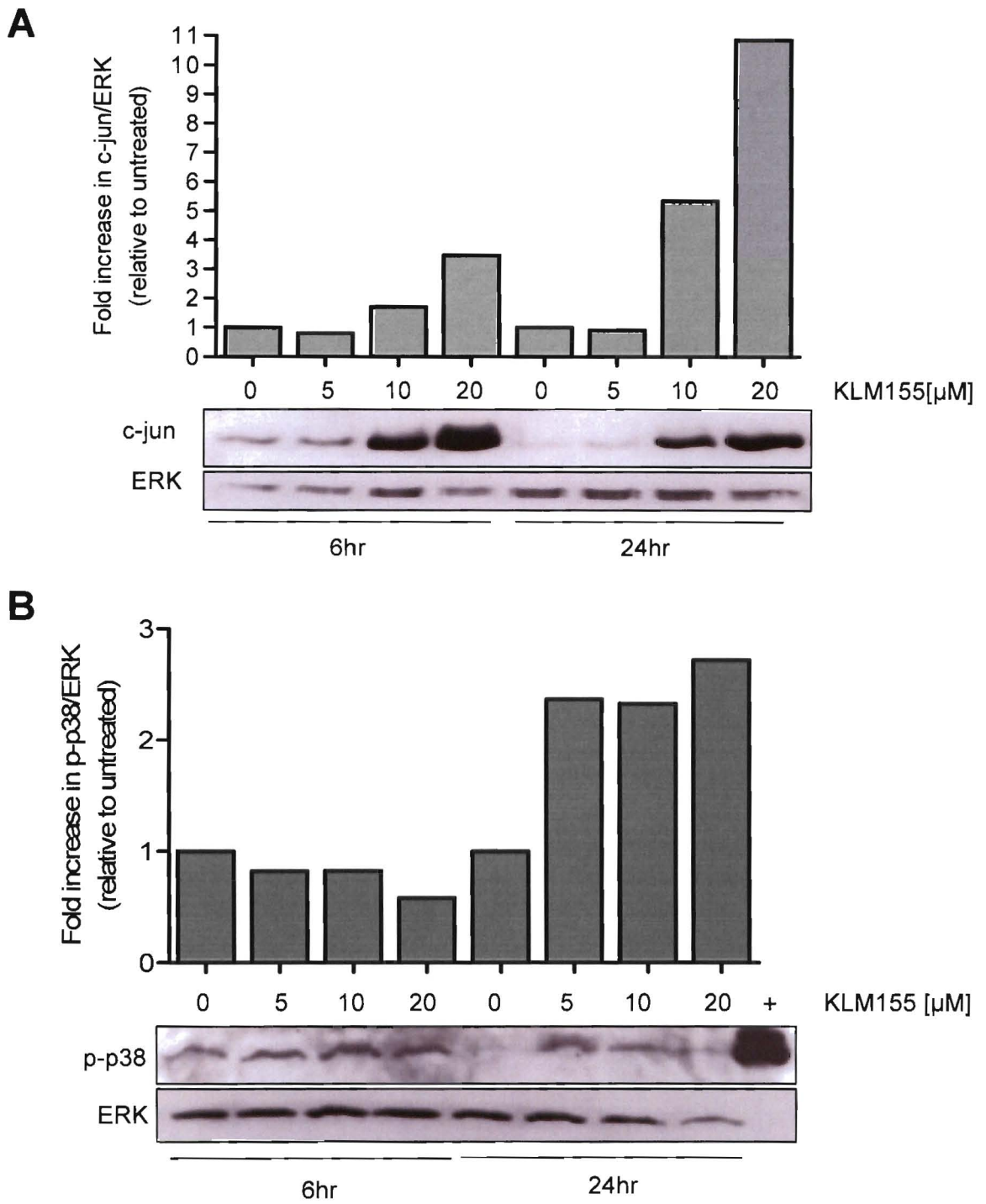

Figure 4.14. Analysis of MAPK signalling molecules c-jun (A) and p-p38 (B) in KLM155 treated cells.

The levels of the MAPK signalling molecules c-jun (A) and p-p38 (B) were analysed by Western Blot. Cell lysates from cells treated with the indicated concentration of KLM155 were harvested at 6 and 24 hours and analysed by Western Blot (as outlined in Materials and Methods). Blots were stripped and reprobed for total ERK1/2. Bands on the autoradiographs were quantitated by densitometry, using total ERK1/2 as a loading control. The positive control in B is cell lysate from UV irradiated Cos cells (kindly provided by A. Abrahams, University of Cape Town, South Africa). These results are representative of two independent experiments.

4.2.5 Effect of Inhibition of c-Jun activity on KLM155 treated cells

To test whether the cell death observed was mediated via signaling through c-Jun we adopted two approaches. In the first, we used a chemical JNK inhibitor II (Calbiochem Cat#420128), that inhibits JNK activity such that phosphorylation of c-Jun does not occur (139). As an independent confirmation of the effects noted with the JNK inhibitor, we used a cell line transfected with the dominant negative mutant of c-Jun, TAM67, that inhibits c-Jun function and compared the effect of KLM155 on parental and tranfected cells.

4.2.5.1. Inhibition of JNK:c-Jun signaling using a chemical inhibitor of JNK

Inhibition of JNK using JNK inhibitor II significantly decreased apoptosis by 55% compared to KLM155 treatment alone ($p<0.05$) (Figure 4.15.A.). JNK inhibition however, had no effect on cell survival in the presence of KLM155 (Figure 4.15.B.). It is possible that the concentration of JNK inhibitor used was insufficient to completely block the cytotoxic and growth inhibitory effects of KLM155.

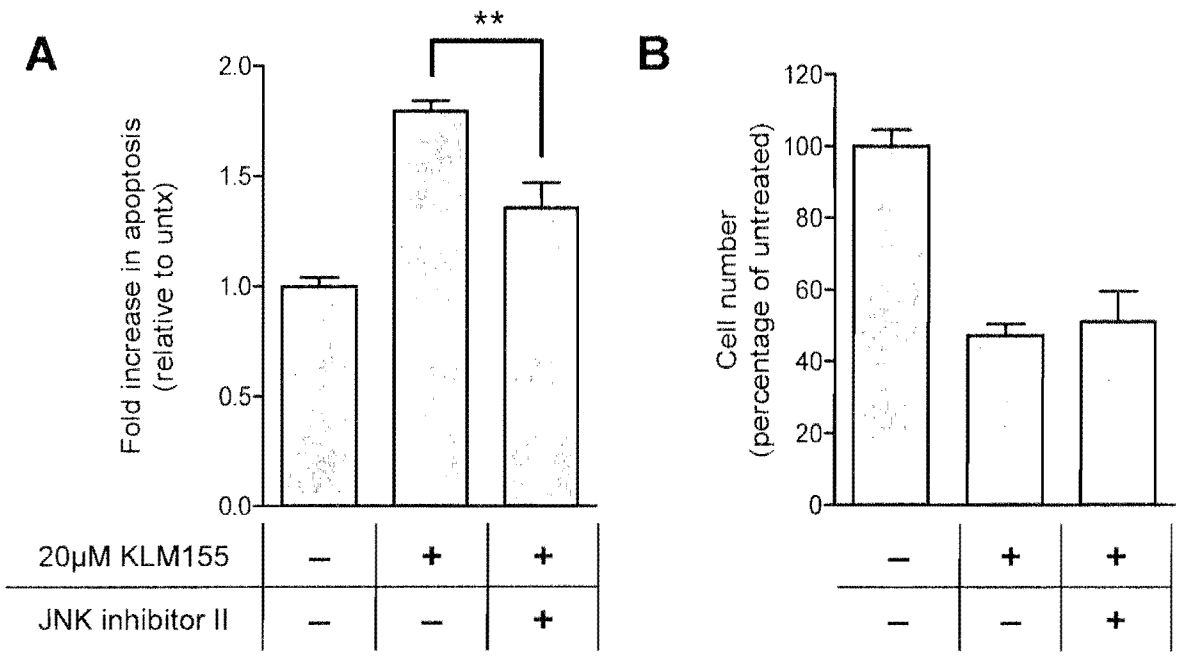

Figure 4.15. Inhibition of KLM155-induced apoptosis (A) and effect on KLM155-induced cell death (B) by the addition of JNK inhibitor II.

Cells were pretreated with JNK inhibitor II (100μM), and one set of wells (in quadruplicate) was treated with KLM155, and one set used as control. After 24 hours, cells were assessed for either apoptosis, using the Caspase-Glo 3/7 kit (A), or cell death/survival, using MTT (B). These values were expressed as fold (A) or percentage (B) of the KLM untreated control for each condition. Values are the mean of triplicate (A) or quadruplicate (B) wells, and error bars indicate standard deviation. (A : ** $p<0.05$). Results are representative of two independent experiments.

4.2.5.2. Inhibition of c-Jun activity with a dominant negative construct (TAM67)

We tested whether abolishing the expression/activity of AP1 (specifically c-Jun) using the dominant negative TAM67, could alter the response of a cell line to the KLMs. TAM67 is a dominant negative mutant of c-Jun which lacks amino acids 3-122, removing the transactivating domain. TAM67 dimerised with wild-type c-Jun, but since it lacks the transactivation domain, the dimers comprising c-Jun and TAM67 are unable to transcriptionally activate any genes (Figure 4.16.) (140).

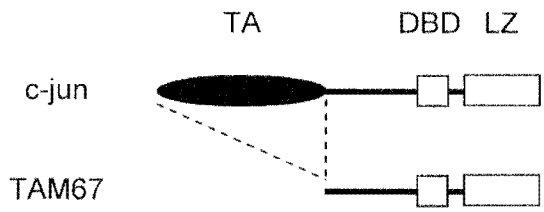

Figure 4.16. Inhibition of c-jun using a dominant negative construct.
The structure of c-jun and TAM67. c-jun consists of a transactivating domain (TA), a DNA binding domain (DBD) and a leucine zipper domain (LZ). TAM67 lacks amino acids 3-122, removing the transactivating domain. TAM67 dimerises with wild-type c-jun, but since it lacks the transactivation domain, it blocks activity of the wild-type c-jun. (Adapted from Hennigan et al. (140))

A doxycycline-inducible TAM67 expressing cell line, Caski/TAM67, was obtained from M.Maritz (Honours thesis, University of Cape Town, 2005). The effect of KLM155 treatment on the parental cells, Caski and Caski-TAM67 grown in the presence of doxycycline was determined. Expression of the inhibitor of c-Jun, TAM67, resulted in the cells being slightly more resistant to KLM155 (IC_{50} = 28 µM, 95% CI 23.2 – 34.6), compared to the parental Caski cells (IC_{50} = 21 µM, 95% CI 18.7 – 25.1).

In addition, cell survival following treatment was increased in both the uninduced (82% survival) and induced (100% survival) Caski/TAM67 cell line in comparison to the parental line (53% survival) (Figure 4.17.A.). The increase in survival compared to the parental line is significant ($p<0.01$), even in the case of uninduced Caski/TAM67 cells. The increased survival observed in the undinduced Caski/TAM67 cells is likely due to leaky expression of TAM67 in the absence of doxycycline. This leakiness was observed by Western Blot analysis, showing some TAM67 expression

in the uninduced cell lysate, and increased expression in the doxycycline treated cells (Figure 4.17.B.).

Taken together, these results suggest that inhibition of c-Jun activity with a dominant-negative mutant interferes with the growth inhibitory and cytotoxic effects of KLM155 and provides further evidence that KLM155 acts via the activation of the JNK:c-Jun signal transduction pathway.

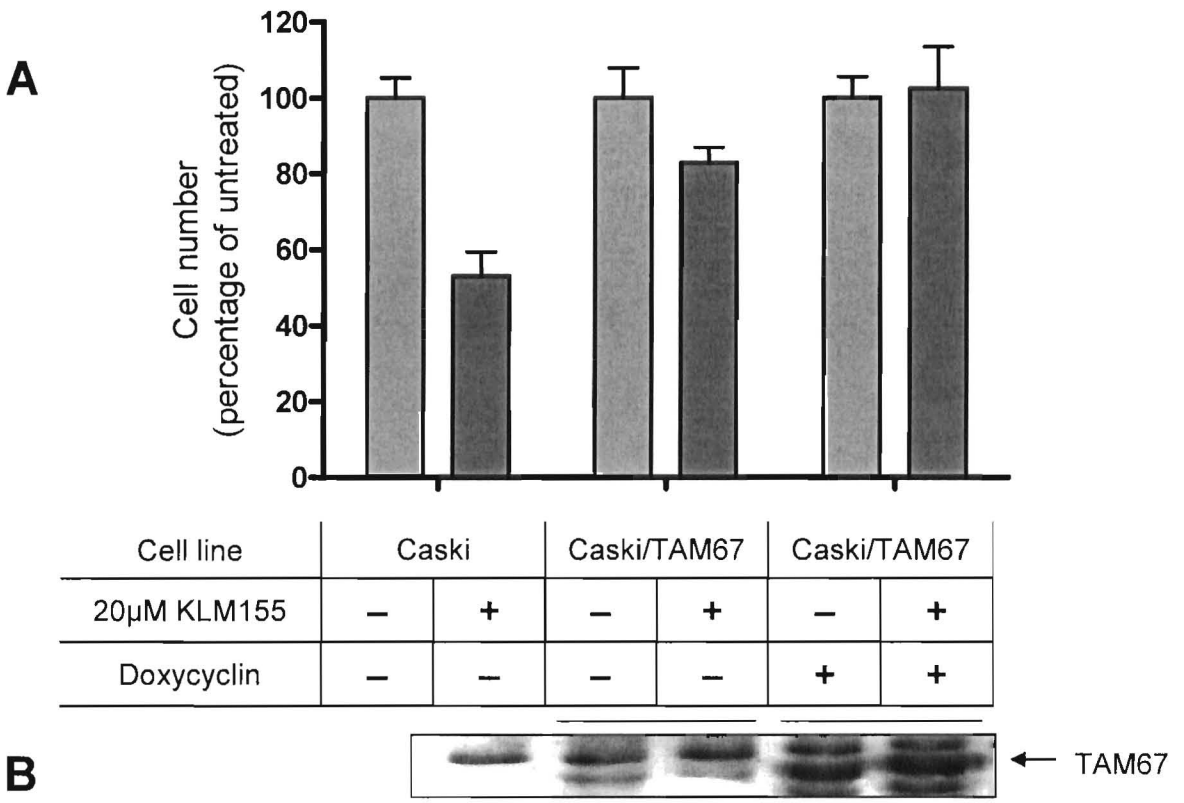

Figure 4.17. Effect of Tam67 on KLM155 induced cell death.
Caski, uninduced Caski/TAM67 cells and induced Caski/TAM67 cells in 96 well plates were treated with 20μM KLM155 or solvent control, and grown for 24 hours. Cell survival was then assessed using the MTT assay according to Materials and Methods. Values are the mean of quadruplicate wells, and are expressed as a percentage of the untreated for that cell line (A). Error bars indicate standard deviation. To confirm that the increased cell survival observed for uninduced Caski/TAM67 cells was due to basal transcription of the TAM67 construct, we harvested protein from treated and untreated cells from Caski, uninduced Caski/TAM67 and induced Caski/TAM67 cells, and ran a Western Blot (according to Materials and Methods) to detect TAM67 (B). The presence of a band in uninduced cells confirms basal expression of this construct in the absence of doxicyclin.

4.3. Discussion

4.3.1. Generation of ROS by KLMs

Compelling evidence in the literature shows that ROS plays a central role in the anti-proliferative activity of other agents that have potential as anti-cancer agents including; i) 4HPR in head and neck squamous carcinoma cell lines (141), ii) diallyl disulfide in neuroblastoma cells (142), iii) paclitaxel in T24 urothelial carcinoma cell lines (65), and iv) heteroarotinoids in HNSCC cell lines (143). We hypothesized that the group of compounds discussed here act by generating ROS based on their structures. We thus evaluated the ability of KLM155 to generate ROS in WHCO1 cells, and determined that ROS is generated in response to KLM treatment. In fact, the pattern of ROS generation seems to match that of apoptosis induction – no/low levels at the lower concentrations (5 and 10 μM), and induction at 20 μM. This led us to make the tentative conclusion that ROS generation is the causative event in KLM155 induced apoptosis. Following this result we tested the time course of ROS production. ROS was generated as early as 15 min after treatment, and levels increased up to 2 hours, which was the limit of the assay. The rapid production of ROS, with ROS levels increasing prior to apoptosis induction, was consistent with our hypothesis that ROS production may be a causative event in KLM-induced apoptosis. This was supported by our observation that the addition of ROS scavengers BHA and Trolox could both decrease levels of apoptosis and improve cell survival after treatment with KLM155 for at least one of the scavengers used. Although BHA treatment substantially blocked KLM155-induced apoptosis, no effect was observed on cell survival. This result requires further investigation.

To confirm that the production of ROS was a feature of the entire group of compounds, all the KLMs were assayed against WHCO1 cells at 20 μM. ROS production varied among the compounds, but appeared to correlate with activity. This was observed by a plot of ROS production at 20 μM (in WHCO1s) against the IC_{50} values for these compounds in WHCO1 cells. A linear relationship was observed, which strengthened our hypothesis that KLM treatment induces apoptosis as a consequence of ROS production. A similar correlation between antioxidant capacity and sensitivity of various cell lines to paclitaxel has been observed (65).

Our observation that ROS production is a relatively early event (within 15 min) is consistent with other reports that also show early ROS production in cells treated

with a variety of compounds that block cell growth and induce apoptosis through ROS-mediated pathways (141;142).

Of all the cell lines tested in this study, SiHa cells were the only line resistant to KLM treatment. SiHa cells have been reported to have high constitutive levels of antioxidant enzymes (124), leading us to theorise that any ROS produced by KLM155 in these cells would be efficiently scavenged, hence the resistance of these cells to KLM155. This also adds strength to our hypothesis that the KLMs induce cell death by producing ROS in the cells.

4.3.2. Mechanism of ROS production by KLMs

At this point, with our knowledge of the metabolism of quinone type compounds, it was possible to develop a model to explain the differences in activity between the compounds. To build the case for the model we are developing, the following background is provided. The KLMs are quinone and hydroquinone structures (with the exception of KLM157 and KLM158). Metabolism of quinones is by either a one or two electron reduction to form a semiquinone or hydroquinone, respectively. The one electron reduction can be catalysed by a range of enzymes including NADPH:cytochrome p450 reductase, NADPH:cytochrome b5 reductase and NADPH:ubiquinone oxidoreductase. The reactive semiquinone intermediate formed as a result of this reduction, can either revert back to the quinone, producing ROS in the process, or undergo another one electron reduction to form the hydroquinone. Quinones can also be metabolized by NADPH:quinone oxidoreductase 1 (NQO1 or DT-diaphorase), which performs a two electron reduction, resulting in the corresponding hydroquinone (Figure 4.18.) (118). The hydroquinone may autooxidise to form the semiquinone. Depending on the microenvironment and the properties of the quinone, an equilibrium between quinone, semiquinone, and hydroquinone will be established (117).

Quinones are generally considered to be more cytotoxic than their hydroquinone metabolites. However, this is highly dependant on the structure, stability and reduction potential of the quinone/hydroquinone pair. In many cases the hydroquinone is less reactive than the quinone, and is metabolized and excreted. However, the hydroquinone can be more active than the quinone : rearrangement of the hydroquinone can occur, giving rise to an alkylating agent, and the hydroquinone conversion to the semiquinone and back again can form a futile redox cycle

generating reactive oxygen species. In fact, several antitumour quinones (e.g. mitomycin C (144;145) and 17-AAG (146;147)) have been shown to require enzymatic reduction to the active species, generally via a two electron reduction to the corresponding hydroquinone, catalysed by NQO1.

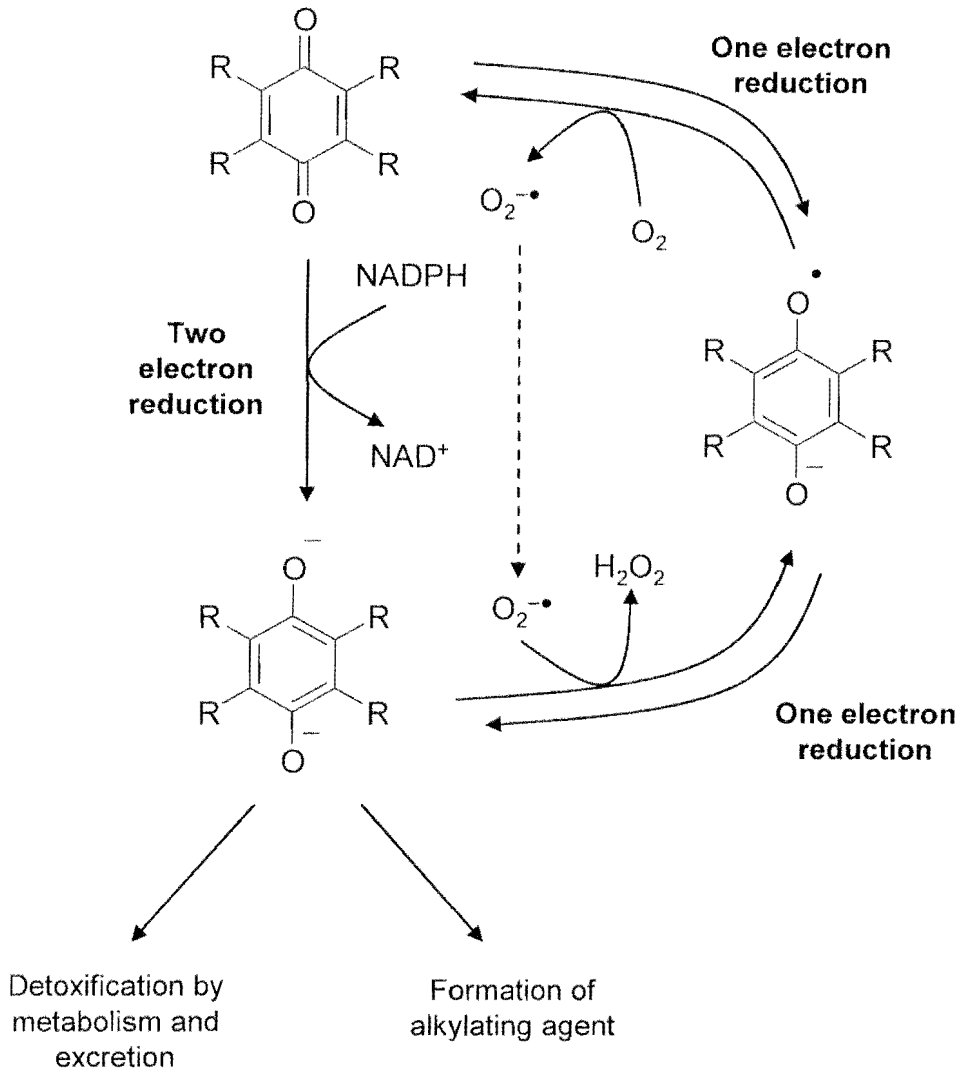

Figure 4.18. Quinone metabolism.

Quinones may be metabolised by either a one or two electron reduction. One electron reduction may be catalysed by a variety of enzymes, including NADPH:cytochrome p450 reductase and NADPH:cytochrome b5 reductase, and give rise to the reactive semiquinone. The two electron reduction is carried out by NADPH:quinone oxidoreductase 1 (NQO1), and gives rise to the corresponding hydroquinone.

The hydroquinone may be metabolised and excreted, but may also be toxic. The hydroquinone can autooxidise to form the semiquinone, and the resulting redox cycle generates reactive oxygen species. The hydroquinone may also form an alkylating agent which can then damage cell constituents including DNA and proteins. (Adapted from Asche *et al* (117))

Our results show that the hydroquinone KLMs (KLM155 and KLM156) are more active than the quinones (KLM153 and KLM154). This leads us to believe that the conversion of hydroquinone to the semiquinone is the most favoured reaction, and allows us to formulate a tentative model for the generation of ROS by these molecules (Figure 4.19.).

4.3.2.1. KLM quinone (KLM153 and KLM154) metabolism

The KLM quinones are converted to both the semiquinone and to the hydroquinone, which then autooxidises to the semiquinone (Figure 4.19,A.). This generates ROS from the autooxidation of a portion of the total molecules, while the one electron reduction does not generate ROS.

4.3.2.2. KLM hydroquinone (KLM155 and KLM156) metabolism

However, the KLM hydroquinones can only be autooxidised to form the semiquinone (Figure 4.19.B.), thus generating more ROS the the metabolism of the quinone.

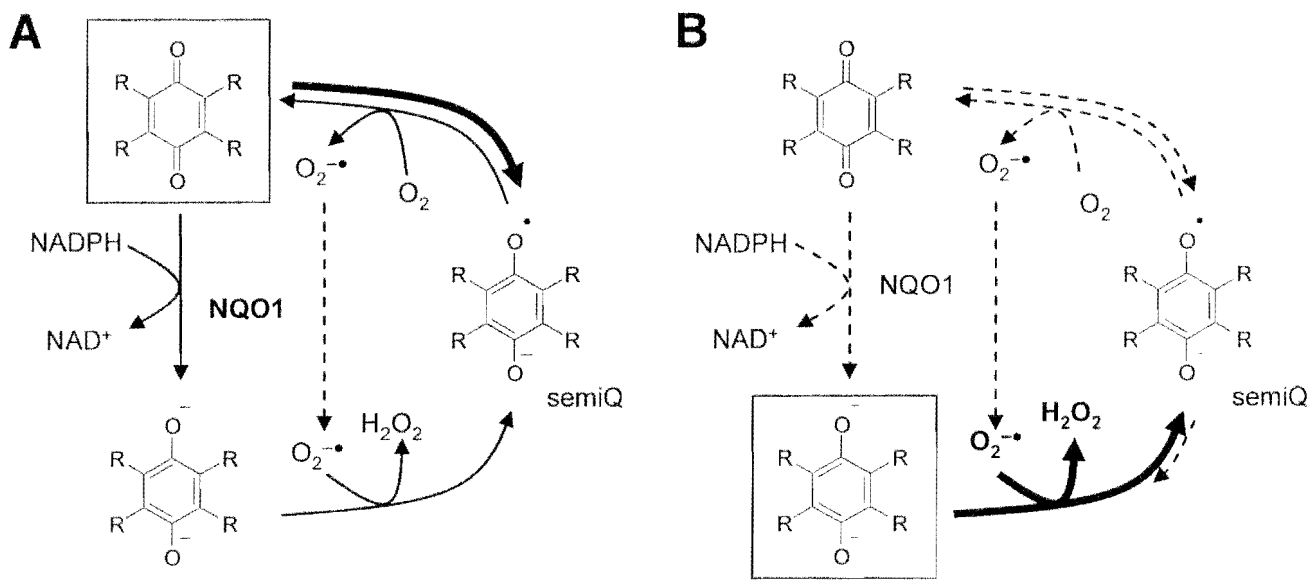

Figure 4.19. Metabolism of the KLM quinones (A) and hydroquinones (B).
Metabolism of the KLM quinone structures is via both one and two electron reductions, generating ROS when the resulting hydroquinone is autooxidised to form the semiquinone (A). However the KLM hydroquinones can only be autooxidised to form the semiquinone, thus generating more ROS than the corresponding quinone (B).

It is difficult to predict the dynamics of these reactions – both the metabolism of the quinone to the hydroquinone by NQO1, and the stability of the hydroquinone – without performing *in vitro* studies with purified enzyme, and determining the reduction potentials of the quinone/hydroquinone pairs. Currently we have insufficient compounds to perform these analyses, but our collaborators are in the process of developing a synthesis protocol to produce large amounts of the KLMs, and related molecules with which we can analyse the relative contributions of the various substitutions and side chain length to the activity of these compounds.

The observation that the KLMs with bent chains (KLM154 and KLM156) are less active than the KLMs with straight chains (KLM153 and KLM155) may reflect differing selectivity of NQO1 for different substrates, though this would not explain the difference in activity between the hydroquinone structures, which would not need activation by NQO1. A more likely explanation is that the altered conformation of the side chain may stabilize the hydroquinone, preventing autooxidation to the semiquinone, and reducing the amounts of ROS produced.

The decreased activity of KLM159 in comparison to KLM155, which differs only in a hydroxyl substituted for the carbonyl on the triprenyl side chain, may be attributable to the same factors – altered activity for the compound by NQO1, or increased stability of the hydroquinone, leading to lower generation of ROS.

If we accept the hypothesis that the KLM quinones are metabolised to the active hydroquinones, this has implications for therapy. NQO1 has been shown to be upregulated in some cancer cells (148;149), and this would increase the sensitivity of these tumours to the KLM quinones, compared to normal tissue. This is a basis for differential activity, and has been demonstrated for some other quinone compounds (145;150).

4.3.3. Effects of ROS production

The production of ROS in cells is a normal cellular event, and is a consequence of a variety of cellular processes such as oxidative phosphorylation and the electron transport chain. However large amounts of ROS can cause damage to every constituent of the cell, including DNA, RNA, proteins and lipids (151;152). The cell's response to this damage is generally to attempt repair (frequently associated with a cell cycle block), followed by cell death if the damage is irreparable (136;153;154). The cellular events we observe following treatment with KLM155 – namely cell cycle arrest and apoptosis – are characteristic of ROS induced cell death (65;142;155).

Cells have a large number of mechanisms in place to deal with reactive oxygen species. Antioxidant enzymes such as superoxide dismutase, glutathione reductase, and others scavenge free radicals. Systems such as the glutathione and thioredoxin systems assist in scavenging ROS, and convert ROS damaged proteins back to their normal conformation, while the heat shock proteins bind to damaged proteins preventing misfolding and aggregation. If the levels of ROS are too high for the cellular antioxidant systems to scavenge, then the cell will undergo apoptosis, or in some cases necrosis.

To determine which pathways are affected by treatment with KLM155, we performed microarray analysis on treated and untreated samples. A number of genes were up or down regulated, and we confirmed this using real time reverse-transcriptase PCR. Several of the genes identified are known responses to an increased level of ROS, and are upregulated in order to deal with the effects of ROS damage.

4.3.3.1. Antioxidant response

We detected the upregulation of a number of genes that encode enzymes associated with an antioxidant response. These included heme oxygenase 1 and thioredoxin, while the levels of MnSOD and glutathione reductase were unaltered. Upregulation of NQO1 was also observed, which may be an indication that this enzyme is indeed involved in the metabolism of the KLMs.

Heme oxygenase 1 (HO1) is one of a family of heme oxygenases, which catalyses the breakdown of heme, a constituent of many proteins. ROS modifications of heme-containing proteins lead to the release of heme, an extremely reactive molecule

(130;156). Thus upregulation of heme oxygenase occurs to deal with increased free heme levels under conditions of oxidative stress (157). HO1 is one of the cell's major activated pathways in response to oxidative stress, and its upregulation as a response to reactive oxygen species is the result of a number of signaling molecules, including AP1 and Nrf1 (158).

While the induction of heme oxygenase is generally considered to be a protective response to ROS stress, there is some evidence that HO1 induction can be a pro-oxidant event (159;160). Since one of the breakdown products of heme is the low-molecular mass iron, which is an extremely redox active form of iron, ferritin is generally upregulated in conjunction with HO1 (we noted a 1.6 fold upregulation of ferritin in our microarray results ($p = 0.021$)). However, in cases where HO1 activity is higher than that of ferritin, excess low-molecular-mass redox-active iron may be generated, and this may contribute to increasing the cellular redox stress (159). Our results, demonstrating exceptionally high upregulation of HO1, suggest that this may be occurring in our system. Further experiments would be needed to confirm this.

Significant upregulation of thioredoxin reductase was observed in KLM155 treated cells. Thioredoxin reductase is a selenoprotein that reduces oxidized protein substrates (161), and forms part of the thioredoxin system which helps regulate the cellular redox balance. This system acts to mediate ROS stress in several ways. First, the thioredoxin molecules are easily oxidized by free radicals, and then reduced by thioredoxin reductase, with NADPH as an electron donor. Thus thioredoxin serves to scavenge ROS molecules (131). Secondly, oxidized thioredoxin translocates from the cytoplasm to the nucleus, where it activates the Ref1, which in turn activates a number of transcription factors including AP1 and NFκB. These in turn upregulate a number of genes which encode molecules which protect the cell from oxidative stress or induce apoptosis (162).

The upregulation of thioredoxin reductase in our system is most likely a reflection of increase oxidized thioredoxin, and serves to reinforce our hypothesis that KLMs induce oxidative stress in treated cells. It seems likely that increased oxidized thioredoxin is one of the signaling events leading to upregulation of AP1 in our system, but this remains to be conclusively shown.

4.3.3.2. Repair of ROS induced damage

DNA-damage inducible transcript 3 (GADD34) is induced in response to DNA damage and plays a role both in halting the cell cycle, and in repairing DNA damage (132). It's upregulation following KLM155 treatment is most likely in response to DNA damage caused by reactive oxygen species.

The heat shock proteins play an important role in the cellular response to oxidative stress. By binding ROS-damaged proteins, they prevent these proteins from misfolding, and from forming aggregates (133). Upregulation of HSP70 can also prevent apoptosis by preventing the release of cytochrome c from the mitochondria, disruption of apoptosome formation, and prevention of procaspase recruitment (163).

4.3.3.3. Apoptosis

Despite the many varied responses to survive oxidative stress, in some cases ROS production, and the resulting damage, overwhelms the cells ability to deal with these events, and cells then undergo apoptosis (164). We demonstrated that KLM155 induces apoptosis, following production of reactive oxygen species in WHCO1 cells.

The mechanism by which KLM155 induces apoptosis in WHCO1 cells has yet to be fully characterized, but we have shown involvement of c-Jun, and that caspase 3 is activated in these cells. Further work will involve examining other pathways, such as NFκB and Nrf in the activation of apoptosis in these cells, and determining if apoptosis is triggered via the mitochondrial or death receptor pathways.

4.3.3.4. AP1 activation

Several cellular signaling pathways may play a role in the cellular response to ROS. Among these are stress response pathways such as p38 and JNK. Treatment of WHCO1 cells with KLM155 in this study specifically activated the JNK/c-Jun pathway and not the p38 pathway.

We hypothesise that at low concentrations of KLM155, low levels of ROS may induce c-Jun (or other signaling pathways), which in turn upregulate antioxidant enzymes that rapidly scavenge the ROS. At higher levels however, the amount of ROS

overwhelms the cell's ability to cope with the stress, and c-Jun becomes pro-apoptotic (134;135).

Our results strongly implicated JNK/c-Jun signaling in mediating compound KLM155-induced apoptosis, with upregulation of c-Jun in KLM155 treated cells, and the observation that the JNK inhibitor abrogated KLM155-induced apoptosis. It was quite intriguing that while the JNK inhibitor blocked the apoptosis induced by KLM155, this inhibitor had no significant effect on the reduction in cell number caused by KLM155 (Figure 4.15.). This should be considered in the context of the results observed for Trolox, which blocked apoptosis to the same extent as the JNK inhibitor, but significantly prevented a reduction in cell number in response to treatment with KLM155. Presumably, the block in apoptosis caused by the JNK inhibitor occurs despite the ROS-induced cellular damage inflicted by treatment of cells with KLM155. Cells may then die through non-apoptotic pathways if denied access to apoptosis, as described before (165). The ability of both Trolox and BHA to block apoptosis and the ability of Trolox to decrease the reduction in cell number caused by treatment with KLM155, reflects the proximal site of action of these ROS scavengers, allowing them to protect cells from extensive ROS-induced damage, and thus precluding the requirement for apoptosis.

The role of ROS in activating JNK (an important upstream activator of c-Jun) through the inactivation of endogenous JNK inhibitors has already been documented, providing a plausible pathway for the induction of c-Jun observed here. Oxidation of thioredoxin causes it to translocate to the nucleus where it interacts with Ref-1, facilitating the Ref-1 mediated reduction of a cysteine residue in the DNA binding domain of fos and c-Jun, causing an increase in DNA binding and transactivation of these molecules (166;167). ROS also affects AP1 activity indirectly, again through thioredoxin. Under normal cellular conditions, reduced thioredoxin is bound to ASK1, a MAPKKK upstream of both JNK and p38 signaling pathways. Oxidation of thioredoxin causes it to dissociate from ASK1, allowing ASK1 to activate the JNK and p38 kinase pathways (166;167).

4.3.4. Production of ROS as a chemotherapeutic strategy

Cancer cells generally are exposed to much higher levels of oxidative stress than normal cells (67). This is based on direct measurements of ROS levels in tumour tissues (168), accumulation of oxidative products in tumour tissue (169), and the presence of oxidised DNA products in the urine of cancer patients (170). Of particular interest for this study, elevated levels of SOD measured in squamous cell carcinomas of the oesophagus relative to normal tissues, suggest that oesophageal tumour tissues are also under increased oxidative stress (171). As a result of the constant assault of oxidative stress, cancer cells have an impaired ability to combat oxidative stress (relative to normal cells) rendering them sensitive to additional oxidative challenges. This diminished ability of cancer cells to mount an effective response to further oxidative challenges may represent a critical therapeutic window that could be exploited to develop more selective anticancer agents (61;67). The central role of ROS in mediating the cytotoxic activity of the family of triprenylquinones and triprenylhydroquinones described here underscores the value of this novel family of compounds as potential lead chemotherapeutic agents for further structure/function analysis.

4.3.5. Conclusion

This chapter describes the anticancer activities of a family of novel compounds of triprenylquinones and triprenylhydroquinones (Figure 3.2.) isolated from the nudibranch *L. millecra* (Figure 3.1.) collected from Algoa bay, South Africa (95).

In Chapter 3 we demonstrated the ability of these compounds to cause cell death and inhibit proliferation in oesophageal cancer cells. We have further shown that the activity of these compounds was directly associated with their ability to generate ROS. Firstly, we were able to directly measure ROS production in cells treated with these agents, secondly, there was a strong inverse correlation between the IC_{50} values of the compounds tested, and ROS production, and lastly, treatment of cells with the ROS scavengers BHA and Trolox reduced the extent of apoptosis caused by treatment with KLM155 (Figure 4.5.). We were able to demonstrate the induction of several antioxidant response molecules including heme oxygenase 1, thioredoxin reductase, GADD34 and HSP70. Increased signaling through the JNK MAPK pathway was detected, and this plays a role in apoptosis induction, since treatment with a JNK inhibitor was able to block apoptosis in KLM155 treated cells.

The strong correlation between the levels of ROS produced by each of the compounds and their IC_{50}'s, and the structural similarity of the family of compounds described here provide an exciting opportunity to further explore the structural elements that confer activity in these molecules. This study and others (172-176) supports the contention that marine benthic organisms from the coast of southern Africa represent a rich, untapped repository of novel and interesting compounds that may hold promise in the development of new chemotherapeutic agents.

CHAPTER 5

CONCLUSION

5.1. Objectives

The objectives of this study were as follows :

1. Establish a screening program, similar in approach to the NCI 60-cell line screen, using oesophageal cancer cell lines to identify compounds that may be of use as chemotherapeutic agents for this cancer.

2. Screen marine extracts, and supply cytotoxicity data to assist with activity-directed fractionation of active compounds.

3. Identify novel compounds active against oesophageal cancer, and assess their mechanism of action.

5.2. Novelty of the approach

The work described in this thesis is novel in the following respects :

1. The cell line used as a primary screen in this study (WHCO1) is derived from oesophageal cancer tumour tissue, and thus is ideal to identify compounds that may be effective against oesophageal cancer.

2. The extracts and compounds used in this study are from organisms collected from the southern African coast. Many of the extracts tested were from previously unidentified organisms, and in some cases from newly identified endemic species, and thus we had access to completely novel source organisms, and compounds.

3. The group of triprenylquinone and hydroquinones identified for further characterization are derived from an organism endemic to the South African Coast, and are unique. We have searched the literature, and found very few similar compounds that have been tested for activity against cancer cells, and where mechanistic assays have been performed.

5.3. Key findings

We established a screening program to identify agents active against an oesophageal cancer cell line. This screen is cheap, rapid (less than a week), and has the capacity to be expanded to include cell lines derived from other cancers of clinical significance in South Africa.

Using this screen, we tested a total of 479 samples. The capacity of this screen is far higher, but the number of samples tested was restricted by the supply. At full capacity this screen could test 50-100 compounds per week using just one researcher.

Our screening of (175 extracts) extracts from marine organisms confirmed previous findings that sponges are the organisms most likely to yield bioactive metabolites. We also identified 5 samples for activity-directed fractionation, which gave rise to a total of 15 compounds with varying activity against oesophageal cancer cell lines.

The aim of this project was not simply to identify active compounds, but also to identify pathways and systems activated by these compounds as they caused cell death. To this end a group of triprenylquinones and hydroquinones was identified as suitable for further characterisation.

We determined that these compounds are cytotoxic to a number of cancer cell lines, and further, that the mode of cell death was via apoptosis, and not necrosis. These compounds exerted their effects by the generation of reactive oxygen species, and signaling via the stress response JNK MAPK pathway. Microarray analysis of treated cells confirmed the oxidative stress response, with a number of genes involved in antioxidant defense being upregulated following treatment with one of these compounds.

The production of ROS has been implicated in the action of many chemotherapeutic agents, and presents a sound strategy for treatment of tumours. There is increasing evidence that tumour cells are under increased oxidative stress, and the generation of excess ROS in these cells may trigger cell death, while normal cells would be unaffected.

5.4. Difficulties encountered in this project

5.4.1. Scarcity of supply

During the course of this project, we identified several extracts from marine organisms that were active against our screening cell line, but were unsuitable for activity-directed fractionation due to the low quantities of sample.

In some cases (such as makaluvamine I), a compound was identified from an active extract, but in such minute quantities that there was insufficient compound to assess its activity against the screening cell line.

Our work determining the mode of action of the KLM compounds was limited since we had relatively small quantities of each compound to work with. In order for these compounds to be validated as potential chemotherapeutic agents, further experimentation would be required, including pharmacological testing and *in vivo* tumourigenicity assays in mice. This would require much larger amounts of compound than is currently available, and if the compounds were to enter clinical trials, even greater amounts would be required. Thus establishing a sustainable supply of these compounds is a critical point in their potential development as chemotherapeutic agents. Our collaborators at Rhodes University have already embarked on a program to synthesise the KLM compounds, and larger amounts of these compounds will soon be available for more extensive biological studies.

5.4.2. Increasing complexity at each stage in the drug discovery process

While our screening assay is relatively rapid (4 days), and is capable of screening large numbers of samples, the following processes of chemical purification and elucidation of structures are labour intensive, and time consuming.

Finally, elucidating the mechanism of action of a compound or group of compounds is even more time consuming.

The increasing research effort required at each stage in this process is evidenced by the number of extracts screened (175), which led to only 5 activity-directed fractionations, identifying 15 compounds, and in the duration of this project, only one group of compounds was evaluated for biological action. This is indicative of the

increased amount of effort and expense at each stage in the drug development process.

5.5. Future directions

5.5.1. Screening assay

It was our intention in establishing this screening assay to identify potential chemotherapeutic agents for the treatment of oesophageal cancer. However, the assay has the potential to be expanded to include other cell lines. For example, we could include a cervical cancer cell line, to identify agents that may be of use in treating cervical cancer, the most common cancer affecting women in South Africa.

During the course of this project, our collaboration with the Department of Chemistry at Rhodes University gave us access to a wide selection of marine extracts and compounds, and this has been the focus of this thesis. However, compounds from other sources could be tested in this assay, and in fact, we have established a collaboration to synthesise and test novel organometallic compounds with the Department of Chemistry at the University of Cape Town.

Of the samples screened, we observed an unusually high rate of activity in samples from Marion Island. It may be advisable to hold another collection at this location to confirm this finding.

5.5.2. KLM compounds

5.5.2.1. Synthesis of the KLMs and analogues

While the current low supply of compounds prevents much further work on the KLMs, our collaborators are currently in the process of synthesizing these compounds and analogues. In the future we hope to be able to assess the contribution of the triprenyl side chain, and altered substitution on the ring on the activity of these compounds. It is also important to validate the results observed for KLM155 for the other compounds. Once sufficient quantities of KLMs are available we are considering submitting these for the NCI 60 cell line screen as this will provide further information as to the suitability of these compounds for the treatment of a wide range of cancers, as well as give more information as to the mechanism of action of these compounds.

5.5.2.2. Further elucidation of the molecular events occurring in KLM treated cells

We also intend to elaborate further on the mechanism by which KLM155 induces apoptosis. We identified the JNK MAPK pathway as being activated, but the molecular events leading to this activation were not explored. The microarray results suggest the involvement of thioredoxin, but other signaling pathways are activated by ROS and may be involved in the antioxidant and cell death response to KLM155 treatment. Our determination that cell death occurred via apoptosis centered around the detection of the activated effector caspase 3. While this is a good indication that apoptosis is occurring, it is the point at which signaling via the mitochondrial and death receptor apoptosis pathways intersect. We intend to establish which of these pathways is activated in response to KLM155 treatment. Determining the signaling and apoptosis pathways induced by KLM treatment may be important in monitoring patient responses to treatment, and in determining drug combinations, should these compounds enter clinical trials at some point in the future.

An important consideration in the assessment of the KLMs as suitable drug leads would be to determine the activity of these agents in mouse xenograph studies or the NCI in vivo hollow fibre studies. We plan to submit these compounds for these whole animal studies as soon as sufficient quantities are available.

5.5.2.3. Determine the involvement of NQO1 in the action of the KLMs

We hypothesise that NQO1 plays a role in activating the KLM quinones. We intend to evaluate the role of NQO1 in metabolizing the KLMs and producing ROS. First, we need to conclusively show that KLM quinones are metabolized by NQO1. This can be determined using pure NQO1 and compounds, and then determining the levels of the parental quinone and corresponding hydroquinone by HPLC. If NQO1 does play a role in activating the KLM quinones, it may be possible to rationally design even more effective KLMs using the known crystal structure of NQO1.

Should NQO1 be involved in activating the KLM quinones, we would determine the level of NQO1 in oesophageal tumour tissue. Previous studies have shown elevated levels of NQO1 in a variety of tumours. Should NQO1 prove to be upregulated in oesophageal tumours, it would indicate the potential for differential activity of the KLMs in these tumours.

5.5.3. ROS production as a therapeutic option

This study and others have shown the potential of agents that produce ROS to kill cancer cells. It may be informative to elaborate on this by assessing the levels of antioxidant enzymes in tumour tissue compared to normal by both quantitative real-time RT-PCR and immunohistochemistry. Should we show that oesophageal tumours have low levels of antioxidant enzymes, it may suggest new therapeutic options for these patients.

5.6. Conclusion

Both the screening program and the group of compounds described in this thesis have the potential to give rise to promising drug leads that can be further developed to provide novel chemotherapeutic agents for the treatment of oesophageal cancer.

CHAPTER 6

MATERIALS AND METHODS

Unless otherwise mentioned, all chemicals were AnalR grade, and purchased from Sigma or Merck. Recipes for all solutions mentioned are listed by experiment in Section 6.14. of this chapter.

6.1. Cell culture

All cell lines were maintained at 37°C, in a 5% CO_2, humidified incubator.

6.1.1. Cell lines and medium requirements

The human oesophageal cancer cell lines designated WHCO (WHCO1, WHCO3, WHCO5, WHCO6) were obtained as a generous gift from Prof R. Veale, University of the Witswatersrand, South Africa. These cell lines were derived from South African patients with squamous cell carcinoma of the oesophagus (83).

The human oesophageal cancer cell lines designated KYSE were obtained as a generous gift from Prof Y. Shimada, Kyoto University, Japan. These cell lines were derived from Japanese patients with squamous cell carcinoma of the oesophagus (177).

SiHa cells (ATCC HTB-35) (178) and ME180 cells (ATCC HTB-33) (179), both cervical cancer cell lines, were obtained from Dr. M. Birrer, National Institute of Health, USA.

MCF12A cells (ATCC CRL-10783) are a breast epithelial line cultured from a non-malignant growth (89), and were obtained from Prof. M.I. Parker, University of Cape Town, South Africa.

The Caski/TAM67 cell line and the parental Caski cell line were obtained from Dr. V. Leaner, University of Cape Town, South Africa. The Caski cell line is a cervical cell line, and the Caski/TAM67 cell line is transfected with the dominant-negative c-Jun mutant TAM67.

Cell line	Medium	% Foetal Calf Serum	Antibiotics (100U/ml penicillin, 100 µg/ml streptomycin)	Supplements
WHCO1	DMEM – (Dulbeccos' Modified Eagle's Medium)	10%	yes	none
WHCO3				
WHCO5				
WHCO6				
KYSE30	DMEM	10%	yes	none
KYSE70				
KYSE180				
KYSE520				
SiHa	MEM (Minimal Eagle's Medium)	10%	yes	none
ME180	McCoy's 5A	10%	yes	none
Caski	DMEM	10%	yes	none
Caski/TAM67	DMEM	10%	yes	5 µg/ml blasticidin
MCF12A	1:1 Ham's F10 : DMEM	5%	no	20ng/ml EGF, 100ng/ml cholera toxin, 500ng/ml hydrocortisone, 10 µg/ml insulin

Table 6.1. Cell lines and medium requirements.

6.1.2. Subculturing protocols

All cell lines were subcultured by removing medium, rinsing once with 2 ml PBS (or 0.5% trypsin in PBS), then trypsinising with 3 ml trypsin. Once cells had rounded, 3 ml of medium were added to neutralize the trypsin, and cells were centrifuged out of the trypsin:medium mix. Cells were then resuspended in the appropriate medium and a portion added to a fresh dish at a 1:6 ratio.

6.1.3. Freezing and thawing protocols

For all cell lines, a confluent dish was trypsinised, neutralized with complete medium, then cells were centrifuged out of the trypsin/medium solution. Cells were resuspended in 3-4 ml of freezing medium (90% complete culture medium, 10% DMSO), and aliquated into cryotubes (1 ml per tube). Tubes were placed in -70°C overnight and then transferred to liquid nitrogen.

6.1.4. Mycoplasma test

All cell lines were tested for mycoplasma contamination every three months. Cells were grown in culture medium free of antibiotics for at least one week, then trypsinised and plated onto coverslips in 60 mm dishes. Following an overnight incubation to allow cells to settle onto coverslips, 5 ml fixative was added to the culture medium, then discarded and replaced with another 2.5 ml fixative. The cells were then immediately washed gently with water and dried by inversion. Once the coverslip was dry, mycoplasma staining solution was added for 30 sec and then thoroughly washed with water. Finally the coverslip was mounted on a slide, using a drop of mounting fluid, and cells were observed using fluorescence microscopy. Cell nuclei stain bright green, and mycoplasma contamination is visualized as minute punctate fluorescence distributed throughout the cytoplasm (180).

6.2. Screening

6.2.1. Crystal violet assay

Initial screening for cytotoxicity was carried out as described previously (176) by plating cells at 1500 cells/well in 90 µl DMEM in CellStar 96 well plates. After 24 hours incubation to allow cells to settle, test compounds were added in 10 µl DMEM to a final concentration of 1, 10 and 50 µg/ml, with solvent (DMSO) at 0.2%. Following 48 hours incubation, observations of cell number and morphology were made, and the plates were then processed for crystal violet staining as follows (88).

Medium was discarded, the plates allowed to drain, and cells were fixed by adding 100 µl methanol to each well. Following a 10 min incubation, the methanol was discarded, and 100 µl of crystal violet staining solution was added to each well for 20

min. Plates were washed thoroughly under running water, and the remaining stain was solubilised using a 50% acetic acid in water solution. Plates were read at 595nm on an Anthos microplate reader 2001 (Austria).

Controls on each plate included a no-cell (medium only) blank, and untreated cells as a 100% control.

6.2.2. Analysis – scoring system

Samples which did not decrease cell number at any concentration were given a score of 0 (e.g. A); samples which decreased cell number to below 10% of untreated at the highest concentration only were scored as 1 (e.g. B); those that decreased cell number to below 10% of untreated at 10 µg/ml were scored as 2 (e.g. C); and those that decreased cell number to below 10% of untreated at the highest concentration (1 µg/ml) were scored as 3 (e.g. D).

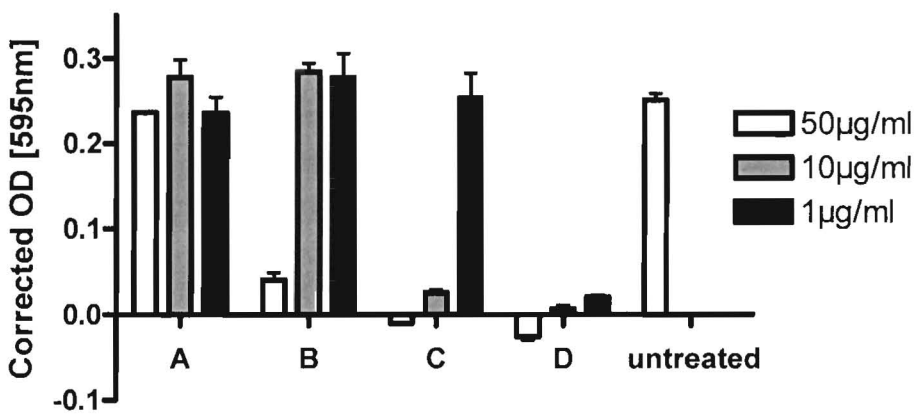

Figure 6.1. Example of screening data.
Samples which did not decrease cell number at any concentration would be scored 0 (e.g. A), samples which decreased cell number to below 10% of untreated at the highest concentration only would be scored 1 (e.g. B). Samples which decreased cell number at the highest and the medium concentration would be scored 2 (e.g. C), and samples which decreased the cell number to below 10% at all concentrations would be scored 3 (e.g. D).

6.3. MTT assay

Samples for the MTT assay (181) were plated in 96 well plates in a final volume of 100 µl. MTT reagent (Roche Cat #1465007) was added at the end of the experiment – 10 µl of MTT reagent was added per well, and plates were incubated for 4 hours at 37°C. Solubilisation solution (100 µl) was then added to each well, and plates were incubated at 37°C overnight. After 16 hours, plates were read at 595nm on an Anthos microplate reader 2001.

6.3.1. IC_{50} determination

For IC_{50} determination, 1500 cells were seeded per well in 90 µl DMEM in Cellstar 96 well plates. Cells were incubated for 24 hours, then test samples were plated at a range of concentrations in 10 µl medium, with a final concentration of 0.2% DMSO. After 48 hours incubation, observations were made, and plates were processed as described above. Plates were read at 595nm on an Anthos microplate reader 2001.

6.3.2. IC_{50} data analysis

The resulting dose-response curve was analysed by non-linear regression analysis (Non-linear regression (Sigmoidal dose response with variable slope)) using GraphPad Prism version 4.00 for Windows (GraphPad Software, San Diego California USA, www.graphpad.com) to yield an IC_{50} value which is specific for the compound against the particular cell line. The formula used is as follows :

$$Y = \text{bottom} + \frac{(\text{top-bottom})}{1 + 10^{(\log IC_{50} - X) \times \text{hillslope}}}$$

Where Y is the absorbance reading, x is the concentration of compound, top is the maximum absorbance, bottom is the minimum absorbance (also the absorbance of the medium blank), and hillslope is the gradient of the curve.

6.4. Cell cycle analysis

Cells were seeded in 60 mm dishes at 0.25×10^6 cells per dish. Following an overnight settling period, compounds were added to the culture medium (to avoid the loss of cycling cells that had detached during division). At appropriate time points, cells were

harvested by trypsinisation (taking care to collect all washes to avoid discarding floating cells), resuspended in 1 ml PBS, and counted. Nine ml of ice cold 70% EtOH was then added to each sample, and samples were stored at –20°C for up to 2 weeks. Cells were then centrifuged out of EtOH, rinsed several times in PBS, and $5x10^6$ cells/ml were incubated in 50 µg/ml RNAse A in PBS for 30 min at room temperature. Cell Cycle Staining solution was added to bring the cell concentration to $1x10^6$ cells/ml, and following a 30 min incubation in the dark, cells were analysed on a Beckman Coulter FACS-calibur flow cytometer. Analysis of cell cycle results was carried out using ModFit 3.0 (Verity Software House).

6.5. Apoptosis assays

6.5.1. Flow cytometry detection

Levels of apoptosis in cells were assessed using the Active Caspase-3 FITC mAb Apoptosis Kit (BD Biosciences BD Cat#550480) according to manufacturer's instructions. Briefly cells were grown in 60 mm dishes, and after the indicated treatments, were harvested by trypsinisation (collecting medium and all washes). The cells were fixed (using the Cytofix/CytoPerm solution provided with the kit), and following two washes (with Perm/Wash buffer, also supplied with the kit), cells were stained for 30 min (protected from light) at room temperature. Cells were washed again, and then resuspended in Perm/Wash buffer, and fluorescence was detected using a Beckman Coulter FACS-calibur flow cytometer.

6.5.2. Caspase-Glo™ 3/7 Assay

Apotosis analysis was carried out by detecting caspase-3 activity in cells using the kit (Promega Cat#G8090), according to manufacturer's instructions. Cells were seeded at 1000 cells/well in 96 well plates in 60 µl. Following 24 hours incubation to allow cells to settle, and in some cases a 2 hour pre-treatment with inhibitors, compounds were added as outlined, and cells incubated for the indicated time periods. Reconstituted caspase reagent was added, and following 1 hour incubation, light emission was detected using a Luminoskan Ascent plate reader.

6.6. Necrosis Assay

Analysis of the levels of necrosis was performed using the CytoTox-ONE Homogeneous Membrane Integrity Assay. This assay detects the release of LDH from cells with compromised cell membranes. LDH is detected by a coupled enzymatic reaction which results in the conversion of resazurin into a fluorescent resorufin product. Cells were plated in 96 well plates in a final volume of 90 µl, and following an overnight incubation to allow cells to settle, treatments were added in 10 µl to a final volume of 100 µl. After the desired incubation time, 100 µl of CytoTox ONE reagent was added, and following a 10 min incubation, 50 µl of Stop solution was added. At each time point Lysis Buffer (a detergent solution supplied with the kit which completely lysed cells, as observed by microscopy) was added to a set of wells as a positive control, and these were processed in the same way as the test wells. Fluorescence was measured on a 96-well plate fluorimeter, and values were expressed as a % of the positive control.

6.7. Trypan Blue Assay

$1x10^5$ cells were seeded in 1 ml/well in 24 well plates. After an overnight incubation to allow cell settling, various agents were added at a 10x concentration in 110 µl. At various time intervals 100 µl of 0.4% trypan blue solution in water was added to duplicate wells, and the cells were incubated at 37°C for 5 min to allow uptake of the dye into non-viable cells. Medium and stain solution were then removed, and the cells washed twice with 2 ml PBS, and then observed using light microscopy.

6.8. Reactive Oxygen Species measurement

Cells were plated in 60 mm dishes at $5x10^5$ cells per dish. Following 24 hours to allow cells to settle, medium was removed, and cells rinsed with 1 ml 37°C Krebs-Ringer (KR) buffer, and 2 ml 25 µM DCF-DA (Sigma Cat#D6883) in KR buffer was added. Following 15 min incubation at 37°C, 5% CO_2 in the dark, 200 µl of 11x stock solution of test compound was added, and cells were incubated for another hour, or for the indicated time at 37°C, 5% CO_2. Cells were then harvested using 0.5% trypsin in PBS (collecting all washes and incubations), neutralizing trypsin by adding 200 µl fetal calf serum to each sample, centrifuged and resuspended in 1 ml KR buffer. Cells were then analysed by flow cytometry on a FACS-Calibur flow cytometer, set to acquire 10 000 events per sample.

6.9. Western blotting

6.9.1. Protein harvest

Cells in 60 mm dishes were treated at the appropriate concentration, and for the indicated times. Medium was removed, cells rinsed with 1 ml PBS, and rinses and media were centrifuged (1000rpm, 5 min) to pellet floating cells. RIPA buffer (200 µl) with protease inhibitor (Roche Complete tablets Cat#11697498001), made up as 10x stock) was added to the dish, and cells were lysed manually using a rubber policeman or disposable 1 ml insulin syringe plunger. The pellet of floating cells was taken up in the resulting lysate, and lysates were stored at -20°C.

6.9.2. Protein quantitation

Lysates were thawed and sonicated at 4°C. Protein quantitation was performed in 96 well plates using the BCA kit (Pierce). Various volumes of lysate (to a total volume of 10 µl) were pipetted into each well in duplicate, and made up to 10 µl with RIPA buffer. Ten µl of each BSA standard (range 10 µg/ml to 2000 µg/ml) were pipetted in duplicate for a standard curve, and 10 µl of RIPA was included as a blank. Reagent A and Reagent B from the kit were mixed at a 1:50 ratio, and 100 µl of this solution was added to each well. Following a 30 min incubation at 37°C, the absorbance at 595nm was measured on an Anthos microplate reader 2001. A standard curve was plotted using Prism, and sample concentrations were calculated from this curve.

6.9.3. SDS-PAGE

10% Acrylamide gels with 5% stacking gel were poured using the Protean II minigel casting apparatus (BioRad). Protein samples were prepared by mixing equal amounts of protein with loading dye, and boiled for 10 min to denature proteins. Samples were loaded onto the SDS-PAGE, and the gel was run at 100 volts, for the appropriate times (depending on the size of the protein of interest). Migration of proteins through the gel was monitored by loading a multicolour protein ladder (Precision Plus Protein Kaleidoscope Standard, BioRad, Cat#1610375).

6.9.4 Transfer

SDS-PAGE gels were removed from between the glass plates, and the transfer apparatus was assembled. Protein was transferred from the gel onto Hybond™-ECL™ nitrocellulose membrane (Amersham RPN203D), and these were sandwiched between filter paper and sponges, and inserted into a transfer cassette. The cassette and an ice pack were inserted into the transfer apparatus, which was filled with transfer buffer, and transfer was carried out at 200 volts for 1 hour.

6.9.5. Ponceau S (membrane) and Coomasie (gel) stains

Following transfer, membranes were stained with Ponceau-S (Sigma, P3504) for 10 min, then destained with dH_2O to assess protein loading and transfer efficiency. Ponceau-S stained membranes were photocopied. Gels were stained, then destained and dried as a permanent record of protein loading.

6.9.6. Washes, blocking and primary antibody

Following Ponceau-S staining, membranes were washed with TBS/0.1% Tween, and then blocked in blocking solution (Table 2). Blocking solution was discarded, and the membrane was then washed with TBS/0.1% Tween, with shaking for three sets of 5 min, changing TBS/0.1% Tween each time. Primary antibody was added at the appropriate dilution, and in the indicated buffer (Table 2), and incubated with shaking overnight at 4°C.

Antibody	Supplier	Cat number	Dilution	Diluted in	Source
c-Jun	Santa-Cruz	sc-44	1 in 500	5% fat free milk in TBS/0.1% Tween	Rabbit polyclonal
p-p38 (Thr180/Tyr182)	Cell Signaling	#9211	1 in 1000	TBS/0.1% Tween	Rabbit polyclonal
ERK	Santa Cruz	sc-154	1 in 1000	2.5% fat free milk in TBS/0.1% Tween	Rabbit polyclonal

Table 6.2. Antibody details and dilutions

6.9.7. Secondary antibody

The primary antibody was removed from the membrane, and the membrane was again washed for three sets of 5 min, changing TBS/0.1% Tween each time. The goat anti-rabbit HRP-conjugated secondary antibody (Pierce 1858415) was added in

5% fat free milk in TBS/0.1% Tween at a 1 in 5000 dilution, and the membrane was incubated with shaking for one hour at room temperature. The secondary antibody was removed, and a final set of three 5 min washes with TBS/0.1% Tween were performed to remove excess antibody. Detection reagent (KPL Lumiglo Reserve) was added, and light emission was detected on X-ray film (AGFA). The bands were visualized by developing the film in developer (AGFA G128) for 1 min, washed for 1 min with water, then fixed for 5 min in fixiative (AGFA G333C) as recommended by the manufacturer.

6.9.8. Stripping Western Blot membrane

After detection, membranes were stripped, as follows. Twenty ml 1 M glycine (pH 2.5) was added to the blot, which was then shaken for 5 min on each side. The solution was neutralized by the addition of 2 ml 1M Tris pH 7.5, and the blot was washed several times with TBS/0.1% Tween and reprobed for other proteins.

6.10. RNA isolation

6.10.1. Trizol extraction

$1x10^6$ cells were plated per 100 mm dish, and allowed to grow for 2 days before compounds were added. After the indicated times, RNA was harvested using Trizol reagent (Invitrogen, Cat# 15596-018). Media was removed, and centrifuged to pellet floating cells. The pellet was taken up in 500 µl Trizol and transferred to the plate, and an additional 700 µl (final volume 1.2 ml) Trizol added to each plate. This was left to incubate for 5 min at room temperature before Trizol was transferred to an eppendorf tube. Chloroform (240 µl) was added, and samples were shaken, then incubated on ice for 10 min. Following centrifugation at 8000 rpm for 15 min at 4°C, the aqueous phase was transferred to a new tube, 600 µl isopropanol was added, and samples were left to precipitate overnight at -20°C. They were then centrifuged at 8000rpm for 30 min at 4°C, and the pellet was washed with 1.2 ml 75% ethanol, centrifuged again and ethanol removed. The pellets were airdried, resuspended in 200 µl DEPC H_2O and transferred to a new tube. Isopropanol (200 µl) and 20 µl 3 M sodium acetate were added, and samples were precipitated at -20°C for an hour, then centrifuged at 15000 rpm for 30 min. Another wash with 70% ethanol was performed, and then the ethanol was removed, and the pellet airdried and resuspended in 50 µl DEPC (diethyl pyrocarbonate) treated water.

6.10.2. Quantitation

RNA was quantitated spectrophotometrically by diluting the RNA solution 1 in 250 and reading the UV absorbance at 260nm and 280nm. The concentration of RNA was calculated using the following equation (extinction coefficient for RNA = 40) :

$$[RNA] = OD_{260nm} \times 40 \times \text{dilution factor } (\mu g/ml)$$

The purity of the RNA was tested using the following condition :

$$\text{Ratio } OD_{260nm}/OD_{280nm} > 1.8.$$

RNA quality was evaluated by electrophoresing ~2 µg of RNA on a formaldehyde gel.

6.10.3. Formaldehyde gel electrophoresis

Approximately 2 µg of each sample of RNA was run on a formaldehyde gel to check RNA quality. One percent agarose was dissolved in 1x MOPS solution, and allowed to cool to touch. 5.4 ml of 37 % formaldehyde and 5 µl EtBr were then added, and the gel poured into the casting tray. Once the gel had set, RNA samples were loaded in 10 µl of RNA loading buffer, and the gel was electrophoresed in 1x MOPS until 18S and 35S bands could be visualized and resolved under UV light.

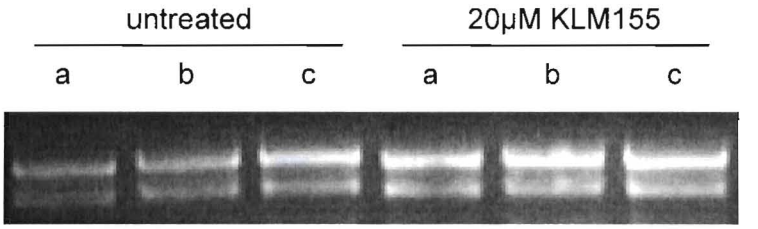

Figure 6.2. Formaldehyde gel electrophoresis of RNA samples used for microarray and real-time RT-PCR analysis.
RNA samples for each treatment condition were electrophoresed on a formaldehyde gel to assess RNA quality. (a,b,c are experimental replicates - RNA harvested from different dishes.)

6.11. Microarray

The microarray format was a cDNA slide. These 11000 element arrays are produced by the National Cancer Institute (NCI) Microarray facility using Incyte Genomics UniGEM clones, and were obtained from Dr. V. Leaner (University of Cape Town, South Africa), and Dr. M. Birrer (National Institute of Health, USA).

6.11.1. First strand synthesis

1 µl of T7-(dT) primer (5'-GGCCAGTGAATTGAATACGACTCACTATAGGAGGCGG-$(dT)_{24}$-3', Genset Corp) was hybridized to 5 µg total RNA at 70°C for 10 min in a total volume of 9 µl, then cooled on ice. The reaction mix was prepared as follows :

4 µl first strand buffer (Invitrogen)
2 µl 0.1M DTT (Invitrogen)
2 µl 10 mM dNTP (Gibco 18090-019)
1 µl RNAsin (Promega N2515)
1 µl Impromp-II Reverse transcriptase (Promega A3802)
9 µl RNA + T7-(dT) primer (from above)

First strand synthesis was then carried out at 42°C for 2 hours, and the product placed on ice.

6.11.2. Second strand synthesis

Second strand reaction mix was prepared as follows :

91 µl sterile ddH_2O
30 µl second strand buffer (Invitrogen)
3 µl 10 mM dNTP mix (Gibco #18090-019)
4 µl *E. coli* DNA polymerase I (Gibco # 18010-025)
1 µl *E. coli* DNA ligase (Gibco #18052-019)
1 µl *E. coli* RNAse H (Gibco #18021-014)

This was added to the product of first strand synthesis for a final volume of 150 µl, and incubated at 16°C for 2 hr. The product was then blunt ended by adding 1.5 µl (x units) T4 DNA polymerase (Gibco #18005-025), and incubating for a further 5 min.

The reaction was stopped by the addition of 10 µl 0.5M EDTA, and 10 µl 1M NaOH, and incubated at 65°C for 10 min, following which 25 µl 1M Tris-HCl (pH 7.5) was added.

6.11.3. DNA clean up

DNA was purified using Phase Lock Gel™ Tubes (Eppendorf #0032 007.953) as follows. Tubes were centrifuged at maximum speed for 30 sec. Sample was mixed with the lower phase of phenol:chloroform:isoamyl alcohol saturated with Tris-HCl/EDTA (Ambion #9732), mixed, and transferred to Phase Lock Tube, then centrifuged at maximum speed for 2 min. The aqueous supernatant was transferred to a new tube, and 1 µl linear acrylamide (Ambion #9520) added. Ninety-six µl 7.5 M ammonium acetate (Sigma #A2706) and 700 µl 95 % ice cold ethanol were added, the pellet vortexed and centrifuged at maximum speed at 4°C for 20 min. The pellet was washed twice with 80 % ethanol, airdried and resuspended in 16 µl sterile ddH_2O.

6.11.4. Transcription

In vitro transcription was carried out using the T7 Megascript kit (Ambion #1334). The reaction mix was prepared as follows :

4 µl 10x reaction buffer
4 µl ATP solution
4 µl CTP solution
4 µl GTP solution
4 µl UTP solution
4 µl enzyme mix

Reaction mix was added to each sample for a final volume of 40 µl, and samples were incubated at 37°C for 6 hours. DEPC treated H_2O (100 µl) was added to each sample to a final volume of 100 µl.

6.11.5. RNA clean-up

RNA was purified using the RNeasy Mini Kit (Qiagen Cat# 74104) as follows.

350 µl Buffer RLT (containing 1 % β-mercaptoethanol added fresh) was added to each sample, and the sample was thoroughly mixed. Two hundred and fifty µl 96 % ethanol was added, and the sample mixed by pipetting. The sample was then applied to an RNeasy mini column placed in a 2 ml collection tube and centrifuged at 8000 xg for 15 sec. The flow through and collection tube were then discarded, and the column transferred onto a new collection tube. Five hundred µl of 1x buffer RPE was then added to the column and centrifuged again at 8000 xg for 15 sec, and the flow through discarded. Another 500 µl of RPE was added and the column centrifuged till dry (approx 2 min) at 8000 xg. The column was then transferred into a 1.5 ml collection tube and 30 µl RNAse-free water pipetted onto the membrane, and the tube centrifuged for 1 min at 8000xg.

The RNA was then quantitated as above.

6.11.6. Labelling (Probe preparation)

5 µg of amplified RNA (and 5 µg of human reference RNA (Stratagene) for each sample) was placed at 65°C for 5 min, then made up to 19 µl with ultrapure H_2O and 2 µl random primers (Gibco #48190-011). Samples were incubated at room temperature for 10 min. Labeling mixes were made up as follows (one Cy3 and one Cy5 mix per sample):

8 µl 5x first strand buffer (Invitrogen)
2 µl 20x low T-dNTP mix (Pharmacia #27-2035-01)
4 µl 0.1M DTT (Invitrogen)
1 µl RNAsin (Promega N515)
2 µl Impromp-II Reverse transcriptase (Promega A3802)
4 µl cy-3 or cy-5 dUTP (NEN #NEL999)

21 µl of mix was added to each probe, with the reference RNA being labeled with cy-3 and samples being labeled with cy-5. Samples were incubated with gentle shaking for 1 hour at 42°C, and the reaction was stopped by the addition of 5 µl 0.5 M EDTA and 10 µl 1 M NaOH. Samples were incubated at 65°C for 15 min, then cooled to room temperature, and 25 µl 1 M Tris-HCl added.

6.11.7. Probe clean-up

Microcon-YM30 columns (Amicon #42410) were prewetted by adding 500 µl 1x TE, and spinning for 5-6 min at 13000 rpm. Flow through was discarded, and columns were checked to ensure a thin film of TE covered the membrane. TE (300 µl) was added to each sample and transferred onto a column, which were then centrifuged for 5-6 min at 13000 rpm. The column was then washed by adding 450 µl TE and spinning as before. A clean eppendorf tube was inverted over each reference RNA column, and probe was eluted by spinning at 14000 rpm for 1 min. The reference RNA probes were then pooled and equal amounts aliquoted into each sample probe. TE (380 µl) was added to each sample, and the column was centrifuged at 13000 rpm until about 7-14 µl remained on the membrane. A clean tube was inverted over the combined column and centrifuged for 1 min at 14000 rpm. The probe volume was then made up to 14 µl with TE and stored at 4°C.

6.11.8. Hybridisation

Prehybridisation buffer was prepared as follows :

250 µl 20x SSC
5 µl 20 % SDS
100 µl 100 mg/ml BSA (Sigma B4287)
645 µl ddH_2O

The hybridization chamber was assembled as follows :

20 µl ddH_2O was added to each humidifying well of the hybridization chamber. The microarray slide was placed in the hybridization chamber, and 40 µl prehybridisation buffer was added to the centre of the slide. A coverslip was placed on top of the prehybridisation buffer, and the cover of the hybridization chamber was firmly screwed in place. Following a 1 hour incubation at 42°C the cover was removed and the slide removed with forceps. The cover slip was allowed to fall off into ddH_2O, and the slide was washed in ddH_2O for 2 min and isopropanol for 2 min. The slide was then placed in a 50 ml blue cap tube and centrifuged at 705 rpm for 4 min to remove moisture.

Fresh 2x hybridization buffer was prepared and warmed to 42°C.

100 µl 20x SSC
100 µl formamide
4 µl 10 % SDS

2 µl COT1 DNA (Gibco #15279-011), 2 µl polyA (Sigma #P9403) and 2 µl yeast tRNA (Sigma #R8759) were added to each sample, and samples were denatured at 100°C for 1 min, then snap cooled on ice. Twenty µl of 2x hybridization buffer was added to each sample to a final volume of 40 µl, and samples were kept at 42°C protected from light until spotted onto the slide.

The hybridization reaction was set up in the same way as the prehybridisation reaction, only with sample replacing the hybridization buffer. The slides were then hybridized for 16 hours at 42°C protected from light.

6.11.9. Slide washes

The slide was removed from the hybridization chamber, and the coverslip was removed by dipping in a 2x SSC, 0.1 % SDS solution. The slides were then washed in 1x SSC, 0.1 % SDS for 4 min, 0.2x SSC for 4 min, and 0.05x SSC for 1 min, then centrifuged at 705 rpm for 4 min or until dry.

6.11.10. Data acquisition

Slides were scanned on a 10 µm resolution GenePix 4000 scanner (Axon Instruments), and images were saved in TIFF format.

6.11.11. Data analysis

The array TIFF images were analysed using GenePix software v3.0 (Axon Instruments). Result files were exported into the NCI microarray database (MaDB) developed by Dr. John Powell.

6.12. Quantitative Real-time RT-PCR

6.12.1. Reverse transcription / cDNA

1 µl of T7-(dT) primer (5'-GGCCAGTGAATTGAATACGACTCACTATAGGAGGCGG-$(dT)_{24}$-3', Genset Corp) was hybridized to 5 µg total RNA at 70°C for 10 min in a total volume of 9 µl, then cooled on ice. The reaction mix was prepared as follows :

4 µl first strand buffer (Invitrogen)
2 µl 0.1 M DTT (Invitrogen)
2 µl 10 mM dNTP (Gibco #18090-019)
1 µl RNAsin (Promega #N2515)
1 µl Impromp-II Reverse transcriptase (Promega A3802)
9 µl RNA + T7-(dT) primer (from above)

First strand synthesis was then carried out at 42°C for 2 hours, and the product placed on ice. Samples were made up to 50 µl with DEPC treated H_2O to a final concentration of 100 ng/µl.

6.12.2. Real Time PCR

Real Time PCR was carried out using the LightCycler FastStart DNA Master SYBR Green I reaction mix (Roche). Two µl of cDNA was added to each capillary, together with 18 µl of reaction mix :

12.6 µl dH_2O
2.4 µl $MgCl_2$
1 µl Hot Start reaction mix
1 µl 20pM sense primer
1 µl 20pM antisense primer

Primers and cycle conditions used are listed in Table 6.3.
Prior to all amplifications samples were denatured at 95°C for 5 min. Melt curves were performed on all samples after each amplification to confirm the presence of a single amplification product.

Gene		Primer sequence	Cycle conditions
Heme oxygenase	forward	5'-GAGGGAAGCCCCCACTCA-3'	40 cycles of 95°C (15sec) 60°C (60sec)
	reverse	5'-AACTGTCGCCACCAGAAAGCT-3'	
Thioredoxin reductase	forward	5'-CGACATAGGATGCTCCAACA-3'	40 cycles of 94°C (30sec) 53°C (60sec) 72°C (30sec)
	reverse	5'-ATTGCCACTGGTGAAAGACC-3'	
MnSOD	forward	5'-GCACTAGCAGCATGTTGAGC-3'	40 cycles of 94°C (30sec) 53°C (60sec) 72°C (30sec)
	reverse	5'-GCGTTGATGTGAGGTTCCAG-3'	
GADD34	forward	5'-TCAATTTGCAGATGGCCAGCGTGCTCC-3'	45 cycles of 95°C (1sec) 58°C (10sec) 72°C (6sec) 62°C (6sec)
	reverse	5'-CCTCGGCTTTCTCCTCCCCTGGGTTCTTAT-3'	
NQO1	forward	5'-TGAAGAAGAAAGGATGGGAGG-3'	45 cycles of 95°C (10sec) 58°C (30sec) 72°C (30sec)
	reverse	5'-AGGGGGAACTGGAATATCAC-3'	
HSP90	forward	5'-GATAAACCCTGACCATTCC-3'	45 cycles of 95°C (15sec) 60°C (45sec) 72°C (10sec) 82°C (1sec)
	reverse	5'-TTTATGAAACTGCGCTCCTGTCTT-3'	
HSP70	forward	5'-GGAGGCGGAGAAGTACA-3'	45 cycles of 95°C (15sec) 60°C (60sec) 72°C (10sec)
	reverse	5'-GCTGATGATGGGGTTACA-3'	
GAPDH	forward	5'-GGCTCTCCAGAACATCATCC-3'	40 cycles of 94°C (30sec) 53°C (60sec) 72°C (30sec)
	Reverse	5'-GCCTGCTTCACCACCTTC-3'	
Glutathione reductase	forward	5'-TTAGGAATAACCAGCGATGGATTT-3'	45 cycles of 95°C (15sec) 60°C (60sec) 72°C (10sec)
	reverse	5'-AATGTAACCTGCACCAACAATGA-3'	

Table 6.3. Primer sequences for Quantitative Real-time RT-PCR.

Several quantitation methods exist for real-time RT-PCR analysis. We chose to use the $2^{-\Delta\Delta CT}$ method (129). The CT (threshold cycle) value for GAPDH for each sample was subtracted from the CT value obtained for that sample for the gene in question (ΔCT). Then one sample was chosen as a reference, and the ΔCT value for this sample was subtracted from the ΔCT for each of the other samples. This gave the ΔΔCT value for each sample, with the reference having a value of 0. The fold upregulation over the reference was then calculated as $2^{-\Delta\Delta CT}$. This gives a value of 1 for the reference sample. Finally the 3 treated samples were averaged, and divided by the average of the untreated samples to give a fold upregulation, with a significance value attached.

$$\text{Fold upregulation} = 2^{-\Delta\Delta CT}$$

CT values (sample gene)	CT values (reference gene)	ΔCT	ΔΔCT	Fold upregulation
A	D	A-D (a)	a-a	$2^{-(a-a)}$
B	E	B-E (b)	b-a	$2^{-(b-a)}$
C	F	C-F (c)	c-a	$2^{-(c-a)}$

Table 6.4. Example of the $2^{-\Delta\Delta CT}$ calculation.

6.13. Data analysis

In all cases, unless otherwise indicated, error bars indicate standard deviation.
For ROS determination, each experimental condition was carried out in triplicate, and results are the mean ± SD and are representative of 2 or more independent experiments.

Apoptosis experiments were carried out in quadruplicate, and results are the mean ± SD, and are representative of 2 independent experiments.

Cell growth and death determinations were carried out in quadruplicate, and results are the mean ± SD and are representative of 2 or more independent experiments. Each concentration for IC_{50} determination was tested in quadruplicate, and each IC_{50} was repeated at least twice.

P-values were calculated using Student's paired 2-tailed t-test.

6.14. Recipes

6.14.1 Cell culture

Trypsin-EDTA

0.5 g trypsin

8 g NaCl

1.45 g $Na_2HPO_4.2H_2O$

0.2 g KCl

0.2 g KH_2PO_4

10 mM EDTA (pH 8.0)

In 1 L PBS

PBS

137 mM NaCl

2.7 mM KCl

4.3 mM $Na_2HPO_4.7H_2O$ (pH 7.4)

1.4 mM KH_2PO_4

Penicillin/streptomycin solution

Add 5 million units Penicillin G Sodium (Highveld Biological) to 5 ml PBS.

Add 5 g 214S Streptomycin Sulphate (Highveld Biological) to 15 ml PBS.

Combine the two and make volume up to 500 ml. Aliquot 5 ml volumes.

Add 5 ml to each 500 ml media.

Mycoplasma detection fixative

1 part glacial acetic acid to 3 parts methanol

Mycoplasma detection Stain solution

0.5 µg/ml Hoeschst No. 33258 in Hanks Buffered Saline Solution (without phenol red or sodium bicarbonate)

Hanks Buffered Saline Solution (without phenol red or sodium bicarbonate)

5.4 mM KCl

0.3 mM Na_2HPO_4

0.4 mM KH_2PO_4

1.3 mM $CaCl_2$

0.5 mM $MgCl_2$

0.6 mM $MgSO_4$

137 mM NaCl

5.6 mM D-glucose

Make up to 1L with dH_2O and pH to 7.4

Mycoplasma detection Mounting Fluid

1.05 g citric acid

1.41 g $Na_2HPO_4.2H_2O$

50 ml glycerol

pH 5.5 (check periodically – critical for optimum fluorescence)

6.14.2. Crystal violet assay

Crystal violet staining solution

1 % crystal violet

50 % MeOH

6.14.3. Cell Cycle analysis

Staining solution

0.1 % Triton X100

2 mM $MgCl_2$

100 mM NaCl

0.01 M PIPES buffer

10 µg/ml propidium iodide

6.14.4. ROS assay

Krebs-Ringer buffer

110 mM NaCl

2.6 mM KCl

1.2 mM $MgSO_4$

1.2 mM KH_2PO_4

25 mM $NaHCO_3$

11 mM glucose

Dissolve in water, pH to 7.4, then make up to 1L.

Filter solution, or make fresh for each experiment to avoid contamination. Can freeze in aliquots.

6.14.5. Western blotting

RIPA buffer

150 mM NaCl

1 % Triton X100

0.1 % SDS

10 mM Tris (pH 7.5)

1 % deoxycholate

Protease inhibitor

1 Complete tablet was dissolved in 5 ml dH_2O to make a 10x solution. This was aliquated and stored at -20°C.

30% Acrylamide

30 g acrylamide

0.8 g bis-acrylamide

0.1 g SDS

Add dH_2O to 100 ml and mix

Store at 4°C

Stacking Buffer

5.9 g Tris

0.4 g SDS

pH to 8.0 and make up to 100 ml with dH_2O. Store at 4°C

Resolving Buffer

36.2 g Tris

0.8 g SDS

pH to 8.9 and make up to 200 ml with dH_2O. Store at 4°C

5x Loading Buffer

1.75 g Tris

30 ml glycine

Make up to about 40 ml with dH_2O

pH to 6.8 with 1 N HCl

Add 5 g SDS

Add H_2O to 50 ml

Loading Dye

200 µl 5x loading buffer

100 µl β-mercaptoethanol

100 µl saturated, filtered bromophenol blue

10x Running Buffer

40 g glycine

63.2 g Tris

10 g SDS or 100 ml 10% stock

Make up to 1 L with dH_2O

Dilute 1 in 10 for 1x running buffer

10x Transfer Buffer

144 g glycine

38 g Tris

Make up to 1 L with dH_2O

1x Transfer Buffer

100 ml 10x transfer buffer

200 ml isopropanol

700 ml dH_2O

Gel stain solution

50 % methanol

10 % glacial acetic acid

0.25 % (w/v) Coomassie Blue

Gel destain solution

10 % methanol

7.5 % glacial acetic acid

Ponceau-S stain solution

0.1 g Ponceau S

1 ml glacial acetic acid

100 ml dH_2O

10x Tris buffered saline (TBS)

60.5 g Tris

87.6 g NaCl

pH to 7.5

make up to 1 L with dH_2O

TBS/0.1 % Tween

100 ml 10x TBS

900 ml dH_2O

1 ml Tween 20

Blocking solutions

5 g fat-free milk powder

Dissolve in 100 ml TBS/0.1% Tween

Fixer (AGFA G333C)

Dilute 100 ml stock solution with 400 ml dH_2O

Developer (AGFA G128)

Dilute 100 ml stock solution with 400 ml dH_2O

6.14.6. RNA isolation

10x MOPS

0.4 M MOPS, pH 7.0

0.1 M sodium acetate

0.01 M EDTA

6.14.7. Microarray

20x SSC

172.32 g Sodium Chloride

88.23 g Sodium Citrate

Make up to 1 L

pH to 7.0

10X TE Buffer

0.1 M Tris-Cl, pH 7.5

10 mM EDTA pH 8.0

REFERENCES

(1) Hendricks D, Parker MI. Oesophageal cancer in Africa. IUBMB Life 2002; 53(4-5):263-268.

(2) World Health Organisation classification of tumours : Pathology and genetics of tumours of the digestive system. Lyon: IARC Press; 2000.

(3) Altorki NK. Radical esophagectomy. Semin Thorac Cardiovasc Surg 1992; 4(4):324-327.

(4) Mqoqi N, Kellerr P, Madhoo J, Sitas F. National Cancer Registry of South Africa. Incidence and geographical distribution of histologically diagnosed cancer in South Africa, 1996-1997. Johannesburg: National Cancer Registry of South Africa, South African Institute for Medical Research; 2003.

(5) Enzinger PC, Mayer RJ. Esophageal cancer. N Engl J Med 2003; 349(23):2241-2252.

(6) Spechler SJ, Goyal RK. Barrett's esophagus. N Engl J Med 1986; 315(6):362-371.

(7) Dreilich M, Bergqvist M, Moberg M, Brattstrom D, Gustavsson I, Bergstrom S et al. High-risk human papilloma virus (HPV) and survival in patients with esophageal carcinoma: a pilot study. BMC Cancer 2006; 6:94.

(8) Yao PF, Li GC, Li J, Xia HS, Yang XL, Huang HY et al. Evidence of human papilloma virus infection and its epidemiology in esophageal squamous cell carcinoma. World J Gastroenterol 2006; 12(9):1352-1355.

(9) Dandara C, Ballo R, Parker MI. CYP3A5 genotypes and risk of oesophageal cancer in two South African populations. Cancer Lett 2005; 225(2):275-282.

(10) Dandara C, Li DP, Walther G, Parker MI. Gene-environment interaction: the role of SULT1A1 and CYP3A5 polymorphisms as risk modifiers for squamous cell carcinoma of the oesophagus. Carcinogenesis 2006; 27(4):791-797.

(11) American Joint Committee on Cancer, American Cancer Society. AJCC cancer staging manual. 6th ed. New York: Springer; 2002.

(12) Mackay S, Stefanou G. Management of oesophageal carcinoma. Aust Fam Physician 2006; 35(4):202-206.

(13) Kuwano H, Nakajima M, Miyazaki T, Kato H. Distinctive clinicopathological characteristics in esophageal squamous cell carcinoma. Ann Thorac Cardiovasc Surg 2003; 9(1):6-13.

(14) Lerut T, Coosemans W, De LP, Van RD, Nafteux P, Moons J. Optimizing treatment of carcinoma of the esophagus and gastroesophageal junction. Surg Oncol Clin N Am 2001; 10(4):863-84.

(15) Leonard GD, McCaffrey JA, Maher M. Optimal therapy for oesophageal cancer. Cancer Treatment Reviews 2003; 29(4):275-282.

(16) Tew WP, Kelsen DP, Ilson DH. Targeted therapies for esophageal cancer. Oncologist 2005; 10(8):590-601.

(17) Bancewicz J, Clark PI, Smith DB, Donnelly RJ, Fayers PM, Weeden S et al. Surgical resection with or without preoperative chemotherapy in oesophageal cancer: a randomised controlled trial. Lancet 2002; 359(9319):1727-1733.

(18) Khushalani NI, Leichman CG, Proulx G, Nava H, Bodnar L, Klippenstein D et al. Oxaliplatin in combination with protracted-infusion fluorouracil and radiation: Report of a clinical trial for patients with esophageal cancer. J Clin Oncol 2002; 20(12):2844-2850.

(19) Urba SG, Orringer MB, Turrisi A, Lannettoni M, Forastiere A, Strawderman M. Randomized trial of preoperative chemoradiation versus surgery alone in patients with locoregional esophageal carcinoma. J Clin Oncol 2001; 19(2):305-313.

(20) Taira N, Doihara H, Oota T, Hara F, Shien T, Takahashi H et al. Gefitinib, an epidermal growth factor receptor blockade agent, shows additional or synergistic effects on the radiosensitivity of esophageal cancer cells in vitro. Acta Med Okayama 2006; 60(1):25-34.

(21) Scheithauer W. Esophageal cancer: chemotherapy as palliative therapy. Annals of Oncology 2004; 15:97-100.

(22) Yim EK, Lee SB, Lee KH, Kim CJ, Park JS. Analysis of the in vitro synergistic effect of 5-fluorouracil and cisplatin on cervical carcinoma cells. Int J Gynecol Cancer 2006; 16(3):1321-1329.

(23) Shirasaka T, Shimamoto Y, Ohshimo H, Saito H, Fukushima M. Metabolic basis of the synergistic antitumor activities of 5-fluorouracil and cisplatin in rodent tumor models in vivo. Cancer Chemother Pharmacol 1993; 32(3):167-172.

(24) Ali BH, Al Moundhri MS. Agents ameliorating or augmenting the nephrotoxicity of cisplatin and other platinum compounds: a review of some recent research. Food Chem Toxicol 2006; 44(8):1173-1183.

(25) Bose RN. Biomolecular targets for platinum antitumor drugs. Mini Rev Med Chem 2002; 2(2):103-111.

(26) Heidelberger C, Chaudhuri, Danneberg P, Mooren D, Griesbach L, Duschinsky R et al. Fluorinated pyrimidines, a new class of tumour-inhibitory compounds. Nature 1957; 179(4561):663-666.

(27) Longley DB, Harkin DP, Johnston PG. 5-fluorouracil: mechanisms of action and clinical strategies. Nat Rev Cancer 2003; 3(5):330-338.

(28) Alter P, Herzum M, Soufi M, Schaefer JR, Maisch B. Cardiotoxicity of 5-fluorouracil. Cardiovasc Hematol Agents Med Chem 2006; 4(1):1-5.

(29) Panigrahi I, Naithani R. Imatinib mesylate: A designer drug. J Assoc Physicians India 2006; 54:203-206.

(30) Workman P. The opportunities and challenges of personalized genome-based molecular therapies for cancer: targets, technologies, and molecular chaperones. Cancer Chemother Pharmacol 2003; 52 Suppl 1:S45-S56.

(31) Sausville EA, Tomaszewski JE, Ivy P. Clinical development of 17-allylamino, 17-demethoxygeldanamycin. Curr Cancer Drug Targets 2003; 3(5):377-383.

(32) Newell DR. How to develop a successful cancer drug - molecules to medicines or targets to treatments? Eur J Cancer 2005; 41(5):676-682.

(33) Decker S, Hollingshead M, Bonomi CA, Carter JP, Sausville EA. The hollow fibre model in cancer drug screening: the NCI experience. Eur J Cancer 2004; 40(6):821-826.

(34) Boyd MR, Paull KD. Some practical considerations and applications of the National-Cancer-Institute in-vitro anticancer drug discovery screen. Drug Dev Res 1995; 34(2):91-109.

(35) Cragg GM. Paclitaxel (Taxol (R)): A success story with valuable lessons for natural product drug discovery and development. Med Res Rev 1998; 18(5):315-331.

(36) Mann J. Natural products in cancer chemotherapy: past, present and future. Nat Rev Cancer 2002; 2(2):143-148.

(37) Cragg GM, Newman DJ. Plants as a source of anti-cancer agents. J Ethnopharmacol 2005; 100(1-2):72-79.

(38) Newman DJ, Cragg GM. Marine natural products and related compounds in clinical and advanced preclinical trials. J Nat Prod 2004; 67(8):1216-1238.

(39) Faulkner DJ. Highlights of marine natural products chemistry (1972-1999). Nat 2000; 17(1):1-6.

(40) Jordan MA, Wilson L. Microtubules as a target for anticancer drugs. Nat Rev Cancer 2004; 4(4):253-265.

(41) Da Rocha AB, Lopes RM, Schwartsmann G. Natural products in anticancer therapy. Curr Opin Pharmacol 2001; 1(4):364-369.

(42) Andersen RJ, Williams DE. Pharmaceuticals from the Sea. In: Hester RE, Harrison RM, editors. Chemistry in the Marine Environment. Cambridge: RSC Press; 2000. 55-79.

(43) Haefner B. Drugs from the deep: marine natural products as drug candidates. Drug Discov Today 2003; 8(12):536-544.

(44) Proksch P, Edrada-Ebel R, Ebel R. Drugs from the Sea – Opportunities and obstacles. Mar Drugs 2006; 1:5-17.

(45) Mayer AMS, Gustafson KR. Marine pharmacology in 2001-2: antitumour and cytotoxic compounds. Eur J Cancer 2004; 40(18):2676-2704.

(46) Blunt JW, Copp BR, Munro MHG, Northcote PT, Prinsep MR. Marine natural products. Nat Prod Rep 2006; 23(1):26-78.

(47) Blunt JW, Copp BR, Munro MHG, Northcote PT, Prinsep MR. Marine natural products. Nat Prod Rep 2005; 22(1):15-61.

(48) Belarbi E, Gomez AC, Chisti Y, Camacho FG, Grima EM. Producing drugs from marine sponges. Biotechnol Adv 2003; 21(7):585-598.

(49) Venter JC, Remington K, Heidelberg JF, Halpern AL, Rusch D, Eisen JA et al. Environmental genome shotgun sequencing of the Sargasso Sea. Science 2004; 304(5667):66-74.

(50) Chin YW, Balunas MJ, Chai HB, Kinghorn AD. Drug discovery from natural sources. AAPS J 2006; 8(2):E239-E253.

(51) Newman DJ, Cragg GM. Advanced preclinical and clinical trials of natural products and related compounds from marine sources. Curr Med Chem 2004; 11(13):1693-1713.

(52) Blay JY, Le CA, Verweij J, Scurr M, Seynaeve C, Bonvalot S et al. A phase II study of ET-743/trabectedin ('Yondelis') for patients with advanced gastrointestinal stromal tumours. Eur J Cancer 2004; 40(9):1327-1331.

(53) Zelek L, Yovine A, Brain E, Turpin F, Taamma A, Riofrio M et al. A phase II study of Yondelis (trabectedin, ET-743) as a 24-h continuous intravenous infusion in pretreated advanced breast cancer. Br J Cancer 2006; 94(11):1610-1614.

(54) Fayette J, Coquard IR, Alberti L, Boyle H, Meeus P, Decouvelaere AV et al. ET-743: a novel agent with activity in soft-tissue sarcomas. Curr Opin Oncol 2006; 18(4):347-353.

(55) Jordan MA, Wilson L. Microtubules and actin filaments: dynamic targets for cancer chemotherapy. Curr Opin Cell Biol 1998; 10(1):123-130.

(56) De Souza MV. (+)-discodermolide: a marine natural product against cancer. ScientificWorldJournal 2004; 4:415-436.

(57) Crews P, Manes LV, Boehler M. Jasplakinolide, A cyclodepsipeptide from the marine sponge, Jaspis sp. Tetrahedron Lett 1986; 27(25):2797-2800.

(58) Carmely S, Kashman Y. Structure of Swinholide-A, A New Macrolide from the Marine Sponge Theonella-Swinhoei. Tetrahedron Letters 1985; 26(4):511-514.

(59) Hurley LH. DNA and its associated processes as targets for cancer therapy. Nat Rev Cancer 2002; 2(3):188-200.

(60) Hurley LH. Secondary DNA structures as molecular targets for cancer therapeutics. Biochem Soc Trans 2001; 29(Pt 6):692-696.

(61) Kong Q, Beel JA, Lillehei KO. A threshold concept for cancer therapy. Med Hypotheses 2000; 55(1):29-35.

(62) Tsang WP, Chau SP, Kong SK, Fung KP, Kwok TT. Reactive oxygen species mediate doxorubicin induced p53-independent apoptosis. Life Sci 2003; 73(16):2047-2058.

(63) Mizutani H, Tada-Oikawa S, Hiraku Y, Kojima M, Kawanishi S. Mechanism of apoptosis induced by doxorubicin through the generation of hydrogen peroxide. Life Sci 2005; 76(13):1439-1453.

(64) Corazzari M, Lovat PE, Oliverio S, Di SF, Donnorso RP, Redfern CP et al. Fenretinide: a p53-independent way to kill cancer cells. Biochem Biophys Res Commun 2005; 331(3):810-815.

(65) Ramanathan B, Jan KY, Chen CH, Hour TC, Yu HJ, Pu YS. Resistance to paclitaxel is proportional to cellular total antioxidant capacity. Cancer Res 2005; 65(18):8455-8460.

(66) Engel RH, Evens AM. Oxidative stress and apoptosis: a new treatment paradigm in cancer. Front Biosci 2006; 11:300-312.

(67) Pelicano H, Carney D, Huang P. ROS stress in cancer cells and therapeutic implications. Drug Resist Updat 2004; 7(2):97-110.

(68) Weiss RB. The anthracyclines: will we ever find a better doxorubicin? Semin Oncol 1992; 19(6):670-686.

(69) Assuncao GC, Linden R. Programmed cell deaths. Apoptosis and alternative deathstyles. Eur J Biochem 2004; 271(9):1638-1650.

(70) Edinger AL, Thompson CB. Death by design: apoptosis, necrosis and autophagy. Curr Opin Cell Biol 2004; 16(6):663-669.

(71) Bremer E, van DG, Kroesen BJ, de LL, Helfrich W. Targeted induction of apoptosis for cancer therapy: current progress and prospects. Trends Mol Med 2006; 12(8):382-393.

(72) Proskuryakov SY, Konoplyannikov AG, Gabai VL. Necrosis: a specific form of programmed cell death? Exp Cell Res 2003; 283(1):1-16.

(73) Boya P, Gonzalez-Polo RA, Casares N, Perfettini JL, Dessen P, Larochette N et al. Inhibition of macroautophagy triggers apoptosis. Mol Cell Biol 2005; 25(3):1025-1040.

(74) Lum JJ, Bauer DE, Kong M, Harris MH, Li C, Lindsten T et al. Growth factor regulation of autophagy and cell survival in the absence of apoptosis. Cell 2005; 120(2):237-248.

(75) Branch ML, Branch G.M. The Living Shores of Southern Africa. Cape Town: Struik; 1992.

(76) Branch GM, Griffiths CL, Branch ML, Beckley LE. Two Oceans. Cape Town: David Philip; 1994.

(77) Davies-Coleman MT. Bioactive natural products from Southern African marine invertebrates. In: Atta-ur-Rahman, editor. Studies in Natural Product Chemistry (Bioactive Natural Products Part L). Amsterdam: Elsevier; 2005.

(78) Riekert C. Drugs from the Sea. 1-20. 1972. Pretoria, The Government Printer.
Ref Type: Report

(79) Silk MH, Saphton HH, Hahn HH. South African pilchard oil. II. Concentrates of highly unsaturated fatty acids and alcohols derived from South African pilchard oil. Biochem J 1954; 57(4):574-577.

(80) de Koning AJ. Phospholipids of marine origin: a review of research in South Africa 1963-2003. S Afr J Sci 2003; 99:521-525.

(81) Nunn JR, Von Holdt MM. Red-seaweed polysaccharides I. *Gracilaria confervoides.* J Chem Soc 1957;1094-1097.

(82) Davies-Coleman MT, Beukes DR. Ten years of marine natural products research at Rhodes University. S Afr J Sci 2004; 100(11-12):539-544.

(83) Veale RB, Thornley AL. Increased single class low-affinity EGF receptors expressed by human esophageal squamous carcinoma cell lines. S Afr J Sci 1989; 85(6):375-379.

(84) Monks A, Scudiero D, Skehan P, Shoemaker R, Paull K, Vistica D et al. Feasibility of a high-flux anticancer drug screen using a diverse panel of cultured human tumor cell lines. J Natl Cancer Inst 1991; 83(11):757-766.

(85) Miller SE, Veale RB. Environmental modulation of alpha(v), alpha(2) and beta(1) integrin subunit expression in human oesophageal squamous cell carcinomas. Cell Biol Int 2001; 25(1):61-69.

(86) Jones GJ, Heiss NS, Veale RB, Thornley AL. Amplification and expression of the TGF-alpha, EGF receptor and c-myc genes in four human oesophageal squamous cell carcinoma lines. Biosci Rep 1993; 13(5):303-312.

(87) Mcleod C, Thornley A, Veale R, Scott E. The anchorage-dependent and anchorage-independent growth of a human SCC cell line - the roles of TGF-Alpha/EGF and TGF-Beta. Br J Cancer 1990; 61(2):267-269.

(88) Saotome K, Morita H, Umeda M. Cytotoxicity test with simplified crystal violet staining method using microtitre plates and its application to injection drugs. Toxicol in Vitro 1989; 3(4):317-321.

(89) Paine TM, Soule HD, Pauley RJ, Dawson PJ. Characterization of epithelial phenotypes in mortal and immortal human breast cells. Int J Cancer 1992; 50(3):463-473.

(90) Rajput J, Moss JR, Hutton AT, Hendricks DT, Arendse CE, Imrie C. Synthesis, characterization and cytotoxicity of some palladium(II), platinum(II), rhodium(I) and iridium(I) complexes of ferrocenylpyridine and related ligands. Crystal and molecular structure of trans-dichlorobis(3-ferrocenylpyridine)palladium(II). J Organomet Chem 2004; 689(9):1553-1568.

(91) Davies-Coleman MT, Froneman W, Keyzers RA, Whibley C, Hendricks D, Samaai T et al. Anti-oesophageal cancer activity in extracts of deep-water Marion Island sponges. S Afr J Sci 2005; 101(11-12):489-490.

(92) Faulkner DJ. Chemical riches from the oceans. Chem Br 1995; 31(9):680-684.

(93) Keyzers RA, Gray CA, Schleyer MH, Whibley CE, Hendricks DT, Davies-Coleman MT. Malonganenones A-C, novel tetraprenylated alkaloids from the Mozambique gorgonian Leptogorgia gilchristi. Tetrahedron 2006; 62(10):2200-2206.

(94) Hooper GJ, Davies-Coleman MT. Sesquiterpene hydroquinones from the South-African soft coral Alcyonium fauri. Tetrahedron Lett 1995; 36(18):3265-3268.

(95) McPhail KL, Davies-Coleman MT, Starmer J. Sequestered chemistry of the Arminacean nudibranch Leminda millecra in Algoa Bay, South Africa. J Nat Prod 2001; 64(9):1183-1190.

(96) Pika J, Faulkner DJ. 4 Sesquiterpenes from the South-African Nudibranch Leminda-Millecra. Tetrahedron 1994; 50(10):3065-3070.

(97) Samaai T, Keyzers R, Davies-Coleman M. A new species of Strongylodesma Levi, 1969 (Porifera; Demospongiae; Poecilosclerida; Latrunculiidae) from Aliwal Shoal on the east coast of South Africa. Zootaxa 2004;(584):1-11.

(98) Schmidt EW, Harper MK, Faulkner DJ. Makaluvamines H-M and damirone C from the pohnpeian sponge Zyzzya fuliginosa. J Nat Prod 1995; 58(12):1861-1867.

(99) Keyzers RA, Samaai T, Davies-Coleman MT. Novel pyrroloquinoline ribosides from the South African latrunculid sponge Strongylodesma aliwaliensis. Tetrahedron Lett 2004; 45(51):9415-9418.

(100) Keyzers RA, Arendse CE, Hendricks DT, Samaai T, Davies-Coleman MT. Makaluvic acids from the South African latrunculid sponge Strongylodesma aliwaliensis. J Nat Prod 2005; 68(4):506-510.

(101) Antunes EM, Copp BR, Davies-Coleman MT, Samaai T. Pyrroloiminoquinone and related metabolites from marine sponges. Nat Prod Rep 2005; 22(1):62-72.

(102) Hooper GJ, Davies-Coleman MT, KellyBorges M, Coetzee PS. New alkaloids from a South African latrunculid sponge. Tetrahedron Lett 1996; 37(39):7135-7138.

(103) Antunes EM, Beukes DR, Kelly M, Samaai T, Barrows LR, Marshall KM et al. Cytotoxic pyrroloiminoquinones from four new species of South African latrunculid sponges. J Nat Prod 2004; 67(8):1268-1276.

(104) Gunasekera SP, Zuleta IA, Longley RE, Wright AE, Pomponi SA. Discorhabdins S, T, and U, new cytotoxic pyrroloiminoquinones from a deep-water Caribbean sponge of the genus Batzella. J Nat Prod 2003; 66(12):1615-1617.

(105) Gunasekera SP, McCarthy PJ, Longley RE, Pomponi SA, Wright AE, Lobkovsky E et al. Discorhabdin P, a new enzyme inhibitor from a deep-water Caribbean sponge of the genus Batzella. J Nat Prod 1999; 62(1):173-175.

(106) Rudi A, Goldberg I, Stein Z, Benayahu Y, Schleyer M, Kashman Y. Sodwanones Ac, 3 New triterpenoids from a marine sponge. Tetrahedron Lett 1993; 34(24):3943-3944.

(107) Carletti I, Long C, Funel C, Amade P. Yardenone A and B: New cytotoxic triterpenes from the Indian Ocean sponge Axinella cf bidderi. J Nat Prod 2003; 66(1):25-29.

(108) Wright AE, Pomponi SA, Mcconnell OJ, Kohmoto S, McCarthy PJ. (+)-Curcuphenol and (+)-curcudiol, sesquiterpene phenols from shallow and deep-water collections of the marine sponge Didiscus flavus. J Nat Prod 1987; 50(5):976-978.

(109) Fusetani N, Sugano M, Matsunaga S, Hashimoto K. (+)-Curcuphenol and dehydrocurcuphenol, novel sesquiterpenes which inhibit H,K-ATPase, from a marine sponge Epipolasis sp. Experientia 1987; 43(11-12):1234-1235.

(110) Karuso P, Skelton BW, Taylor WC, White AH. The constituents of marine sponges .1. the isolation from Aplysilla sulfurea (Dendroceratida) of (1R Star, 1'S Star, 1'R Star, 3R Star)-1-acetoxy-4-ethyl-5-(1,3,3-trimethylcyclohexyl)-1,3-dihydroisobenzofuran-1'(4),3-carbolactone and the determination of its crystal structure. Aust J Chem 1984; 37(5):1081-1093.

(111) Molinski TF, Faulkner DJ. Metabolites of the Antarctic sponge Dendrilla membranosa. J Org Chem 1987; 52(2):296-298.

(112) Pettit GR, Xu JP, Hogan F, Williams MD, Doubek DL, Schmidt JM et al. Isolation and structure of the human cancer cell growth inhibitory cyclodepsipeptide dolastatin 16. J Nat Prod 1997; 60(8):752-754.

(113) Pettit GR, Kamano Y, Herald CL, Tuinman AA, Boettner FE, Kizu H et al. Antineoplastic Agents .136. the isolation and structure of a remarkable marine animal antineoplastic constituent - Dolastatin 10. J Am Chem Soc 1987; 109(22):6883-6885.

(114) Simmons TL, Andrianasolo E, McPhail K, Flatt P, Gerwick WH. Marine natural products as anticancer drugs. Mol Cancer Ther 2005; 4(2):333-342.

(115) Son BW, Kim JC, Choi HD, Kang JS. A radical scavenging farnesylhydroquinone from a marine-derived fungus Penicillium sp. Arch Pharmacal Res 2002; 25(1):77-79.

(116) Li XF, Choi HD, Kang JS, Lee CO, Son BW. New polyoxygenated farnesylcyclohexenones, deacetoxyyanuthone A and its hydro derivative from the marine-derived fungus Penicillium sp. J Nat Prod 2003; 66(11):1499-1500.

(117) Asche C. Antitumour quinones. Mini Rev Med Chem 2005; 5(5):449-467.

(118) Karczewski JM, Peters JGP, Noordhoek J. Quinone toxicity in DT-diaphorase-efficient and -deficient colon carcinoma cell lines. Biochem Pharmacol 1999; 57(1):27-37.

(119) Riss TL, Moravec RA. Use of multiple assay endpoints to investigate the effects of incubation time, dose of toxin, and plating density in cell-based cytotoxicity assays. Assay Drug Dev Technol 2004; 2(1):51-62.

(120) Su YT, Chang HL, Shyue SK, Hsu SL. Emodin induces apoptosis in human lung adenocarcinoma cells through a reactive oxygen species-dependent mitochondrial signaling pathway. Biochem Pharmacol 2005; 70(2):229-241.

(121) Chen ZH, Na HK, Hurh YJ, Surh YJ. 4-Hydroxyestradiol induces oxidative stress and apoptosis in human mammary epithelial cells: possible protection by NF-kappaB and ERK/MAPK. Toxicol Appl Pharmacol 2005; 208(1):46-56.

(122) Aiello A, Fattorusso E, Luciano P, Macho A, Menna M, Munoz E. Antitumor effects of two novel naturally occurring terpene quinones isolated from the Mediterranean ascidian Aplidium conicum. J Med Chem 2005; 48(9):3410-3416.

(123) Cadenas E. Antioxidant and prooxidant functions of DT-diaphorase in quinone metabolism. Biochem Pharmacol 1995; 49(2):127-140.

(124) Foppoli C, De MF, Blarzino C, Perluigi M, Cini C, Coccia R. Biological response of human diploid keratinocytes to quinone-producing compounds: role of NAD(P)H:quinone oxidoreductase 1. Int J Biochem Cell Biol 2005; 37(4):852-863.

(125) Watanabe N, Forman HJ. Autoxidation of extracellular hydroquinones is a causative event for the cytotoxicity of menadione and DMNQ in A549-S cells. Arch Biochem Biophys 2003; 411(1):145-157.

(126) Oyama Y, Hayashi A, Ueha T, Maekawa K. Characterization of 2',7'-dichlorofluorescin fluorescence in dissociated mammalian brain neurons: estimation on intracellular content of hydrogen peroxide. Brain Res 1994; 635(1-2):113-117.

(127) Hasui M, Hirabayashi Y, Kobayashi Y. Simultaneous measurement by flow cytometry of phagocytosis and hydrogen peroxide production of neutrophils in whole blood. J Immunol Methods 1989; 117(1):53-58.

(128) Ruiz-Ramos R, Cebrian ME, Garrido E. Benzoquinone activates the ERK/MAPK signaling pathway via ROS production in HL-60 cells. Toxicol 2005; 209(3):279-287.

(129) Livak KJ, Schmittgen TD. Analysis of relative gene expression data using real-time quantitative PCR and the 2(-Delta Delta C(T)) Method. Methods 2001; 25(4):402-408.

(130) Galbraith R. Heme oxygenase: who needs it? Proc Soc Exp Biol Med 1999; 222(3):299-305.

(131) Holmgren A, Johansson C, Berndt C, Lonn ME, Hudemann C, Lillig CH. Thiol redox control via thioredoxin and glutaredoxin systems. Biochem Soc Trans 2005; 33(Pt 6):1375-1377.

(132) Haneda M, Xiao H, Hasegawa T, Kimura Y, Nakashima I, Isobe K. Regulation of mouse GADD34 gene transcription after DNA damaging agent methylmethane sulfonate. Gene 2004; 336(1):139-146.

(133) Parsell DA, Lindquist S. The function of heat-shock proteins in stress tolerance: degradation and reactivation of damaged proteins. Annu Rev Genet 1993; 27:437-496.

(134) Seanor KL, Cross JV, Nguyen SM, Yan M, Templeton DJ. Reactive quinones differentially regulate SAPK/JNK and p38/mHOG stress kinases. Antioxid Redox Signal 2003; 5(1):103-113.

(135) Brantley-Finley C, Lyle CS, Du L, Goodwin ME, Hall T, Szwedo D et al. The JNK, ERK and p53 pathways play distinct roles in apoptosis mediated by the antitumor agents vinblastine, doxorubicin, and etoposide. Biochem Pharmacol 2003; 66(3):459-469.

(136) Matsuzawa A, Ichijo H. Stress-responsive protein kinases in redox-regulated apoptosis signaling. Antioxid Redox Signal 2005; 7(3-4):472-481.

(137) Pandey S, Wang E. Cells en-route to apoptosis are characterized by the up-regulation of c-Fos, c-Myc, c-Jun, cdc2 and Rb phosphorylation, resembling events of early cell-cycle traverse. J Cell Biochem 1995; 58(2):135-150.

(138) Sng JCG, Taniura H, Yoneda Y. Inhibition of histone deacetylation by trichostatin A intensifies the transcriptions of neuronal c-fos and c-jun genes after kainate stimulation. Neurosci Lett 2005; 386(3):150-155.

(139) Bennett BL, Sasaki DT, Murray BW, O'Leary EC, Sakata ST, Xu WM et al. SP600125, an anthrapyrazolone inhibitor of Jun N-terminal kinase. Proc Natl Acad Sci U S A 2001; 98(24):13681-13686.

(140) Hennigan RF, Stambrook PJ. Dominant negative c-jun inhibits activation of the cyclin D1 and cyclin E kinase complexes. Mol Biol Cell 2001; 12(8):2352-2363.

(141) Kim HJ, Chakravarti N, Oridate N, Choe C, Claret FX, Lotan R. N-(4-Hydroxyphenyl)retinamide-induced apoptosis triggered by reactive oxygen species is mediated by activation of MAPKs in head and neck squamous carcinoma cells. Oncogene 2006; 25(19):2785-2794.

(142) Filomeni G, Aquilano K, Rotilio G, Ciriolo MR. Reactive oxygen species-dependent c-Jun NH2-terminal kinase/c-Jun signaling cascade mediates neuroblastoma cell death induced by diallyl disulfide. Cancer Res 2003; 63(18):5940-5949.

(143) Chun KH, Benbrook DM, Berlin KD, Hong WK, Lotan R. The synthetic heteroarotinoid SHetA2 induces apoptosis in squamous carcinoma cells through a receptor-independent and mitochondria-dependent pathway. Cancer Res 2003; 63(13):3826-3832.

(144) Seow HA, Penketh PG, Belcourt MF, Tomasz M, Rockwell S, Sartorelli AC. Nuclear overexpression of NAD(P)H:quinone oxidoreductase 1 in Chinese hamster ovary cells increases the cytotoxicity of mitomycin C

under aerobic and hypoxic conditions. J Biol Chem 2004; 279(30):31606-31612.

(145) Phillips RM, Burger AM, Fiebig HH, Double JA. Genotyping of NAD(P)H:quinone oxidoreductase (NQO1) in a panel of human tumor xenografts: relationship between genotype status, NQO1 activity and the response of xenografts to Mitomycin C chemotherapy in vivo(1). Biochem Pharmacol 2001; 62(10):1371-1377.

(146) Kelland LR, Sharp SY, Rogers PM, Myers TG, Workman P. DT-Diaphorase expression and tumor cell sensitivity to 17-allylamino, 17-demethoxygeldanamycin, an inhibitor of heat shock protein 90. J Natl Cancer Inst 1999; 91(22):1940-1949.

(147) Guo W, Reigan P, Siegel D, Zirrolli J, Gustafson D, Ross D. The bioreduction of a series of benzoquinone ansamycins by NAD(P)H:quinone oxidoreductase 1 (NQO1) to more potent heat shock protein 90 (Hsp90) inhibitors, the hydroquinone ansamycins. Mol Pharmacol 2006; 70(4):1194-1203.

(148) Cresteil T, Jaiswal AK. High levels of expression of the NAD(P)H:quinone oxidoreductase (NQO1) gene in tumor cells compared to normal cells of the same origin. Biochem Pharmacol 1991; 42(5):1021-1027.

(149) Siegel D, Ross D. Immunodetection of NAD(P)H:quinone oxidoreductase 1 (NQO1) in human tissues. Free Radic Biol Med 2000; 29(3-4):246-253.

(150) Winski SL, Swann E, Hargreaves RH, Dehn DL, Butler J, Moody CJ et al. Relationship between NAD(P)H:quinone oxidoreductase 1 (NQO1) levels in a series of stably transfected cell lines and susceptibility to antitumor quinones. Biochem Pharmacol 2001; 61(12):1509-1516.

(151) Barzilai A, Yamamoto K. DNA damage responses to oxidative stress. DNA Repair (Amst) 2004; 3(8-9):1109-1115.

(152) Sakharov DV, Bunschoten A, van WH, Wirtz KW. Photodynamic treatment and H2O2-induced oxidative stress result in different patterns of cellular protein oxidation. Eur J Biochem 2003; 270(24):4859-4865.

(153) Temple MD, Perrone GG, Dawes IW. Complex cellular responses to reactive oxygen species. Trends Cell Biol 2005; 15(6):319-326.

(154) Slupphaug G, Kavli B, Krokan HE. The interacting pathways for prevention and repair of oxidative DNA damage. Mutat Res 2003; 531(1-2):231-251.

(155) Shackelford RE, Kaufmann WK, Paules RS. Oxidative stress and cell cycle checkpoint function. Free Radic Biol Med 2000; 28(9):1387-1404.

(156) Prawan A, Kundu JK, Surh YJ. Molecular basis of heme oxygenase-1 induction: implications for chemoprevention and chemoprotection. Antioxid Redox Signal 2005; 7(11-12):1688-1703.

(157) Kirkby KA, Adin CA. Products of heme oxygenase and their potential therapeutic applications. Am J Physiol Renal Physiol 2006; 290(3):F563-F571.

(158) Maines MD. The heme oxygenase system: update 2005. Antioxid Redox Signal 2005; 7(11-12):1761-1766.

(159) Lamb NJ, Quinlan GJ, Mumby S, Evans TW, Gutteridge JM. Haem oxygenase shows pro-oxidant activity in microsomal and cellular systems: implications for the release of low-molecular-mass iron. Biochem J 1999; 344 Pt 1:153-158.

(160) Weng YH, Tatarov A, Bartos BP, Contag CH, Dennery PA. HO-1 expression in type II pneumocytes after transpulmonary gene delivery. American Journal of Physiology-Lung Cellular and Molecular Physiology 2000; 278(6):L1273-L1279.

(161) Biaglow JE, Miller RA. The thioredoxin reductase/thioredoxin system: novel redox targets for cancer therapy. Cancer Biol Ther 2005; 4(1):6-13.

(162) Nguyen P, Awwad RT, Smart DD, Spitz DR, Gius D. Thioredoxin reductase as a novel molecular target for cancer therapy. Cancer Lett 2006; 236(2):164-174.

(163) Beere HM, Green DR. Stress management - heat shock protein-70 and the regulation of apoptosis. Trends Cell Biol 2001; 11(1):6-10.

(164) Ciriolo MR. Redox control of apoptosis. Antioxid Redox Signal 2005; 7(3-4):432-435.

(165) Zhang XD, Wu JJ, Gillespie S, Borrow J, Hersey P. Human melanoma cells selected for resistance to apoptosis by prolonged exposure to tumor necrosis factor-related apoptosis-inducing ligand are more vulnerable to necrotic cell death induced by cisplatin. Clin Cancer Res 2006; 12(4):1355-1364.

(166) Chen YR, Shrivastava A, Tan TH. Down-regulation of the c-Jun N-terminal kinase (JNK) phosphatase M3/6 and activation of JNK by hydrogen peroxide and pyrrolidine dithiocarbamate. Oncogene 2001; 20(3):367-374.

(167) Bernardini S, Bernassola F, Cortese C, Ballerini S, Melino G, Motti C et al. Modulation of GST P1-1 activity by polymerization during apoptosis. J Cell Biochem 2000; 77(4):645-653.

(168) Zhou Y, Hileman EO, Plunkett W, Keating MJ, Huang P. Free radical stress in chronic lymphocytic leukemia cells and its role in cellular

sensitivity to ROS-generating anticancer agents. Blood 2003; 101(10):4098-4104.

(169) Senthil K, Aranganathan S, Nalini N. Evidence of oxidative stress in the circulation of ovarian cancer patients. Clin Chim Acta 2004; 339(1-2):27-32.

(170) Chiou CC, Chang PY, Chan EC, Wu TL, Tsao KC, Wu JT. Urinary 8-hydroxydeoxyguanosine and its analogs as DNA marker of oxidative stress: development of an ELISA and measurement in both bladder and prostate cancers. Clin Chim Acta 2003; 334(1-2):87-94.

(171) Janssen AM, Bosman CB, van Duijn W, Oostendorp-Van De Ruit MM, Kubben FJ, Griffioen G et al. Superoxide dismutases in gastric and esophageal cancer and the prognostic impact in gastric cancer. Clin Cancer Res 2000; 6(8):3183-3192.

(172) Davies-Coleman MT, Dzeha TM, Gray CA, Hess S, Pannell LK, Hendricks DT et al. Isolation of homodolastatin 16, a new cyclic depsipeptide from a Kenyan collection of Lyngbya majuscula. J Nat Prod 2003; 66(5):712-715.

(173) Keyzers RA, Arendse CE, Hendricks DT, Samaai T, Davies-Coleman MT. Makaluvic acids from the South African latrunculid sponge Strongylodesma aliwaliensis. J Nat Prod 2005; 68(4):506-510.

(174) Knott MG, Mkwananzi H, Arendse CE, Hendricks DT, Bolton JJ, Beukes DR. Plocoralides A-C, polyhalogenated monoterpenes from the marine alga Plocamium corallorhiza. Phytochemistry 2005; 66(10):1108-1112.

(175) Davies-Coleman MT, Dzeha TM, Gray CA, Hess S, Pannell LK, Hendricks DT et al. Isolation of homodolastatin 16, a new cyclic depsipeptide from a Kenyan collection of Lyngbya majuscula. Journal of Natural Products 2003; 66(5):712-715.

(176) Whibley CE, Keyzers RA, Soper AG, Davies-Coleman MT, Samaai T, Hendricks DT. Antioesophageal cancer activity from Southern African marine organisms. Ann N Y Acad Sci 2005; 1056:405-412.

(177) Shimada Y, Imamura M, Wagata T, Yamaguchi N, Tobe T. Characterization of 21 newly established esophageal cancer cell lines. Cancer 1992; 69(2):277-284.

(178) Friedl F, Kimura I, Osato T, Ito Y. Studies on a new human cell line (Siha) derived from carcinoma of uterus .1. Its establishment and morphology. Proc Natl Acad Sci U S A 1970; 135(2):543-545.

(179) Sykes JA, Whitesca J, Jernstrom P, Nolan JF, Byatt P. Some properties of a new epithelial cell line of human origin. J Natl Cancer Inst 1970; 45(1):107-122.

(180) Battaglia M, Pozzi D, Grimaldi S, Parasassi T. Hoechst-33258 staining for detecting mycoplasma contamination in cell cultures - A method for reducing fluorescence photobleaching. Biotech Histochem 1994; 69(3):152-156.

(181) Vistica DT, Skehan P, Scudiero D, Monks A, Pittman A, Boyd MR. Tetrazolium-based assays for cellular viability: a critical examination of selected parameters affecting formazan production. Cancer Res 1991; 51(10):2515-2520.